EXPERIMENTAL STUDY ON

AN IMPACT VIBRATION ABSORBER

by

İHSAN CEM DEŞEN, B.S.M.E.

A THESIS

IN

MECHANICAL ENGINEERING

Submitted to the Graduate Faculty
of Texas Tech University in
Partial Fulfillment of
the Requirements for
the Degree of

MASTER OF SCIENCE

MECHANICAL ENGINEERING

Approved

Accepted

Dean of the Graduate School

May, 2000

ACKNOWLEDGEMENTS

I am grateful for the consistent guidance and support of my advisor, Dr. Stephen Ekwaro-Osire, who made this experience enjoyable as well as challenging. Without him, this work would never have been possible. I also want to thank him for helping me improve myself professionally. Special thanks are due to my committee members, Dr. Atila Ertas, to whom I am also indebted for realizing my ideals, and to Dr. Timothy T. Maxwell.

I also would like to thank all the staff and faculty of the Department of Mechanical Engineering at Texas Tech University for their help and support. I enjoyed working for my classes, as well as working for my professors as their teaching assistant, including the teaching assignment, which I took extreme pleasure from doing. I am also grateful for the support of my friends and colleagues at the department, especially those of the Dynamical Systems and Vibrations Lab.

Very special thanks are due to my professors at Bogazici University of Istanbul, Turkey. Without the support of Dr. Gunay Anlas and Dr. Ozer Arnas, I would not have been able to realize my dreams. In addition, the help of Dr. Eren Semercigil of Mechanical Engineering-Victoria University of Technology, Australia is greatly appreciated. His expertise on impact vibration absorbers has helped me throughout my research, and I am grateful for his never-ending support.

However, above all, I want to thank my mother and father, Puran and Erdogan Desen, for helping me be the man that I am today, and for their support and understanding through all my life. Finally, my gratitude is extended to my love, Guldal, for her encouragement, understanding, and support.

TABLE OF CONTENTS

ABSTRACT

An Impact Vibration Absorber (IVA), which is also referred to as an impact damper, consists of a free mass moving between the motion limiting stops of a primary system. When the amplitude of vibration of the primary system exceeds the gap between the stops, the absorber mass collides with the stop. Under sufficient excitation, the IVA undergoes cyclic motion, colliding intermittently with the stops. By this mechanism, the IVA reduces the vibration of the primary system through momentum transfer by collision and dissipation of kinetic energy as acoustic and heat energy.

The aim of the current study is to investigate the effects of mass ratio, clearance between stops, and excitation amplitude on IVA effectiveness and system dynamics. Vibration absorption is studied for both free and forced vibrations. Constant frequency and frequency sweep experiments are conducted to study system dynamics. Coherence between the forcing function and primary mass response is studied, as a first step in proposing a new method for determining the efficiency of vibration absorbers.

Extensive parametric studies were performed on the IVA. Free vibration studies revealed the effect of system parameters on rate of decay of vibrations. For forced vibrations, it was shown that an optimum clearance exists for which the energy absorption is greatest. The efficiency of the absorber is highest around the natural frequency of the primary structure, and diminishes as excitation frequency moves away from the natural frequency. The characteristic jump phenomenon was observed for the case without the IVA, at different locations for upsweep and downsweep. In the absence of the IVA, the high response amplitude at resonance caused the coherence to drop. The introduction of the IVA was shown to attenuate the vibrations in such a manner that the response amplitude of the primary mass is consistently low for the whole range of the swept frequency. This results in a coherence function that is close to unity for the range of the swept frequency. Therefore, coherence between the forcing function and response of a system may be used as a measure the absorber effectiveness.

LIST OF FIGURES

LIST OF SYMBOLS

f	Frequency of vibration, excitation frequency (Hz).
f_n	Natural frequency (Hz).
w	Frequency of vibration, excitation frequency (Rad/s).
w_n	Natural frequency (Rad/s).
r	Frequency ratio, f/f_n or w/w_n.
t	Time (s).
A	Zero-to-peak amplitude of excitation (m).
e	Coefficient or restitution.
x	Deflection of primary mass from equilibrium position (m).
z	Deflection of IVA from equilibrium position (m).
$\dot{z}$	Velocity of impact vibration absorber (m/s).
k	Stiffness (N/m^2).
m_1	Mass of primary mass (kg).
m_2	Mass of impact vibration absorber (kg).
μ	Mass ratio, m_2/ m_1.
c	Damping ratio (N-sec/m).
l	Length of pendulum (m).
d	Clearance between walls (m).
θ	Angle of rotation of pendulum (degrees).
$G_{xx}(f)$	Auto (Power) Spectral density function of input.
$G_{yy}(f)$	Auto (Power) Spectral density function of output.
$G_{xy}(f)$	Cross-Spectral density function.
$\gamma^2_{xy}(f)$	Coherence function.

CHAPTER 1
INTRODUCTION

1.1 Introduction

Vibration is the study of the repetitive motion of objects. Vibration is caused by anything that oscillates and it is transmitted through continuous media. Therefore, vibrations caused by a system effect other systems, unless the systems are separated by vacuum, as in space. It is observed in nature as well as in man-made devices and structures. When talking about vibration, one usually refers to the displacement, velocity and acceleration of a point on the vibrating structure. These quantities are functions of time, and are referred to as signals. Throughout the text, vibration signals will be referred to simply as vibration. Vibration, or vibration signals, can be divided into two main categories with respect to the characteristics of signals, namely, deterministic and non-deterministic. Deterministic vibration, which can be categorized further as in Figure 1.1, can be periodic or non-periodic. Furthermore, on one hand periodic vibration is classified as sinusoidal or complex periodic, on the other hand non-periodic vibration is classified as almost periodic or transient (Bendat and Piersol, 1986). Sinusoidal vibration has the form of a sine signal, while complex periodic vibration may have the form of a combination of sine signals of different frequency and amplitude, or it may be any other signal that is periodic. Vibration caused by the rotation of unbalanced machinery such as turbines, wheels and shafts is an example to sinusoidal vibration. The vibration of an engine, however, is complex periodic since the components of the engine move periodically with different periods. Vibration that is present in the nature, e.g., vibration caused by earthquakes, often shows non-deterministic characteristics, hence the term random vibration. For repeated observations under basically identical conditions, random vibrations do not depict the same time histories. Therefore, statistical and probabilistic tools, e.g., mean and correlation, are used to study these vibrations. Transient vibration is another case of non-periodic vibration. In this case, an initial displacement, velocity or acceleration, or a sudden change in one of these quantities caused by an external element, causes the structure to experience vibrations that decay with time. Transient vibration is

also referred to as free vibration, since the primary structure is not forced to move continuously, but instead, it vibrates freely due to initial conditions that are imposed on the structure.

Vibration is used in different fields for numerous applications. Vibrating mixers and sieves are used in production systems for use in automated production, e.g., automatic feeders. Vibrating sieves and tools are used in construction, e.g., pneumatic drills. In medicine, vibrating machines are used by doctors to cure diseases, e.g., sound waves are used to break kidney stones, as in the lithotripter, which is used for Extracorporeal Shock Wave Lithotripsy (ESWL) treatments.

Although there are some applications that benefit form vibrations, in general, vibration is not desired in mechanical systems and engineering structures. The cyclic characteristic of vibration introduces dynamic stresses in members, which cause fatigue and can eventually lead to failure. Vibrations caused by earthquakes may cause structures to fail unless they are designed properly. Vibration of the passenger compartments of vehicles cause discomfort to the passengers.

The concept of resonance is very important and has a high priority in the study of forced vibrations. The term forced vibration is used for cases where the structure is excited continuously by an external source, e.g., a sinusoidal force. The forcing frequency is the frequency of this forcing function, e.g., the frequency of the sine wave. For a vibratory system, resonance occurs when the forcing frequency is equal to the natural frequency, also referred to as the resonant frequency, of the structure. Under resonance, displacement of a nodal point reaches its highest value. Since displacements are maximum at resonance, resonance imposes the highest strains and stresses on the structural members, and therefore causes the most damage. The idea in using a vibration absorber in a system is mainly to reduce the destructive vibrations that the primary system experiences when it is excited at or around its natural frequency, i.e., when it experiences resonance. A vibration absorber can be described as an auxiliary system connected to the primary system of concern, which attenuates the vibrations of the primary system by absorbing and/or dissipating its kinetic energy. Vibration absorbers have found extensive use in engineering systems for about a hundred years. The first

hydraulic vibration absorber was actually used in 1909 to reduce the rolling motion of ships (Frahm, 1909). As the technology advances, applications require more efficient, smaller and lighter vibration absorbers.

1.2 Vibration Control

1.2.1 Introduction

There are different methods to control vibration. If the system is not designed for vibration, problems may be faced once vibration is observed during operation. In this case, a vibration control strategy needs to be employed to reduce the levels of vibration and enable reliable and comfortable operation. Vibration control can be divided into three main categories, namely, passive, active, and hybrid vibration control (Figure 1.2). Passive vibration control systems function without external assistance, e.g., they do not require a power source, simply because they are driven by the vibration itself. In most cases, they offer the fastest, simplest and cheapest solution to the problem. They require little or no maintenance, and installation is relatively simple. The tuned mass damper, which consists of a mass-spring-damper system, is a common example for vibration absorbers that operate on this principle. However, passive control may not be sufficient in some applications, and active vibration control systems may be required. Contrary to passive systems, active vibration control systems depend on a power source. They require power for operating the sensors that sense the level of vibration, the control systems that process the sensor signals and send driving signals, and the driving devices that apply forces to reduce the level of vibration. Active vibration control systems are mostly more complex and expensive than passive systems, require maintenance, and there is a higher possibility of failure, but they may show better performance or be the only solution in some cases. Active vibration control systems used in buildings that protect them from the destructive effects of earthquakes is a good example for this category. Hybrid control systems utilize both passive and active components.

1.2.2 Passive Vibration Control

1.2.2.1 Introduction

Passive vibration control methods (Figure 1.2), which are usually simpler compared to active methods, involves modifying the existing design, or adding extra components to the system. These modifications may be changing the structural design, making localized additions to the system, adding damping to the system, using resilient isolation, or a combination of these methods. Changing the structural design may be done by changing the dimensions, shapes or materials of some elements in order to change stiffness, damping and mass of the structure. Making additions involves adding localized or continuous components, e.g., vibration absorbers, or adding damping to the main system. Using vibration isolators between components is an example of the resilient isolation technique. Depending on the design considerations, space, weight and cost constraints, a decision can be made on the passive vibration control method to be used.

1.2.2.2 Passive Vibration Control by Structural Design

It is best to take vibration considerations into account while designing a structure. This will mostly include designing the structure so that the natural frequencies of the system are far from the frequencies of operation, and the levels of vibration are acceptable. The most general methods used for controlling vibrations by structural design are detuning, reducing the number of responding modes, nodalizing, decoupling, optimizing the structural geometry, structural stiffening and selecting the best material. Detuning implies modifying the structure in such a way that its resonance frequencies do not coincide with the excitation frequencies. Reducing the number of responding modes is applicable to finite-band random excitation. Undamped continuous structures under harmonic excitation possess points at which the vibration displacement is zero, referred to as nodes. Nodalizing involves locating the sources of excitation at the nodes, by so doing minimizing the response amplitude throughout the entire structure. Increasing the stiffness of the structure reduces the number of modes that fall in the frequency band of excitation, which causes the total response to decrease. Decoupling is done by relocating the masses on the structure to minimize the vibrational power flow between the modes

and parts of the structure. The material selection and stiffening methods refer to modifying the stiffness in order to reduce the response levels (Mead, 1998).

1.2.2.3 Passive Vibration Control by Localized Additions

In some cases, the most effective and economic method for reducing vibration is to add an extra system at a discrete location on the main system. This addition can be in the form of a mass-spring-damper system attached to a single point on the main system, i.e., lumped parameter absorbers, or it can be a beam attached to the main system from its end points, i.e., continuous absorbers. In both cases, the added systems are attached to the main system at discrete points, rather than being connected continuously along the primary structure, and therefore are localized additions. Different types of absorbers can be connected to the primary structure as localized additions.

Lumped parameter absorbers have two distinguishing characters. The absorber mass is located at a discrete point, i.e., its mass is concentrated in a smaller volume compared to the main structure, and therefore it can be modeled as a discrete mass. The connection of the absorber mass to the main system is also discrete. The simplest type of absorber that falls in this category is the well-known mass-spring-damper system, commonly known as the tuned mass damper, as shown in Figure 1.3. M_S is the main system and M_T is the absorber mass. Another example is the pendulum absorber, which can be tuned to any harmonic excitation (Crossley, 1953), used as a dynamic damper for absorbing torsional vibrations (Figure 1.4). Mustafa and Ertas (Mustafa and Ertas, 1995) utilized the pendulum absorber for damping vibrations of flexible structures, where a single mass is connected to the primary structure via a pendulum (Figure 1.5). The three-mass pendulum absorber, which consists of three interconnected masses, is another example of this type of absorbers (Figure 1.6) (Korenev and Reznikov, 1993).

In the case of continuous absorbers, the absorber mass is distributed along its length, in which case the mass of the absorber can not be modeled as discrete. The absorber may also be connected to the primary structure at multiple points, or along its length, instead of being connected at a single point. Examples to this type are beam-mass absorbers, beam-pendulum absorbers, and liquid dampers. Ibrahim and Sullivan proposed

in 1990 a beam-mass absorber, where a beam-mass system is used as an absorber to another beam-mass structure. Ibrahim *et al.* (1989) studied a beam-mass absorber for a nonlinear building model (Figure 1.7). Sevin (1961) proposed a beam connected to two linkages at its ends, as an absorber (Figure 1.8). Liquid dampers, which consist of containers partially filled with liquids, (Figure 1.9) have been proposed and used for vibration absorption.

The absorber mass of an Impact Vibration Absorber (IVA) may either be connected to the primary mass as in the case of the tuned mass damper, or it may be free to move in a cavity with no connections with the primary structure. The distinguishing character of IVAs is the existence of the walls, the movement limiting stops that constrain the range of movement of the absorber mass. The first IVA was proposed by Paget (Figure 1.10) in 1937 to damp the vibrations of turbine blades (Paget, 1937). Here, the impact mass (c) is a steel ball, which is free to move along the rectangular section (a) that is cut into the turbine blade.

1.2.2.4 Passive Vibration Control by Added Damping

Damping causes the decay of transient vibrations, by removing the energy from the system. The energy is either removed from the system by radiation, or it is dissipated within the system. Using layers of high-damping materials in or on a structure increases damping. By increasing the damping, the energy dissipation is increased. If more energy is dissipated from a vibratory system, there will be less kinetic energy left, which will cause the velocities and displacements related to vibration to be lower (Ungar, 1992). This method is most effective for reducing flexural vibrations of beams, plates and cylinders, but usually ineffective for torsional and longitudinal vibration. The internal damping of beams can be increased by using stainless steel instead of aluminum, or by adding viscoeleastic materials to dissipate energy. The radiation damping of a vibrating beam can also be increased, e.g., by clamping it to a supporting structure instead of suspending it by wires (Crandall, 1970).

1.2.2.5 Passive Vibration Control by Resilient Isolation

Vibration isolation refers to the use of comparatively resilient elements for reducing vibrations that are induced on a system by another system (Ungar, 1992). For physically connected systems, it is not possible to eliminate vibration transmission completely, but it can be minimized by isolating the two systems using resilient interconnections, referred to as vibration isolators. The resilient elements can be modeled as spring damper systems, as shown in Figure 1.11. Mechanical applications include anti-vibration mounts by which the engines of vehicles are attached to the main structure. Applications in civil structures include solid viscoeleastic dampers, fluid viscoeleastic devices and fluid viscous devices that are used in buildings to restrict the transmission of earthquake, wind or traffic caused vibration (Penalba, 1999).

1.3 Impact Vibration Absorbers

1.3.1 Introduction

Since the introduction of the IVA, different types of IVAs have been proposed, studied and used in practical applications. The IVAs that have been proposed up to date can be classified as (a) single-unit IVAs, (b) multi-unit IVAs, (c) hybrid IVAs, and (d) compound IVAs (Figure 1.12). Single-unit IVAs consist of a single mass moving freely in the primary system (Figure 1.12 (a)), whereas multi-unit IVAs utilize multiple impact masses contained either in the same cavity (Figure 1.12 (b)), or in separate cavities. Hybrid IVAs are IVA systems combined with other absorbers, e.g., an IVA connected to a mass-spring-damper absorber (Figure 1.12 (c)). On the other hand, the impact mass in compound IVAs is connected to the primary system, e.g., by a pendulum or leaf spring (Figure 1.12 (d)). Although the absorber mass in the current study is connected to the encoder by a pendulum, it does not fall into the compound category since the holding mechanism is separate from the primary mass. The IVA in the current study belongs to the single-unit IVA class.

1.3.2 Single-Unit Impact Vibration Absorbers

Single-unit IVAs are the simplest type of IVAs. The first IVA proposed by Paget (1937) was of this type. He studied the effect of clearance on the efficiency of the IVA under transient excitation in the vertical direction, and found out that the IVA increased the rate of energy dissipation of the system up to 60 times. Grubin (1956) found theoretically for harmonic excitation that the IVA was most efficient at resonance. Masri and Caughey (1966) presented the exact solution of the two-impacts-per-cycle motion, for harmonic excitation (Figure 1.13). Masri (1969) also showed that best attenuation was achieved by highest coefficient of restitution and highest mass ratio. He also stated that lightly damped systems that operate over a frequency band needed lower coefficient of restitution for stability. Furthermore, he showed that the sensitivity of tuning to clearance increased with increasing gap, decreased with decreasing coefficient of restitution. He also proved theoretically that when the IVA experienced stable steady state motion, with two-impacts-per-cycle, impacts were equispaced and motion was symmetric. Masri and Ibrahim (1973) studied the response of the IVA to white noise random excitation and observed the best vibration attenuation for $0.2<e<0.8$. The authors showed that even with small mass ratios, substantial attenuations were possible, e.g., 50% attenuation for a 5% mass ratio, and that IVA performance was enhanced if there is little or negligible viscous damping in the system. Roy *et al.* (1975) investigated the application of IVAs on simply supported and clamped beams both experimentally and theoretically, and showed the effect of mass ratio, clearance, and excitation on absorption effectiveness. Thomas *et al.* (1975) applied the IVA for vibration reduction of boring bars and found at that boring bars effectiveness was improved with the installation of an IVA, giving increases in stable metal removal rates. They also showed IVA performance was insensitive to the excitation frequency. Skipor and Bain (1980) applied the IVA to a rotary printing equipment for reducing response of system to transient vibrations, studied the maintenance, wear, and failure of the IVA, and showed that oscillations were reduced to 21% of their undamped values within one cycle of vibration. Popplewell *et al.* (1983) showed that best attenuations were obtained when frequency ratio of 1, and the performance of the ID detoriates noticeably if frequency ratio was lower than 1. For this

reason, the authors proposed that driving frequency or speed would require close controls. Masri *et al.* (1989) proposed an actively controlled IVA with variable clearance, and found it quite effective in reducing peak response of vibrating structures under swept sine and random excitation, including non-stationary wide-band random excitation. Chalmers and Semercigil (1991) studied the performance on the IVA applied to a long aluminum beam under harmonic excitation. Cases of single IVA at the tip, single IVA at 2nd mode, and two IVAs at both locations were studied and the authors determined the desired location for second IVA for the second mode of the beam. It was shown that using two IVAs gave much better vibration reduction and also using hard rubber on impact surfaces increased reduction, while also reducing the sensitivity of the system response to clearance. Hoang and Semercigil (1992) proposed an IVA to control the excessive transient vibrations of a single-link flexible robot arm for transient excitation, e.g., after a sudden stop or after hitting a stop block. The authors demonstrated experimentally that the IVA was capable of attenuating up to 95% of the vibrations, with a simple, self-contained construction and without any obstruction to the tasks to be performed by the robot. The previous study was extended by numerical simulations and experiments, and it showed that the performance of the IVA detoriates slightly if the impacts take place in the vertical direction (Figure 1.14)(Chen and Semercigil, 1993). The authors proposed a new IVA employing an oscillator rather than a loose mass, since it would have consistent damping in both horizontal and vertical directions, and showed that the new IVA was as effective in the vertical direction as the horizontal direction. Cao and Semercigil (1994) studied a semi-active controller to change the clearance of an impact damper to control the excessive transient vibrations of light flexible systems. Bapat (1995) studied an IVA operating on an inclined surface, showing that effects of gravity and friction were detrimental and reduced stability ranges in most cases and considered using compressed air to accelerate the IVA. Ema and Marui (1995) applied the IVA to boring bars and drills to reduce chatter vibration, considering operation in vertical and horizontal direction. The authors showed that the damping capability was increased by eight-fold or more. Moore *et al.* (1995) developed an IVA for turbo-pumps. The authors stated the difficulty of damping of such machinery due to cryogenic

temperatures and low viscosity of the operating fluid. The optimum operating amplitudes for different modes and mass ratios were determined experimentally and analytically, and the damping performance is characterized by an equivalent viscous damping coefficient to compare performance of IVA by other dampers. The results proved the ID to be a viable means to suppress vibration in cryogenic rotor-bearing systems. Oledzki *et al.* (1999) used a self contained IVA in the fuselage of the motorized hang-glider in Figure 1.15, where the arrow shows the location of the IVA, showing that it decreased the resonance amplitude up to four times, and especially at idling speeds of the motor which caused resonance. The authors investigated impact phenomena between bodies with plastic inserts, found optimum values for mass ratio, clearance, and stated that small amounts of friction force would benefit the efficiency, while efficiency did not depend on frequency ratio.

1.3.3 Multi-Unit Impact Vibration Absorbers

As the name suggests, multi-unit IVAs utilize multiple impact masses. The impact masses can be enclosed in a single cavity, as in Figure 1.12 (b), or they may be enclosed in their respective cavities, e.g., three impact masses in three cavities. Also, the impact masses can be connected to each other, as in the case of hanging chain dampers. Paget (1937) was also the first to utilize a chain as an IVA. Reed (1967), showed that the IVA increased the damping of a 70-foot tall erected launch vehicle by a factor of up to 3, and utilized the IVA effectively to reduce transverse vibrations caused by wind excitation (Figure 1.16). Masri (1968) obtained the exact solution for the two-impacts-per-particle-per-cycle motion, and showed that a properly designed multiple-unit IVA was more efficient than an equivalent single-unit IVA in regard to vibration reduction and noise level of operation. The model used in this study is a good example for multi-mass/multi-cavity IVAs (Figure 1.17). Semercigil and Popplewell (1988) proposed the use of the "beanbag damper," a bag filled with lead shots, as an IVA. The authors showed experimentally that the beanbag damper reduced the vibrations of systems under random excitation by about 40%, whereas the traditional IVA was quite ineffective. They also showed that the beanbag damper attenuated the accelerations due to impacts, and

operation was quiet, and commented that the beanbag dissipated more energy because of its design and more plastic behavior. Popplewell and Semercigil (1989) studied the beanbag damper (Figure 1.19) for sinusoidal excitation and showed that it had better performance over the single-unit IVA. They also utilized optical sensors to measure the displacement of the beanbag damper with respect to the primary mass. Jo *et al.* (1989) used multiple IVAs for absorbing wind and road excited vibrations of highway light poles (Figure 1.18), while coating contact surfaces with polyurethane for noise reduction. By attaching IVAs to the inside of the pole, the authors were able to obtain 90% reduction in vibration amplitudes, while also proposing a self-contained design. Koss and Melbourne (1995) utilized the hanging chain damper for reducing wind-induced vibrations of communication towers. Hanging chain dampers were employed inside the towers to increase their structural damping, and it was shown that the impacts occurred not only at the free and but along most of the length of the chain as vibration became more severe. The authors also proposed that energy dissipation was by inelastic impact of chain against the wall of the cylinder and by the internal friction of the chain links. Yokomichi *et al.* (1996) studied the effects of the damper parameters, mode shapes and damper locations, and showed that good vibration reduction was achieved when the damper was applied to points of large modal amplitudes. Papalou and Masri (1998) showed that replacing a single-particle IVA with smaller particles of equal total mass improved the surface detoriation, reduced noise and sensitivity of efficiency to excitation amplitude with a compromise in reduction in the peak efficiency. The model used in this study (Figure 1.20) is a good example to multiple-unit IVAs in a single cavity.

1.3.4 Hybrid Impact Vibration Absorbers

Ying and Semercigil (1991) were the first to propose this type of an IVA. The authors demonstrated that the inclusion of an impact damper as an extra system may improve the capabilities of the conventional tuned mass absorbers for random excitation (Figure 1.21), and suggested installing the system in existing absorbers to provide extra protection in the event of unexpected excitation such as earthquakes. Moore *et al.* (1997) studied a hybrid friction-impact vibration absorber (Figure 1.22) for high-speed rotor

dynamic applications at cryogenic temperatures. The authors stated that since the coefficient of restitution is a weak function of temperature, the IVA was effective at cryogenic temperatures as well. According to the authors, the friction damper shows superior performance at low amplitudes and speeds, while the IVA requires a certain acceleration to initiate impacting motion, and therefore yields optimal performance at higher amplitudes and speeds. The two dampers complement each other providing vibration suppression over the full speed range. Collette (1998) analyzed the effectiveness of the combined tuned mass absorber-IVA for a three-story building model under random excitation, and studied its sensitivity to variations of clearance, coefficient of restitution, and mass ratio. Performance of the combined absorber is compared to the conventional tuned absorber. Collette and Semercigil (1998) and Collette *et al.* (2000) studied similar systems under transient vibration.

1.3.5 Compound Impact Vibration Absorbers

Kato *et al.* (1976) studied an IVA connected to the primary mass with a spring (Figure 1.23), under swept sinusoidal excitation, and showed that IVA of one-sided impact design is superior in damping effect to one of two-sided impact design. The authors stated that choosing a proper static distance between the IVA and the stopper and a Wn_{IVA}/Wn_{PM} ratio between 0.6 to 0.8, achieves damping effect over a wide range of frequencies. It is worthwhile to note that in the case of compound IVAs, it is necessary to tune the IVA as in the case of tuned mass absorbers, as well as tuning IVA parameters. Steinberg (1977) utilized IVAs he named "snubbers," in the form of resilient rubber posts attached to the center of adjacent boards and separated by a gap of a few hundredths of an inch, for damping printed-circuit boards in order to protect them form vibrating under dynamic loads and results of cracked solder joints, broken leads and loose components. He reported that snubbers limited vibration to a safe amplitude by coupling boards together for added structural support. Fuse (1989) proposed a dynamic damper with an IVA connected to the primary mass with a leaf spring. The primary mass and the IVA is coupled in this case, since they are connected (Figure 1.24). In fact, The IVA would be a TVA if there were no impacts. This study is interesting, since this absorber can be

thought of a TVA for smaller displacements and as an IVA for displacements large enough to cause impacts. Ogawa *et al.* (1992) proposed an IVA with a mass connected to a cable suspended from the top of a 2 m. tower model whose vibrations are to be reduced. Since there is no initial clearance, this design is also effective for small vibration amplitudes. Ogawa *et al.* (1997) studied the vibration absorption of a hanging mass IVA (Figure 1.25) for transient and wind tunnel excitation. Since neoprene was used on impact surfaces, the noise levels are reported to be lower than 60 dB. This IVA was used to suppress wind-induced vibration of a bridge pylon by increasing the structural damping of the pylon, in order to increase the galloping onset wind velocity. El-Sayad *et al.* (1999) proposed an IVA system in the form of a simple pendulum (Figure 1.26) impacting with the walls of a tank whose vibrations are to be reduced.

1.4 Objectives

The objective of this research is to study the effectiveness of the IVA under swept and constant sinusoidal excitation, and the effect of the system parameters on system dynamics. This involved determining the effect of mass ratio, excitation amplitude, and clearance on absorber efficiency and on system dynamics.

1.5 Scope of Work

For free vibration experiments, the time series data for the primary mass and the IVA are recorded. For forced vibration, the time series data for the forcing function, which is the excitation amplitude, the primary mass displacement, and IVA displacement are collected. The time series data is used to obtain the motion plots, phase portraits, frequency response plots and coherence curves at selected frequencies, and for a range of frequencies by sweeping the frequency range in both directions. Data is also utilized to show the effect of system parameters on system response. The results are analyzed and where appropriate, compared with published results

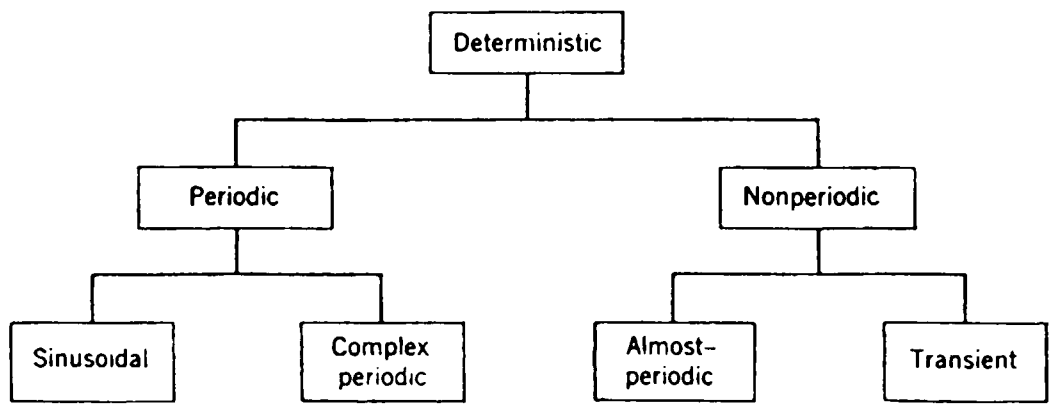

Figure 1.1: Classification of Deterministic Vibration (Bendat and Piersol, 1986).

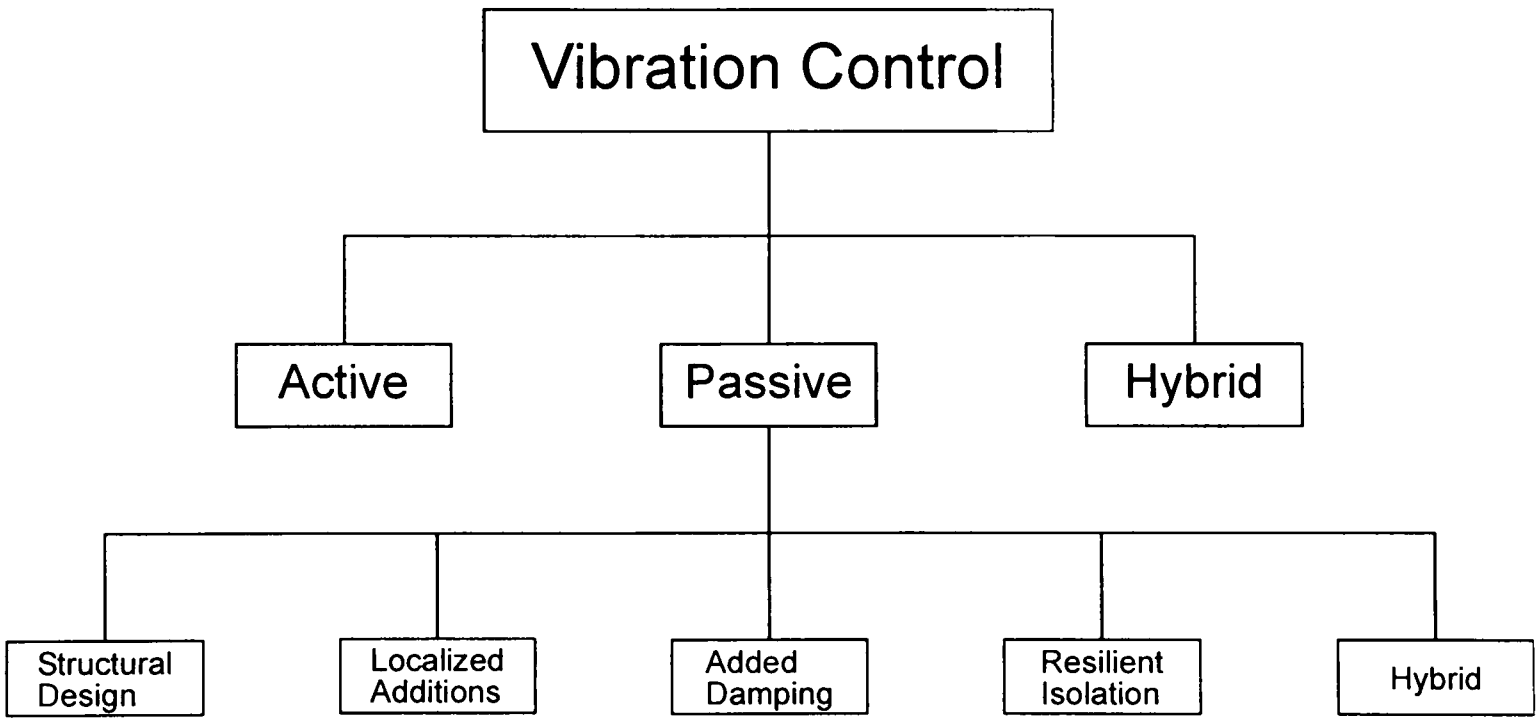

Figure 1.2: Vibration Control Methods

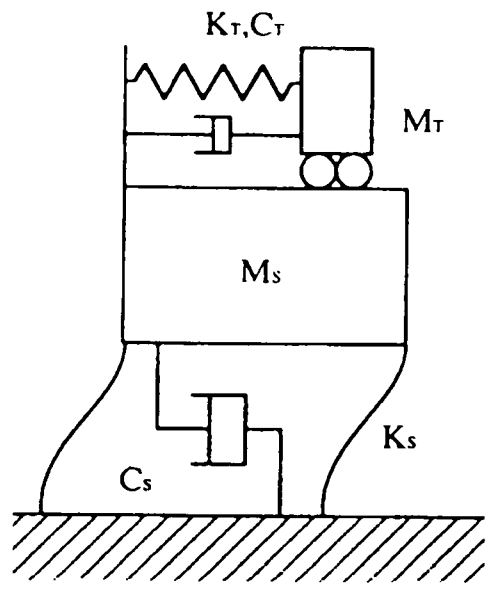

Figure 1.3: 2-DOF Model of Main Structure and Tuned Mass Damper (Iemura, 1994)

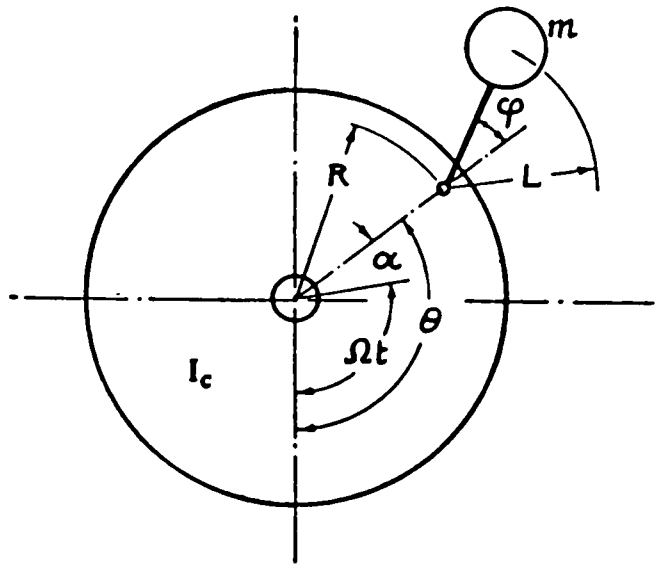

Figure 1.4: Centrifugal Pendulum Absorber

(Crossley, 1953)

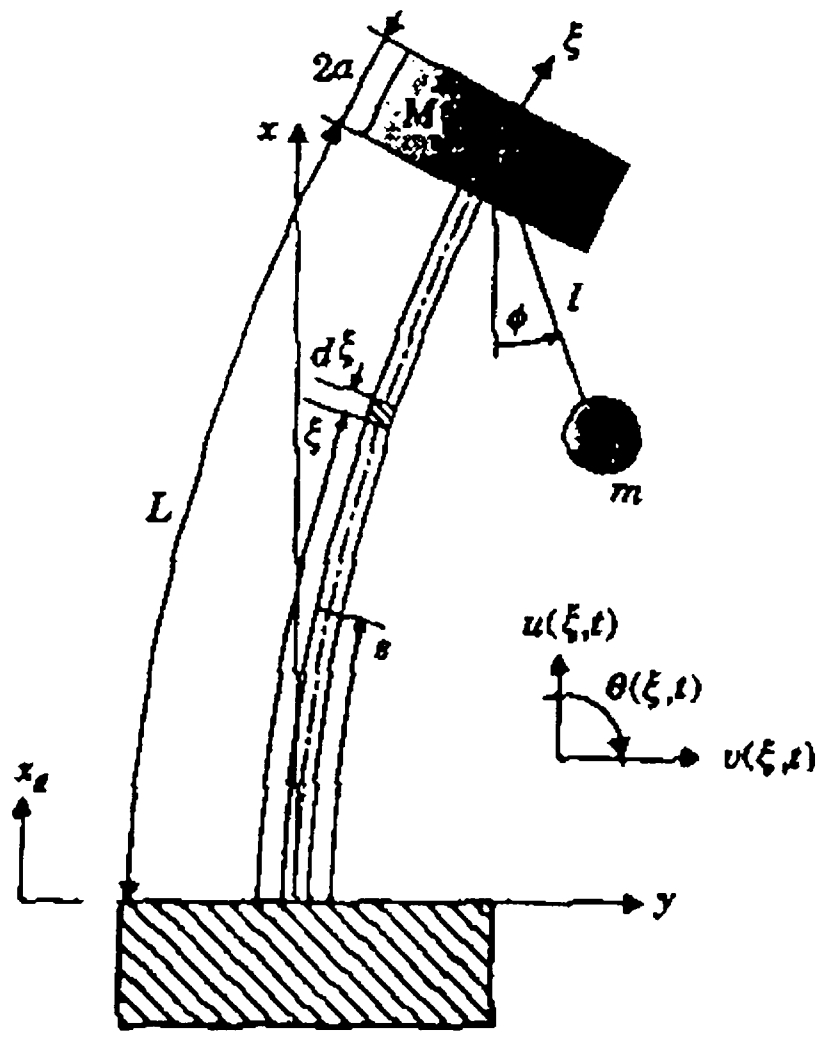

Figure 1.5: A Pendulum Absorber-Column with a tip appendage

(Mustafa and Ertas, 1995)

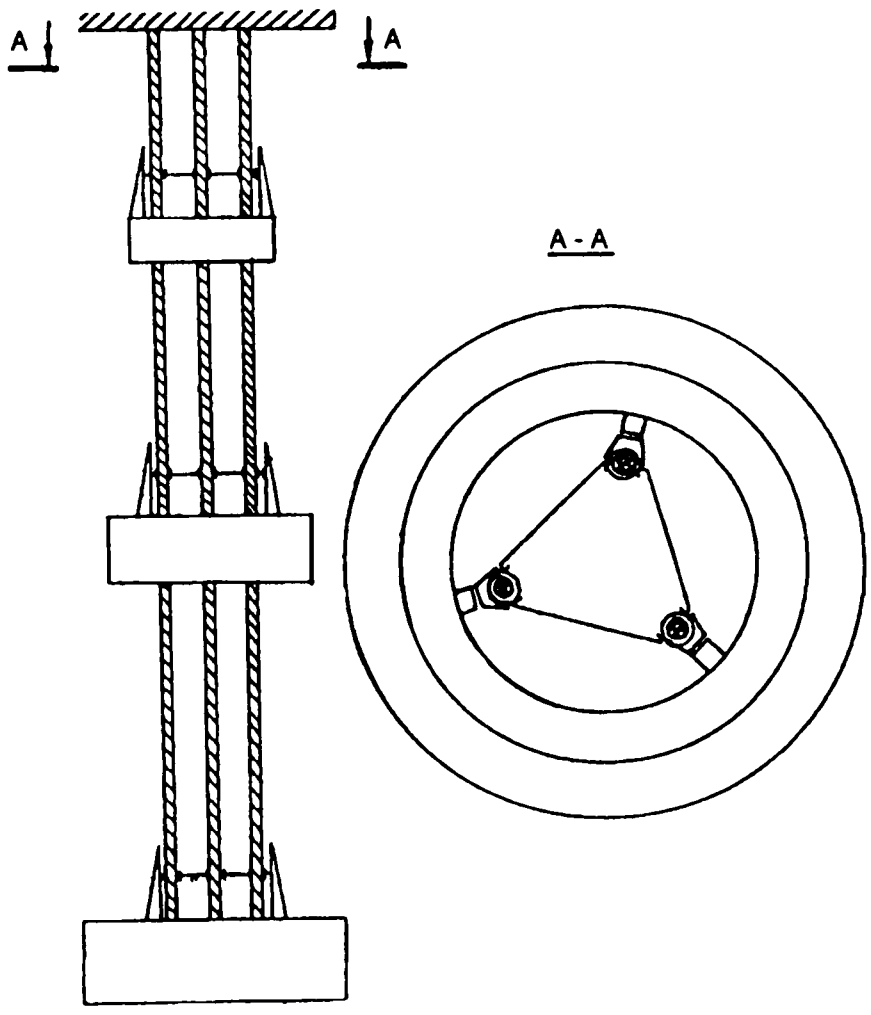

Figure 1.6: Three-mass Pendulum Absorber.

(Korenev and Reznikov, 1993)

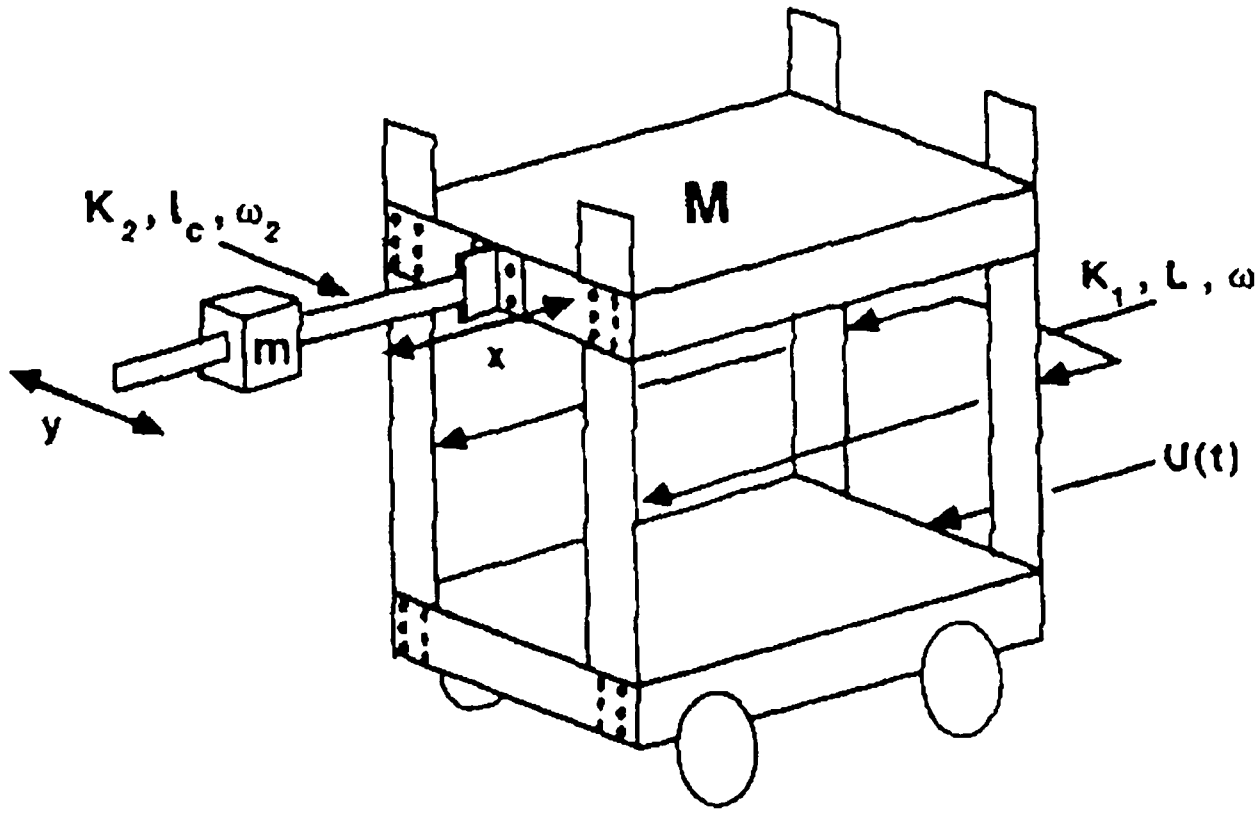

Figure 1.7: A Beam-Mass Absorber

(Ibrahim *et al.*, 1989)

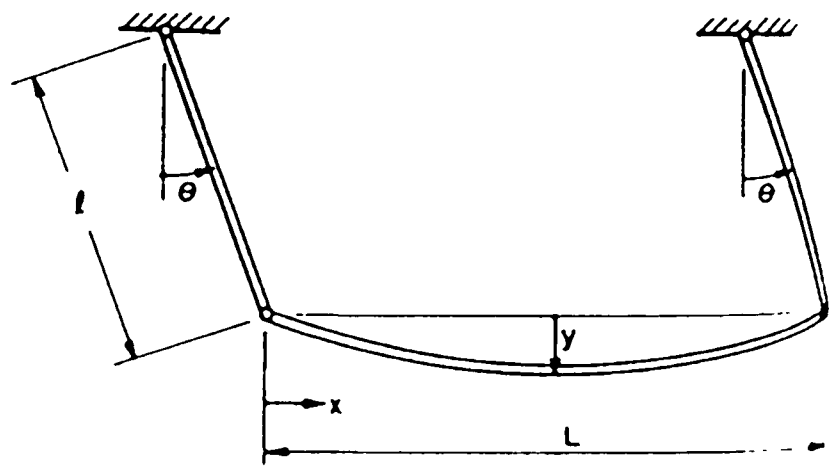

Figure 1.8: Beam-Pendulum Absorber

(Sevin, 1961)

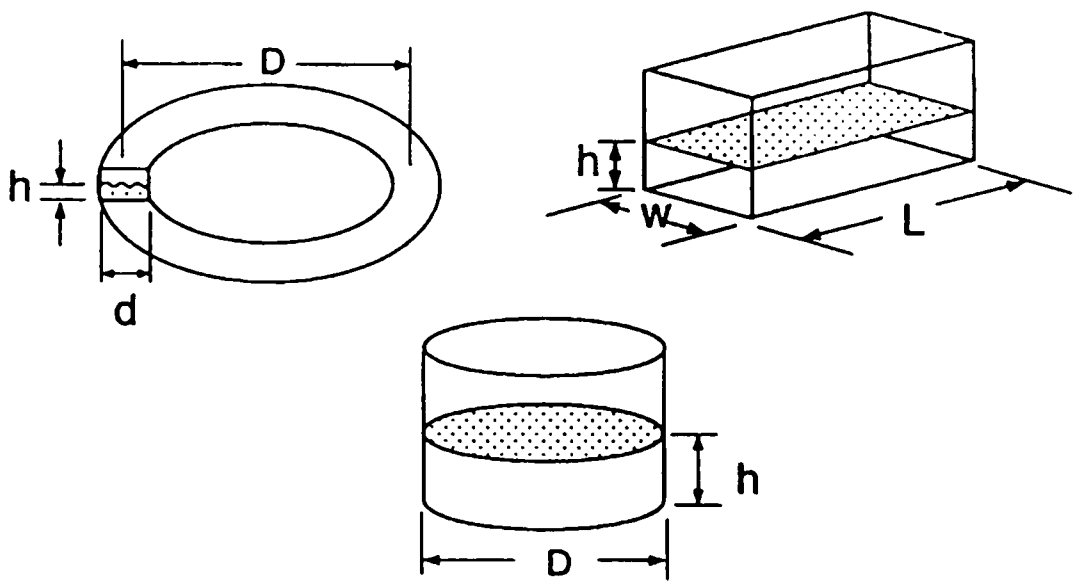

Figure 1.9: Liquid Dampers

(Modi and Seto, 1998)

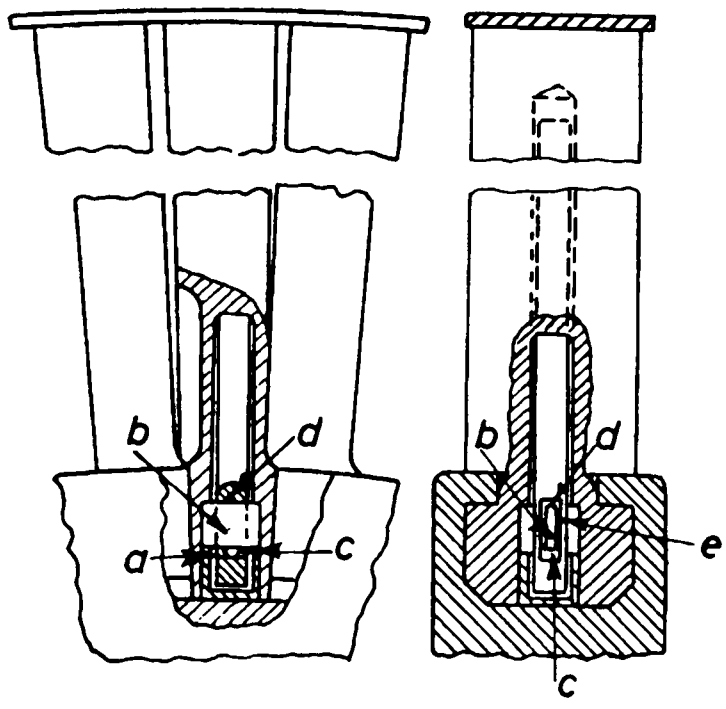

Figure 1.10: Impact Damper for Damping Turbine Blade Vibration
(Paget, 1937)

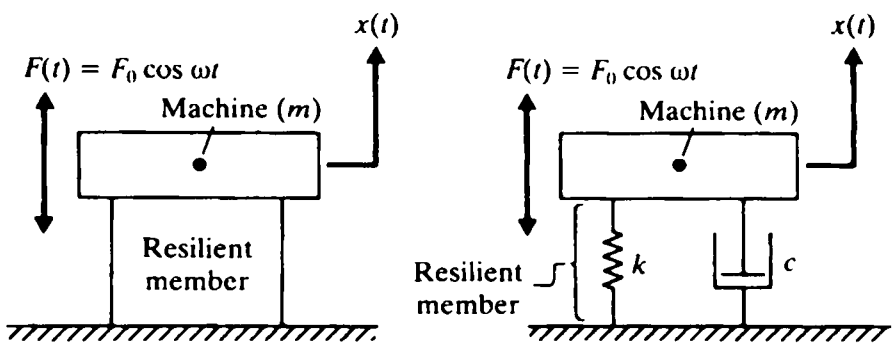

Figure 1.11: Vibration Isolator

(Rao, 1995)

Figure 1.12: Types of Impact Vibration Absorbers

(a) Single-Unit-IVA, (b) Multi-Unit IVA, (c) Hybrid IVA, (d) Compound IVA.

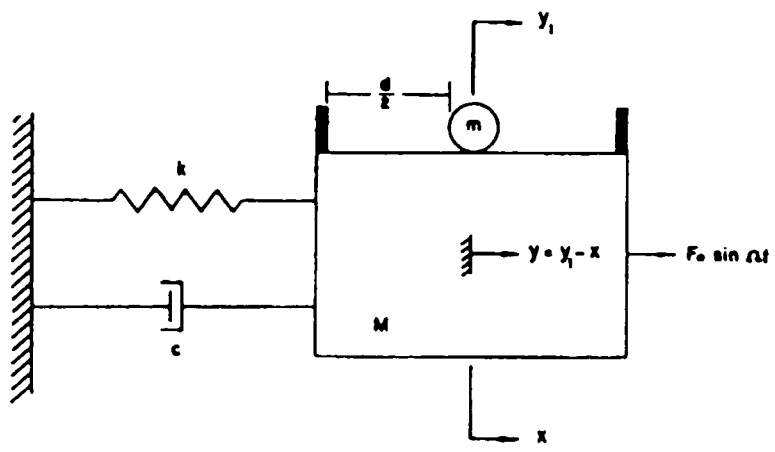

Figure 1.13: Theoretical model of IVA system.
(Masri and Caughey, 1966)

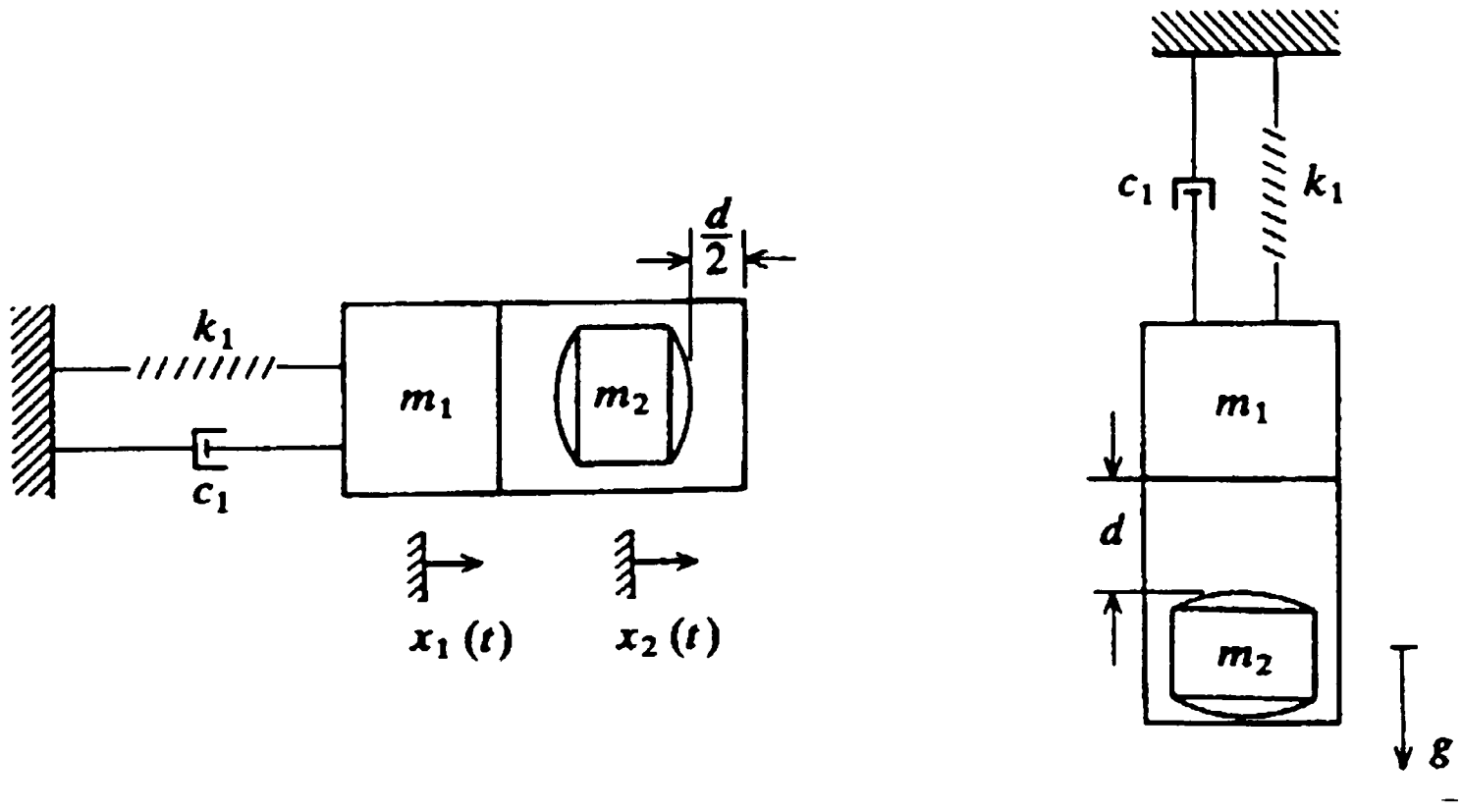

(a) (b)

Figure 1.14: IVA operating in the (a) horizontal and (b) vertical direction.
(Chen and Semercigil, 1993)

Figure 1.15: IVA installed in motorized hang glider.

(Oledzki *et al.*, 1999)

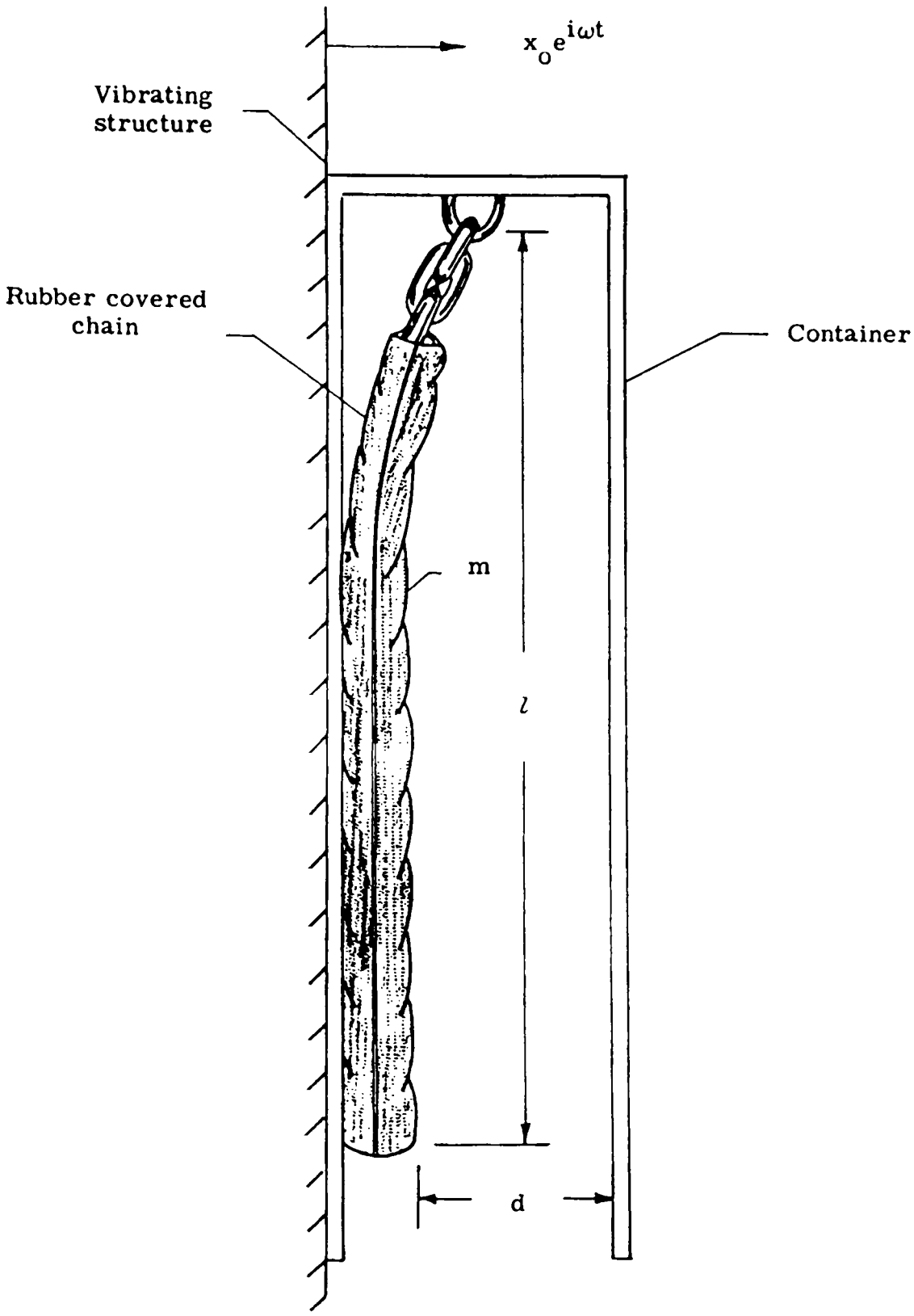

Figure 1.16: Hanging Chain Damper

(Reed, 1967)

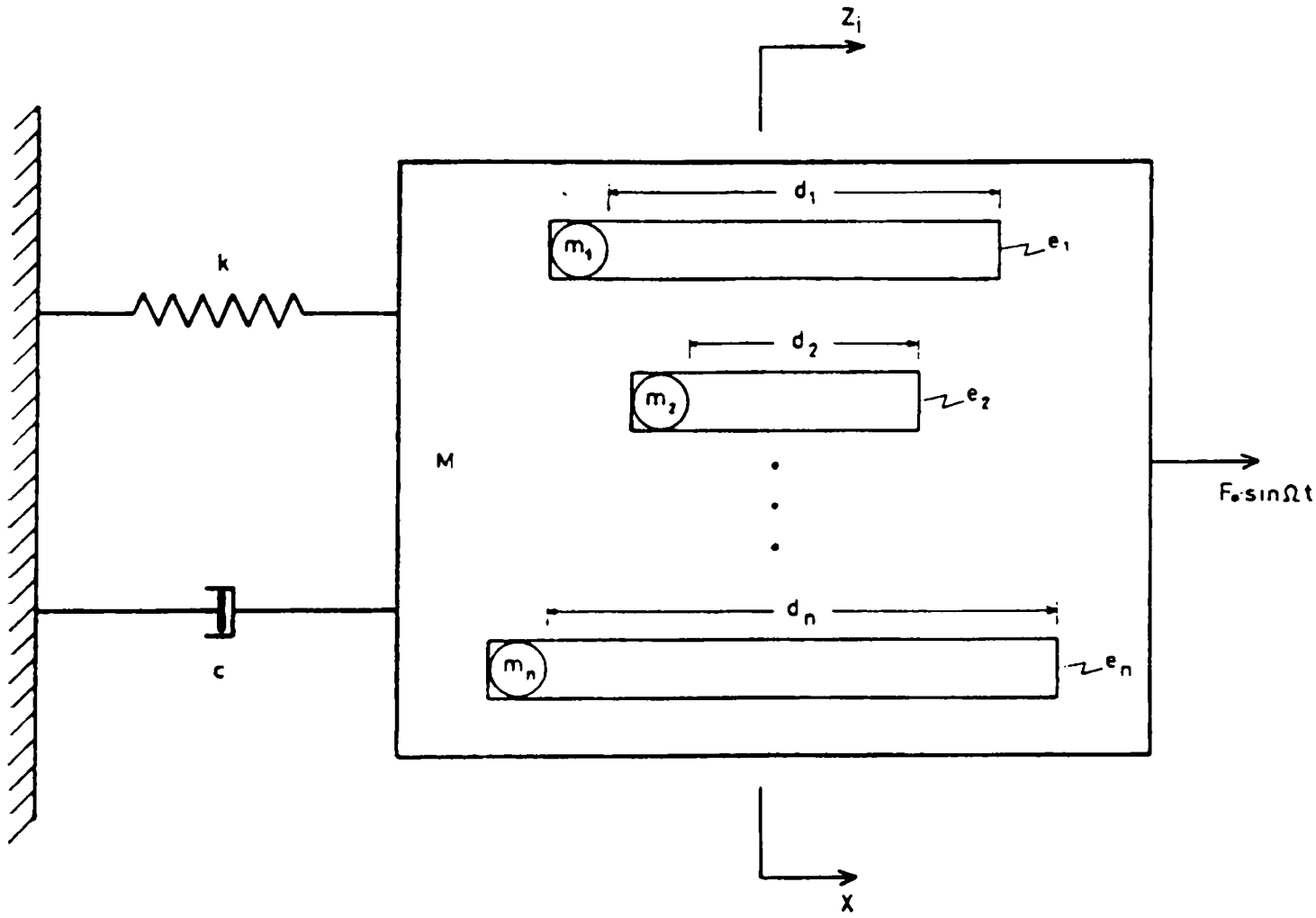

Figure 1.17: Multi-unit IVA.

(Masri, 1968)

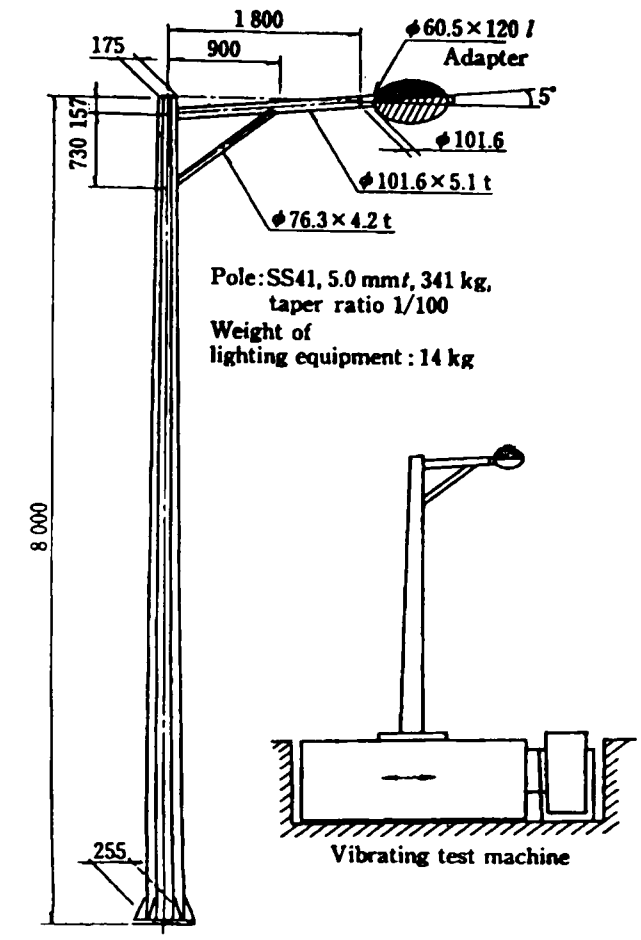

(a)

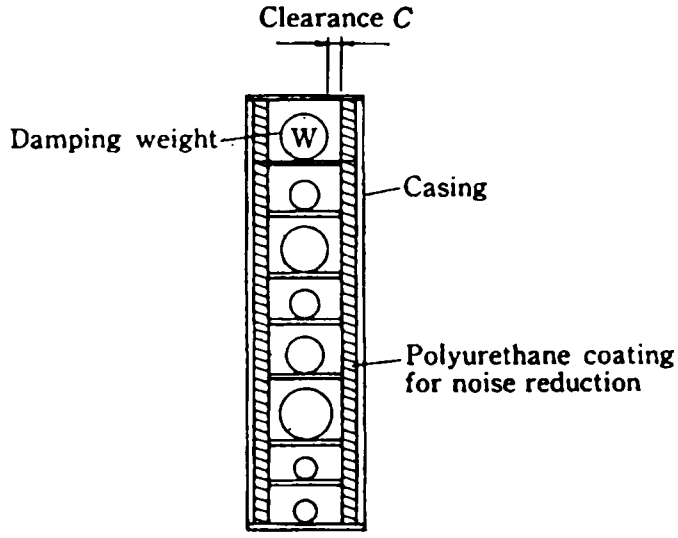

(b)

Figure 1.18: Multi-unit IVA for reducing highway light pole vibration.
(a) Highway light pole and test machine, (b) Multi-unit IVA configuration.
(Jo *et al.*, 1989)

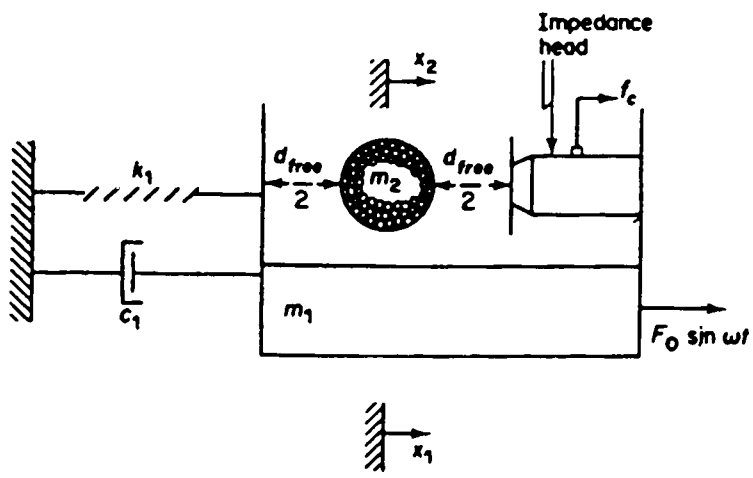

Figure 1.19: Beanbag damper.
(Popplewell and Semercigil, 1989)

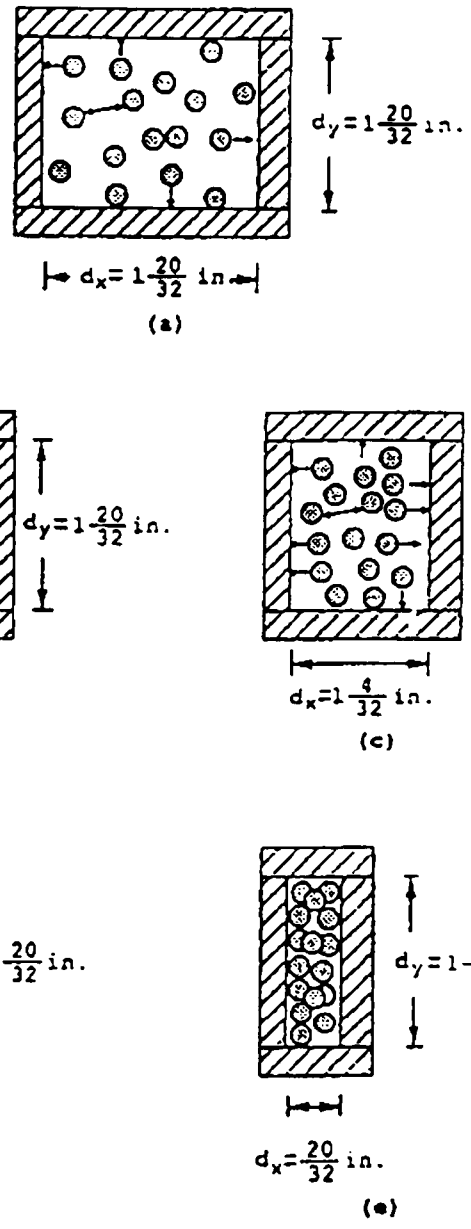

Figure 1.20: Multi-unit IVA with single cavity.

(Papalou and Masri, 1998)

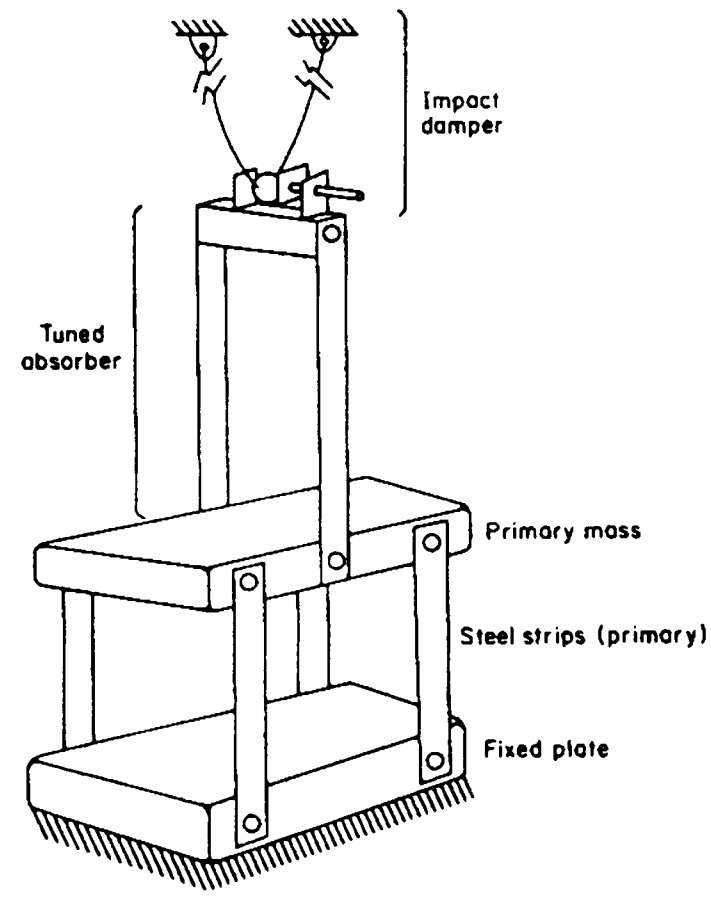

Figure 1.21: Combined IVA-TMA system.

(Ying and Semercigil, 1991)

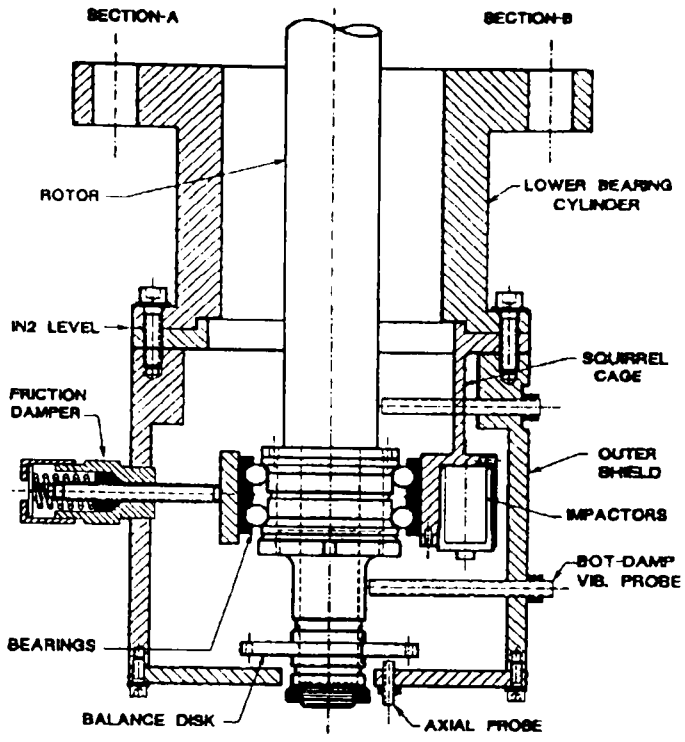

(a)

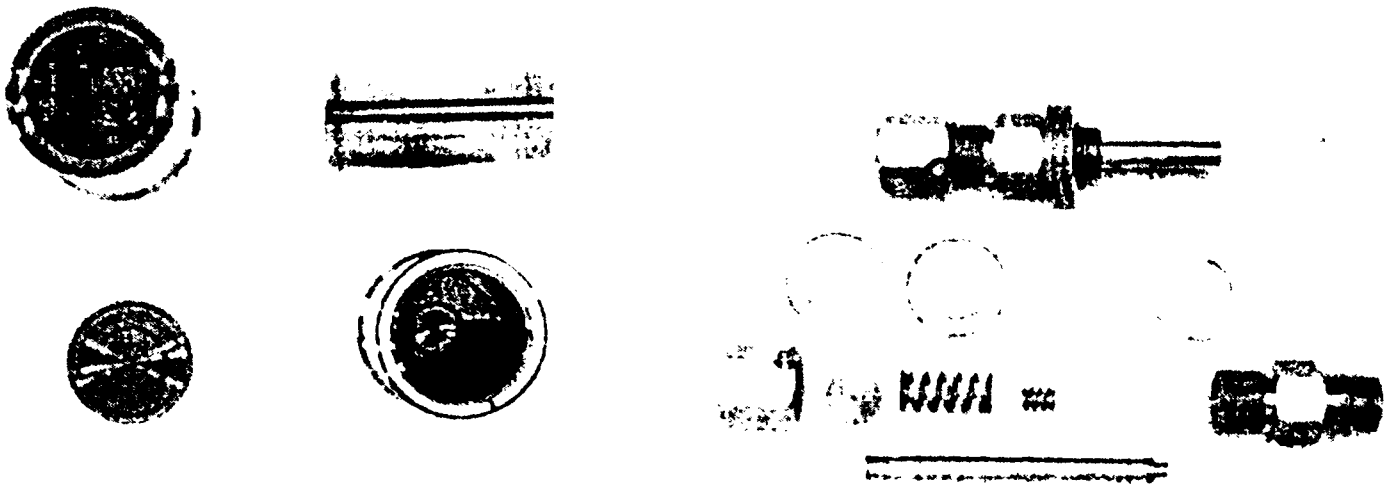

(b) (c)

Figure 1.22: Hybrid friction-impact damper.

(a) Assembly, (b) Close-up of IVA design, (c) Friction damper exploded view.

(Moore *et al.*, 1997)

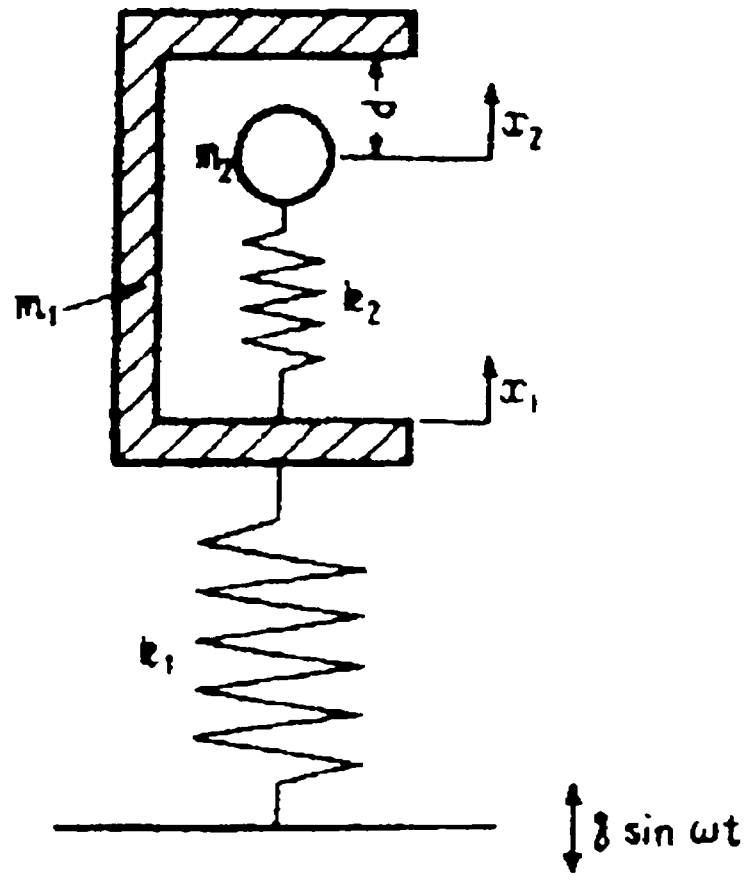

Figure 1.23: IVA with spring-supported mass.

(Kato *et al.*, 1976)

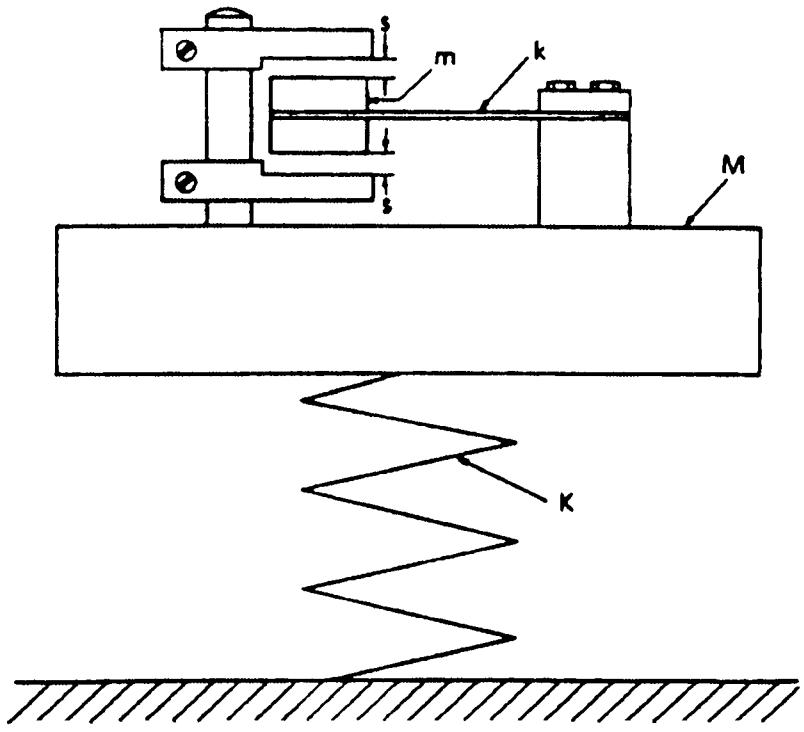

Figure 1.24: IVA connected to the primary mass with leaf spring.
(Fuse, 1989)

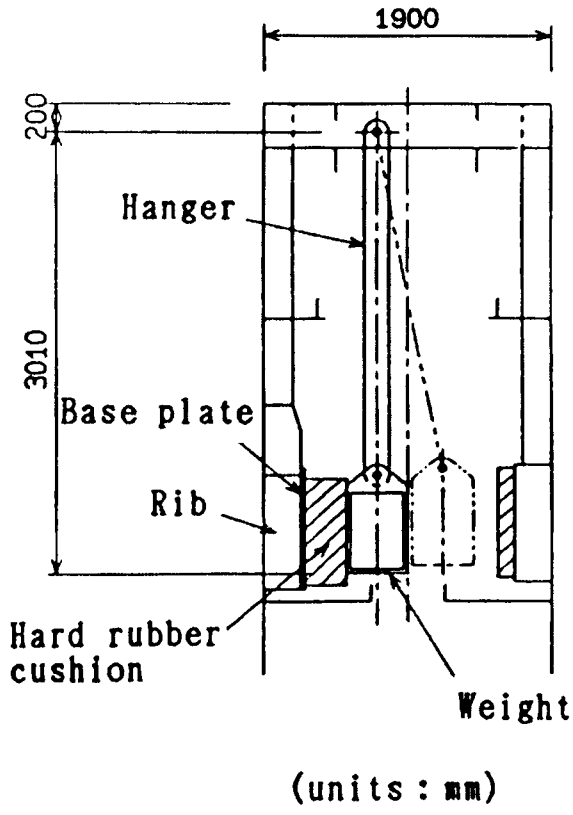

Figure 1.25: IVA for controlling wind-induced excitation.

(Ogawa *et al.*, 1997)

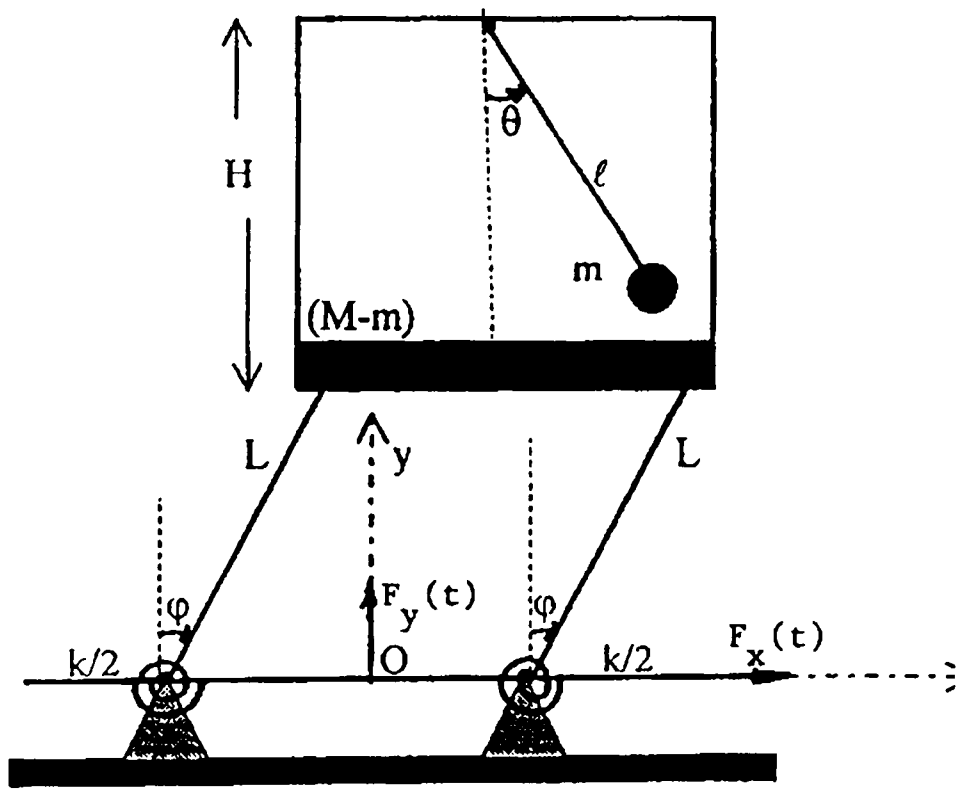

Figure 1.26: Hydrodynamic sloshing impactor.

(El-Sayad *et al.*, 1999)

CHAPTER 2
EXPERIMENTS

2.1 Introduction

The experimental model was designed and built to enable the variation of the parameters to be studied. The experiment setup contains mechanical and electronic components from different manufacturers. Each of these components had to be setup to function properly with one another. Feedback control is utilized to control the shaker. Each set of experiments is run with and without the IVA to gather displacement data in the time domain. The data is later used for studying the absorption and dynamics of the system. The effects of parameters such mass ratio, amplitude of excitation, and clearance are also studied. Three different excitation amplitudes are used to show the effect of the amplitude on the system response, as well as the absorption efficiency and region. Figure 2.1 shows the different experiments done and the parameters that are studied.

2.2 Model

The experimental model (Figure 2.2) consists of two aluminum plates connected with four 1.65 *mm* Thick, 25.4 *mm* wide, and 220 *mm* long steel beams, which function as leaf springs. The lower plate rests on four wheels, and is free to move forward and backward. The shaker is connected to the bottom plate, which can be considered as the base of the primary mass, the top plate. Therefore, when the shaker is excited, base excitation is imposed on the primary mass. There are two L-shaped pieces, on the top plate that act as motion stops. The motion stops are also referred to as walls. The top plate has slots machined through the surface, where the walls are bolted. The clearance between the walls can be adjusted as desired, since the slots enable the bolts to be located anywhere on the plate.

The impact mass, which is referred to as the IVA, connected to an encoder via a pendulum, collides intermittently with the walls and reduces the vibrations of the primary mass. The IVA to be used for preliminary experiments was made of steel. However, since the shaker is electromagnetic, the magnetic field produced by the shaker caused the IVA

to stick to the walls on some occasions. Therefore, a nonmagnetic material was required to isolate the IVA from all magnetic forces. The other considerations for the material selection were that a high-density material was needed in order to obtain the desired mass without making the IVA too large, and the hardness of the material needed to be high enough not to deform the IVA by impacts during operation. Stainless steel was selected as the material, since it combines all the above properties in sufficient proportions. The IVA was designed to provide four mass ratios without changing the diameter. The IVA assembly (Figure 2.3) consists of a main mass of 38.1 mm diameter and mass of 86 g, with a curved circumference, i.e., it is a disc of varying diameter, which can be attached to the secondary masses. The impacts occur on the circumference of the main mass, i.e., the IVA and the walls contact on the circumference of the IVA. Point contact is desired during impacts, instead of line or area contact. Therefore the final design of the IVA was chosen as above, although the prototype IVA was simply a disc, which experienced line contact with the walls. The main mass also has a hole through its center along the diameter, through which the pendulum is inserted in order to attach the IVA to it. The four secondary masses are discs of 33-mm diameter, one pair of which weigh 46 g, and the other pair 93 g. They can be attached to the main mass in 4 different combinations to provide 4 different mass ratios. All the masses, including the main mass, also have two holes through their thickness. Setting pins, each weighing 3 g, are inserted through these holes to hold the masses together. The holes were machined so that the pins fit through them tightly, allowing the omission of setscrews. The pendulum that connects the IVA to the encoder was a hollow carbon rod, which has a relatively high strength to density ratio compared to most other materials that could be used for this purpose, e.g., steel. The carbon rod was used in order to concentrate all the mass of the IVA on the IVA itself, so that we can make a reasonable assumption that the IVA is a free mass moving between the walls. The IVA was connected to the pendulum by using setscrews. However, since the carbon rod was not stiff enough to withstand the pressure applied by the setscrews, a slotted brass sleeve was inserted into the hole of the IVA, and the rod was inserted into the sleeve. In this way, the pressure applied by the setscrews was distributed to a larger area on the rod, and cracking of the rod was prevented. The rod was connected to the

shaft of the encoder in a similar way, utilizing an aluminum connector to translate the rotation of the shaft into translation of the IVA. The length of the carbon rod, and therefore the pendulum, was 211 mm. Since the angular rotation of the pendulum is very small, it can also be assumed that the IVA is translating linearly, rather that rotating about a pivot. A detailed three-dimensional drawing of the experiment layout is shown in Figure 2.4.

2.3 Setup

The experiment setup is shown in Figure 2.5. The setup consists of (a) controller, (b) amplifier, (c) shaker, (d) accelerometer, (e) signal conditioner, (f) primary system, (g) absorber, (h) encoder system, and (i) acquisition and analysis system. Feedback control is used to control the frequency and amplitude of the signal. A personal computer with Data Physics SignalCalc 550 Vibration Controller software is used for this purpose. The drive signal is sent to an MB Dynamics Model S6K Power Amplifier, which drives the shaker. The function of the shaker is to excite the model under investigation with a signal of specified amplitude and frequency content. The shaker used was an MB Dynamics Model C-10 Type E electromagnetic shaker.

An accelerometer mounted on the shaker table provides the feedback signal for the vibration control system. A PCB Piezotronics Model 353B52 accelerometer is used with a PCB Model 480C02 signal conditioner for the experiments without the IVA, while a PCB Model 353B34 accelerometer and a PCB Model 480B10 signal conditioner is used for experiments that include the IVA. The reason for this change is the noise created by the IVA. When the IVA is not in operation, the signal from the accelerometer has a high enough signal-to-noise ratio for using it as the control signal. However, when the IVA is operating, the impacts introduce high frequency noise into the signal, therefore using the acceleration data for control reduces the performance of the controller. The integrating switch on the 480B10 signal conditioner can be used to convert acceleration signal from the accelerometer into low-noise displacement signal. This is expected since integration reduces noise, in a mathematical perspective (Chapra and Canale, 1998). The reason for using different accelerometers was that the 353B34 accelerometer signal is always

recorded in displacement mode to track the driving force. The reason for using different types of signal conditioners was that the 480B10-signal conditioner does not provide enough voltage to power the 353B52 accelerometer. The selected control signal was fed to the controller, while at the same time the shaker displacement signal was recorded by the data acquisition system. The vibration control program uses this feedback signal to keep the shaker displacement within the desired values specified by the user.

The displacement data from the primary mass is obtained by a 350A14 accelerometer and a 480B10 signal conditioner in displacement mode. During the earlier preliminary experiments, a strain-gage and a piezo-film were used to measure the position of the primary mass, but it was later decided that an accelerometer should be used due to reliability and repeatability considerations. However, an MEM Type CEA-06-250UR-350 strain gage installed on one of the steel beams is used to determine the initial displacement applied to the model in transient vibration experiments. The strain gage is connected to a Vishay Measurements Group Model P3500 strain indicator. An optical encoder and an Allen-Bradley digital programmable control system are used to measure the angular position of the IVA. This measurement system produces a voltage proportional to the angular position of the pendulum. The encoder was calibrated in such a way that the voltage is zero when the pendulum is in the downward vertical position. The voltage increases linearly with the rotation angle from 0 to 10 V, as the pendulum turns clockwise, until it reaches the vertical upward position. Turning it clockwise from the vertical upward to the downward position, the voltage changes from –10 to 0 V. In other words, the voltage is negative to the right of the vertical axis and positive to the left. Details about this measurement system can be found in the article by Ertas and Mustafa (1992). The displacement data is recorded by a personal computer equipped with a National Instruments model SCB-68, AT MIO-16E-2 data acquisition board, using National Instruments LabVIEW 5.1 software.

A jig is built to suspend the encoder and the IVA from above the top plate. The jig is designed in a way to accommodate different pendulum lengths; however, it was decided that the pendulum length would not affect the results significantly, and a single pendulum is used in all experiments. The jig is also designed in a rigid manner so that it

is not affected by vibrations. The two screw at the bottom of two legs allow the adjustment of the length of those legs, which enables adjusting the jig to stand in a vertical position.

2.4 Controlling the Shaker

2.4.1 Feedback Control

As stated in the previous sections, the control signal is chosen as displacement or acceleration, for different experiments. This is done because the controller performs better using different signals for different experiments. The reason for the difference in performance is related to the coherence, which will be discussed in section 2.4.2.

Constant displacement mode is selected for all forced vibration experiments. Therefore, the controller operates to keep the zero-to-peak value of the shaker table displacement at the desired value that is input to the program. The controller calculates the acceleration value that should be produced by the specified zero-to-peak displacement during the period of the specified sine wave. This is the desired acceleration value that the controller tries to establish. The controller then compares the feedback signal with the desired value, and adjusts the driving volts to keep the feedback signal as close as possible to the desired signal. The controller always uses acceleration for comparing the signals, i.e., even though the feedback signal is displacement, it is converted to acceleration first for comparing with the desired acceleration. Further details about the control system may be found in the manuals (Data Physics Corporation, 1999).

2.4.2 Coherence

For pairs of random records from two different stationary random processes, coherence function is an important joint statistical property. The coherence function is a measure of the accuracy of the assumed linear input/output model, and can also be computed from the measured auto spectral and cross-spectral density functions, $G_{xx}(f)$ and $G_{xy}(f)$, respectively. The coherence function $\gamma^2_{xy}(f)$ of two quantities x(t) and y(t) is the ratio of the square of the absolute value cross-spectral density function to the product of the auto spectral density functions of the two quantities:

$$\gamma^2_{xy}(f) = \frac{|G_{xy}(f)|^2}{G_{xx}(f)G_{yy}(f)} \quad .$$

For all f, the quantity $\gamma^2_{xy}(f)$ satisfies $0 \leq \gamma^2_{xy}(f) \leq 1$, i.e., the coherence is bounded by zero and unity. This ordinary coherence function measures the extent to which y(t) may be predicted from x(t) by an optimum linear least squares relationship (Bendat and Piersol, 1986).

A zero value means there is no linear dependence and a value of unity means there is a perfect linear dependence between the signals at the frequency f. A coherence value that is less than unity at one or more frequencies is usually indicative of one of the following situations (Piersol, 1992):

1. Noise is present in the measurements.
2. The frequency resolution of the frequency spectrum is too wide.
3. The relation between y(t) to x(t) is dependent on time.
4. The relation between y(t) and x(t) is not linear.
5. The output y(t) depends on other inputs as well as x(t).

2.4.3 Controllability

In the case of controlling the shaker, the input refers to the driving volts supplied by the controller to the shaker, while the output refers to the actual displacement of the shaker table, which is fed back to the controller as the feedback signal. For all systems utilizing feedback control, there needs to be a relation between the input and the output for the control to work efficiently. The stronger this relation, the higher the coherence and vice-versa. A stronger relation, i.e., higher coherence will enable better control. The coherence value varies between 0 and 1. A coherence of 0.5 means that there is a 50% probability that the feedback control system will be able to control the system. For every type of experiment, e.g., with/without IVA, sweep/dwell, the feedback signal was chosen as displacement or acceleration, so that the coherence was as high as possible.

2.5 Experimental Procedure

2.5.1 Introduction

The natural frequency of the primary system was tuned while the absorber was not in place. The primary mass is given an initial excitation and let to oscillate freely, while the displacement data is recorded for 10 seconds. By using a power spectral density (PSD) program written in LabVIEW, the natural frequency of the model was obtained. For this study the natural frequency was adjusted to 9 Hz, by changing the stiffness of the system. The stiffness was adjusted by making use of the formula $w_n = (k/m)^{1/2}$. For a leaf spring (steel beam), the stiffness increases by decreasing length, and vice versa.

Since the amplitude of excitation was in the order of 0.25 mm, the distance between the walls need to be measured very precisely. For this purpose, a telescoping gage and a micrometer were used. The walls were installed in such a way that the impact surfaces were parallel to each other but perpendicular to the direction of motion of the IVA. This and the curved surface of the IVA assure perpendicular point contact during the impacts.

The desired mass ratio was obtained by assembling the IVA as required. When experiments without the IVA are to be conducted, the IVA was elevated above the walls by moving the encoder higher along the jig.

A data acquisition rate of 70 scans/sec was used to acquire data. This rate was selected due to the speed involved in the dynamics of the system, as well as the sensitivity of the encoder. The scan rate was also set to avoid antialliasing. The encoder sends 2048 pulses per revolution of its shaft, therefore the smallest angle it can measure is 360/2048 degrees. Since the pendulum is forced to move at around 9 Hz throughout the experiment, higher scan rates cause data points to be at the same level, e.g., 1 V of voltage at two consequent data points although the pendulum has rotated slightly, but the rotation is not enough for the encoder to give a different signal.

2.5.2 Transient Vibration

Transient vibration experiments were done by applying an initial displacement to the primary mass. The same initial displacement was applied to the system, with and without the IVA, by using the strain gage. The primary mass was displaced from its equilibrium position by pulling it, until the desired value was read from the strain indicator, and the system was let to oscillate. Four displacement initial displacements were applied to the system, while four clearances and four mass ratios were used. The parameters that are used are shown in the table in the appendix.

2.5.3 Forced Vibration

2.5.3.1 Introduction

Feedback control is utilized for all the forced vibration experiments. For every such experiment, the frequency and displacement content of the desired shaker displacement signal is input to the program. Dwell (constant frequency) and sweep (varying frequency) experiments are conducted. The non-dimensional frequency ratio is obtained by dividing the excitation frequency by the natural frequency of the primary mass, which is 9 Hz. The frequency range of interest is 8.7 to 9.3 Hz, which corresponds to a non-dimensional frequency ratio range of 0.967 to 1.033. The frequencies where data was collected is seen in the table in the appendix. A smaller frequency increment was used around resonance and jump points.

2.5.3.2 Sweep

The frequency of excitation is swept in both directions, namely, upsweep and downsweep. The sweep rate was chosen as 0.001 Hz/sec, which is the lowest sweep rate the control system supports. The system is let to dwell at the starting frequency for 20 seconds, until it reaches steady state before the sweep starts and data is collected.

2.5.3.3 Dwell

For constant frequency experiments, the dwell option of the controller is chosen to specify the dwell frequency and the duration of the dwell. All the dwell frequencies are

programmed in sequence, so that when one measurement for one frequency is taken, the controller ramps down the drive, stops the shaker completely, and then ramps up at the next frequency.

The data for each discrete frequency value is recorded for 25 seconds after the system has been excited with the same frequency for at least 15 seconds. This initial time is necessary for the system to reach steady state before data is taken. To determine the time the system needs to reach steady state, the real time data is analyzed while the experiment is running, and the system is assumed to have reached steady state when three consecutive sets of data show the same trend, i.e., when the displacement amplitude reaches a constant value.

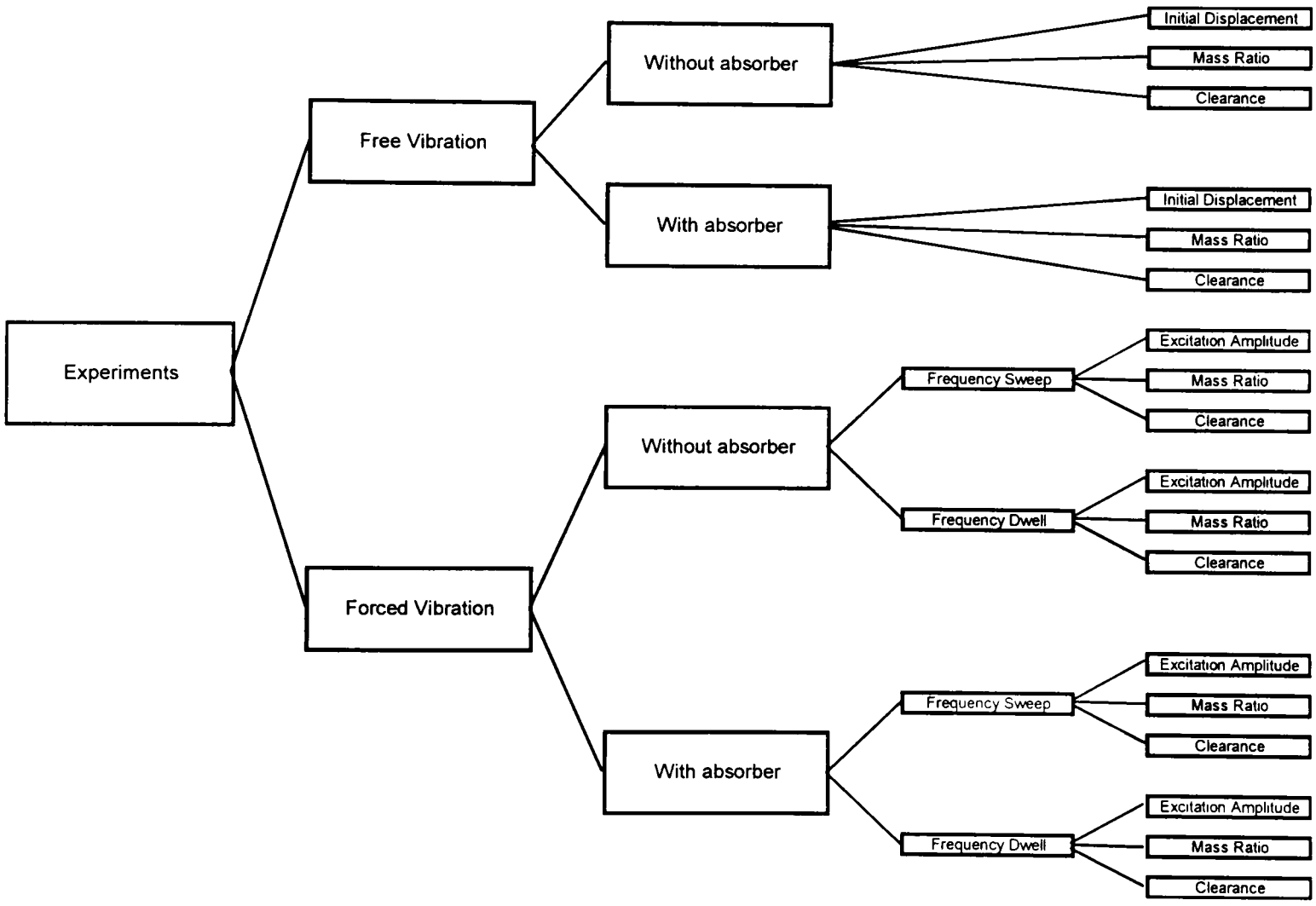

Figure 2.1: Experiments done and parameters studied.

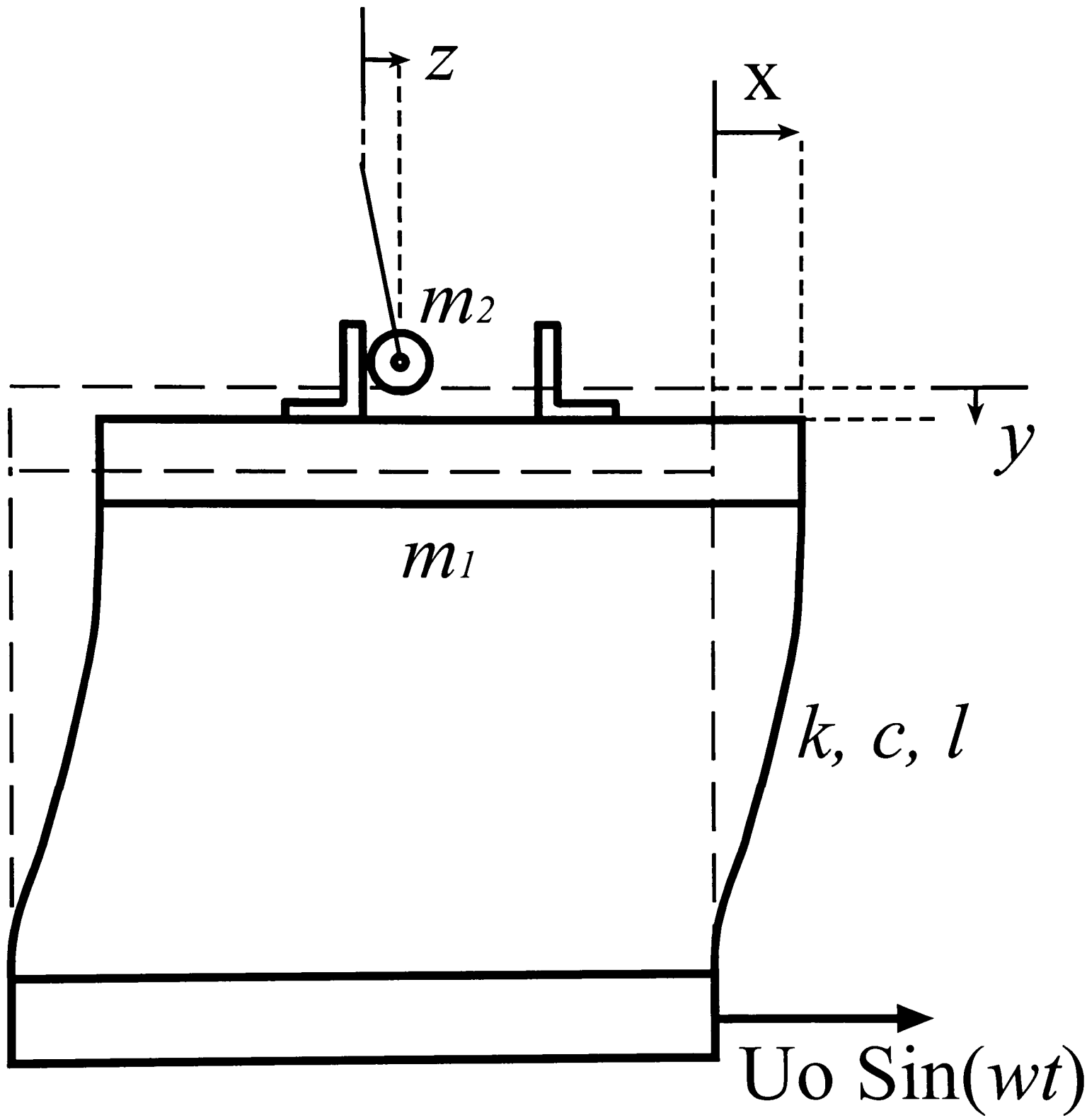

Figure 2.2: Model.

Figure 2.3: IVA assembly.

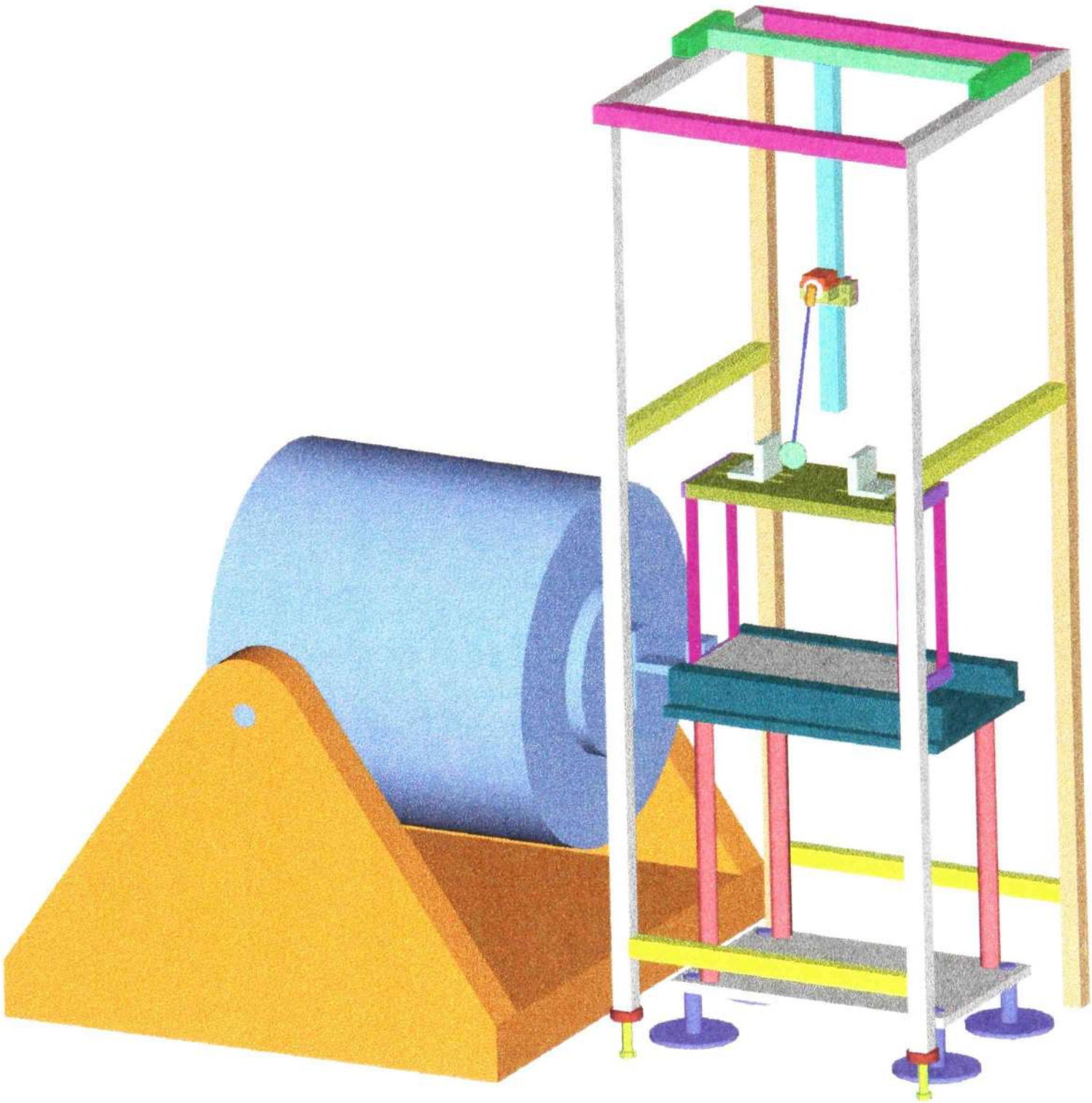

Figure 2.4: Experiment layout.

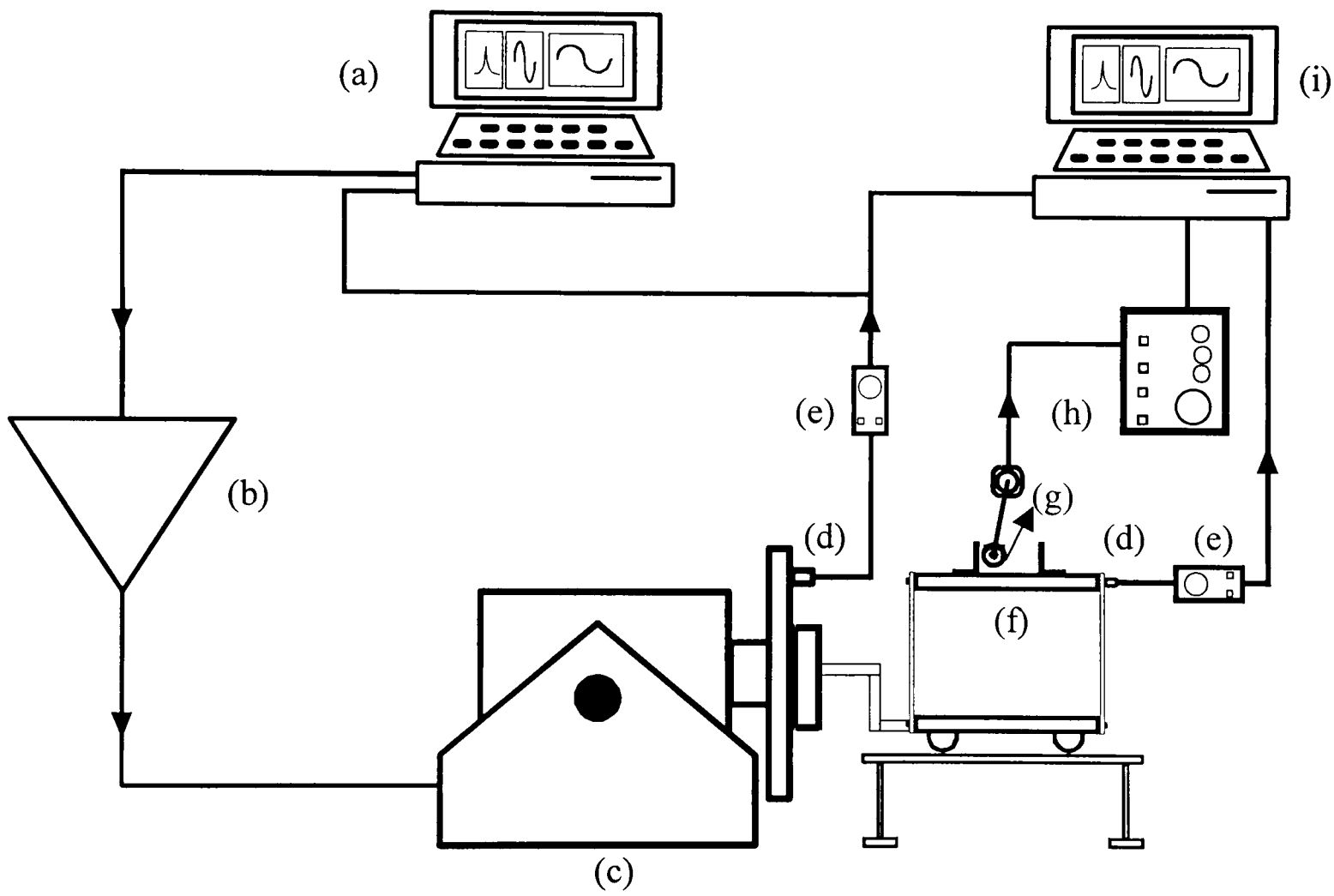

Figure 2.5: Experiment setup.

CHAPTER 3
RESULTS AND DISCUSSION

3.1 Introduction

In all plots, the parameters used to get the data is illustrated by the legend. Transient vibration experiments can be with or without the IVA, and the data is illustrated by the legend as w/o IVA-ID or MxCx-ID, respectively, where the term w/o IVA means without IVA, ID stands for initial displacement, the x's in Mx and Cx are the mass ratio and clearance of the IVA, hence the presence of Mx means the IVA is in operation. The initial displacement is the strain applied to the steel beams, in microstrains, e.g., if the number shown is 400, the initial displacement applied to the primary mass causes a strain of 400 microstrains. A Stands for amplitude, M stands for mass, or mass ratio, and C stands for clearance. The data is organized in such a way that A4>A3>A2>A1, M4>M3>M2>M1, and C4>C3>C2>C1. The values for these parameters that were used for the experiments are shown in Appendix. Forced vibration experiments are organized in a similar manner, except that the amplitude of excitation is shown by an additional parameter, A.

Displacement values are the voltage values read by the data acquisition board. Since the transducers' output is a linear function of displacement, the data is qualitative, even though it is not quantitative.

3.2 Transient Vibration

3.2.1 Linear vs. Exponential Decay

The time series displacement data of the primary mass without the absorber is shown in Figure 3.1. The data depicts the characteristic decay of damped systems under free vibration. Using the LabVIEW program utilizing power spectral density analysis, the natural frequency of the primary mass is seen to be 9 Hz (Figure 3.2), since there is a peak at 9 Hz.

A typical time series data for transient vibration is shown in Figure 3.3. The black line represents the position of the primary mass in the absence of the IVA, while the red

line represents the position of the primary mass when the IVA is operating. It is observed that in the latter case, the vibrations are reduced much faster compared to the case without the IVA, due to faster energy dissipation. When the IVA is not in place, the slow decay is a result of the internal damping in the system.

A LabVIEW program was used to locate the maximum displacement points in a data file. Figure 3.4 shows these points for the first 11 seconds of motion, for the cases without and with the IVA. Fitting curves to the peak points proves that for the case without the IVA, the decay is exponential, whereas for the case with the IVA the decay is linear until the vibrations of the primary mass go below a certain level that impacts are not observed anymore. This result is in agreement with the results presented by Bapat and Sankar (1985). The damping inclination formula proposed by the authors is related to the slope of the line, for the cases with the IVA. In this case, the higher the absolute value of the slope, the steeper the line, the higher the damping inclination, and faster the attenuation of vibrations.

3.2.2 Parametric Studies

Figure 3.5 shows the results for transient vibration experiments for studying the effect of mass ratio, while all other parameters are kept constant. It is seen that a higher mass ratio causes faster absorption, since the slope of the line increases as the mass ratio is increased. This result is also consistent with the results of other researchers (Bapat and Sankar, 1985; Chen and Semercigil, 1993; Ema and Marui, 1994).

The effect of clearance is shown in Figure 3.6, while all other parameters are kept constant. It is seen from the equations of the best fit lines that the fastest absorption corresponds to the largest clearance, but this trend is not consistent with the other clearance values, e.g., the absorption corresponding to C2 is better than that of C3. Similar results were reported by Bailey and Semercigil (1994), and Araki *et al.* (1989). In this case, more clearance values need to be studied to make conclusions.

The effect of initial displacement on the rate of decay is presented in Figure 3.7. Four experiments were done with the same mass ratio and clearance, while initial displacement was changed for each case. It was observed that higher initial displacements

result in faster vibration attenuations. This may be attributed to the severity of impacts when the initial displacement is higher. Since the spring force is directly proportional to the initial displacement, the primary mass may gain more speed, resulting in a higher relative impact speed. From the theory of impact, coefficient of restitution, which effects the amount of energy dissipated by an impact, depends on the velocities of the bodies at the instant of impact (Babitsky, 1998). The change in coefficient of restitution may cause faster attenuations.

3.3 Forced Vibration

3.3.1 Time Series Data

A sample of time series data for the shaker, the primary mass and the IVA is shown in Figure 3.8, for an excitation amplitude of 0.254 mm, clearance of 2.112 mm, mass ratio of 0.193 and excitation frequency of 9 Hz. The voltage signals from the transducers connected to the latter two are multiplied by 10, to display the signals on the same graph. The reason for the large amplitude of the shaker signal is due to the high sensitivity of the accelerometer used to control the shaker. From the nature of operation of the IVA, it requires impacts to change its direction of motion. The instants of impact of the IVA can be located as the highest and lowest points on the time series data. Observation of this graph reveals that there are two impacts per cycle of excitation. Masri and Caughey (1966) studied this type of motion theoretically and stated that two impacts per cycle motion is necessary for the stability of the system. Further observation of Figure 3.8 reveals that there is a phase difference between the displacement of the shaker and the primary mass. This is due to the leaf spring connecting the base and the primary mass.

3.3.2 Motion Plot

Although Kato *et al.* (1976) and Popplewell and Semercigil (1989) have used non-contact displacement transducers to measure the position of a compound and a multi-unit IVA, respectively, this study is the first one to show the position of the impact mass of a single-unit IVA experimentally. The motion of the IVA is presented in Figure 3.9.

where the two-impacts-per-cycle motion can be observed. Since the impact mass is smaller than the primary mass, impacts cause the impact mass to change direction, while the velocity of the primary mass is reduced. The primary mass also changes direction after the impacts, but this is due to the cyclic characteristic of vibrations.

3.3.3 Frequency Response Plots and Parametric Studies

Figure 3.10 shows the amplitude of vibrations of the primary mass without the IVA, and with the IVA for four different impact masses. The curve for the case without the IVA shows the traditional trend of vibratory systems around resonance, reaching a maximum at natural frequency. As in the case of transient vibration, a higher mass ratio provides better absorption. This result is consistent by the results reported, among others, by Roy *et al.* (1975), and Popplewell and Liao (1991).

For cases when the IVA is active, the non-dimensional displacement ratio is obtained by dividing the displacement of the system with the IVA, with the displacement of the system without the IVA. Similarly, dividing the forcing frequency by the natural frequency of the model establishes the dimensional frequency ratio r.

Figure 3.11 shows the effect of mass ratio on the amplitude ratio. As stated above, a higher mass ratio increases the attenuations. The absorption is best around resonance, and absorber effectiveness diminishes as the excitation frequency moves away from the natural frequency. In addition, the IVA amplifies the vibrations in some cases, i.e., the amplitude ratio may go above 1. These results are in agreement with the results published by Roy *et al.* (1975) and Popplewell and Liao (1991). In addition, the trends of the curves are similar to the ones in the aforementioned studies.

The effect of clearance on the displacement ratio is presented in Figure 3.12. From the four different clearances studied, C3 shows the best performance, followed by C2 and C1. C4, which is the largest clearance, attains the worst absorption. This is because of the fact that the clearance in this case is too large for the system to reach steady state and perform two impacts per cycle motion.

Figure 3.13 shows the excitation levels as measured by the control accelerometer located on the shaker table. It is observed that the system controls the shaker within desired accuracy limits.

The effect of excitation amplitude on displacement ratio is shown in Figure 3.14. The excitation amplitude A3 offers the best performance along the frequency range of interest. The performance with A4 is better than A2 and A1, except for $r<0.94$. The excitation amplitude A2 shows better performance than A1. These results suggest that, for constant clearance, the performance of the system for a certain excitation amplitude differs along the frequency spectrum, i.e., a different excitation amplitude is most efficient in different regions. However, it is not possible to change the excitation amplitude in real systems where vibration is a problem, i.e., the aim in using absorbers is to reduce the amplitude; therefore the clearance may be changed to improve performance in some cases.

Figure 3.15 shows the frequency response plots for upsweep, without the IVA. For two different excitation amplitudes, the shape of the curve is similar even though the jump phenomenon (Nayfeh and Mook, 1979) and maximum amplitudes are observed at different frequencies. The same behaviors are observed for downsweep (Figure 3.16).

The effect of mass ratio is also studied by sweep experiments. For both upsweep (Figure 3.17) and downsweep (Figure 3.18), IVA efficiency is best around resonance, and diminishes as excitation frequency moves away from the resonant frequency. As in the case of dwell experiments, higher mass ratio enables better absorption. For the smallest mass ratio M1, the shape of the response curve with the IVA is similar to the shape of the response curve without the IVA, except that the peak point of the curve has shifted to a lower frequency. This behavior is similar to the case of tuned-mass absorbers where the primary mass and the absorber are coupled, and the introduction of the absorber dislocates the resonant amplitudes (Iemura, 1994). A similar peak in response may also be observed at a higher frequency. In general, the shapes of the response curves are similar to those presented in previous studies (Masri, 1969; Masri, 1973; Roy *et al.*, 1975; Chatterjee *et al.*, 1996)

The frequency response plots obtained from dwell and sweep experiments are presented together in Figure 3.19. This data was obtained for the highest excitation amplitude A4, and the highest mass ratio M4. Jump phenomenon is observed at different frequencies for upsweep and downsweep. Also, the dwell data seems to correspond with the downsweep data. Absorption is observed, and it is seen that the IVA generally keeps the amplitude of vibration below a certain level, when the impact mass is large enough.

3.3.4 Coherence Measurements

The coherence measurements were done for the same conditions stated above (Figure 3.20). As stated in Section 2.4.2, coherence is a measure of the linear relationship between two signals, e.g., input and output of a system, and is measured on a scale of 0 to 1. For a vibratory system, the excitation can be considered as the input to the system, while the response can be considered as the output. For such a system, around resonance, the response of the system reaches very high amplitudes regardless of the level of excitation. This causes coherence to drop, since the output of the system is greatly exaggerated. However, for the same excitation level, the response of the system is considerably lower as excitation frequency moves away from natural frequency, and therefore coherence is higher. When the IVA is introduced to the system, since the high amplitudes of vibration around resonance are absorbed, coherence goes up to approximately 1. Although coherence was first studied to measure the performance of feedback control, it is shown that it can be used to determine absorption, and possibly vibration absorber efficiency. Furthermore, comparing Figure 3.19 and Figure 3.20 reveals that the frequencies where coherence is lowest for both upsweep and downsweep (Figure 3.20) corresponds to the frequencies where the jump phenomenon is observed in the frequency response curves (Figure 3.19).

3.3.5 Phase Portrait

Figure 3.21 shows the phase portrait of the IVA signal. In this case, all parameters are kept constant and measurements are taken at two different dwell frequencies. It has been shown before that the performance of the IVA is highest around resonance, and

drops as excitation frequency moves away from the natural frequency of the system. It is observed from the figure that for the case of efficient absorption (8.98 Hz), the motion of the IVA is periodic and symmetric, and it has reached steady state. On the other hand, when the efficiency diminishes, the displacement and velocity of the IVA is higher, and the motion is observed to be somehow periodic, but unstable (8.69 Hz). Therefore, the theoretical results by Masri (1969) have been proven experimentally.

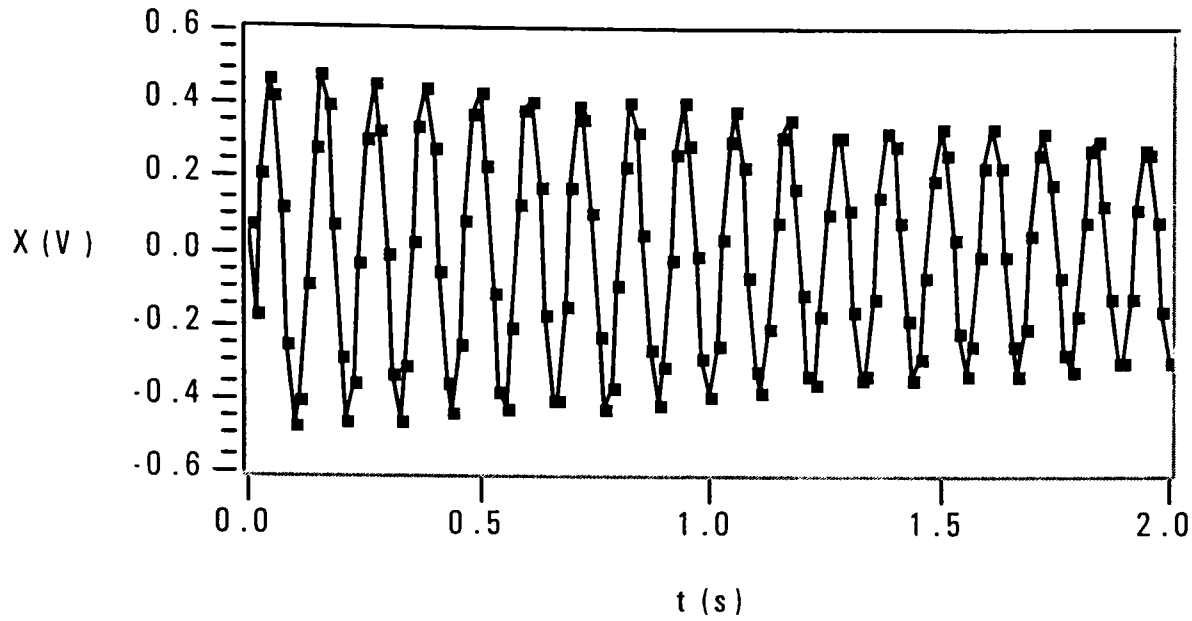

Figure 3.1: Transient vibration without IVA-time series.

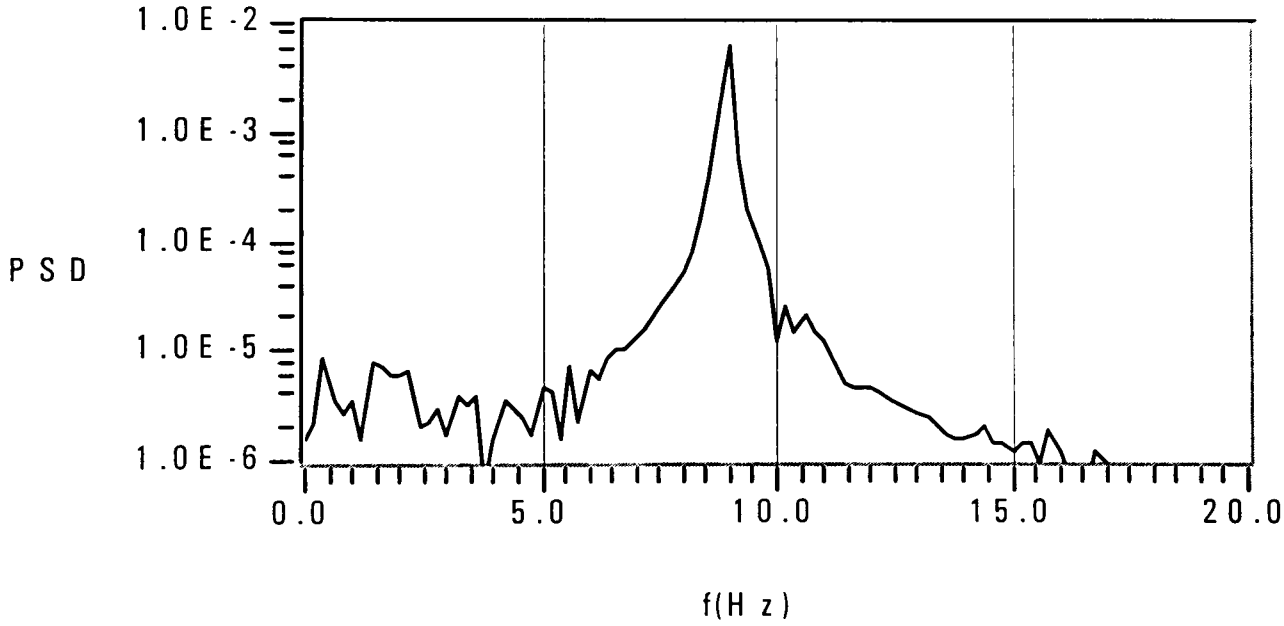

Figure 3.2: PSD of time series.

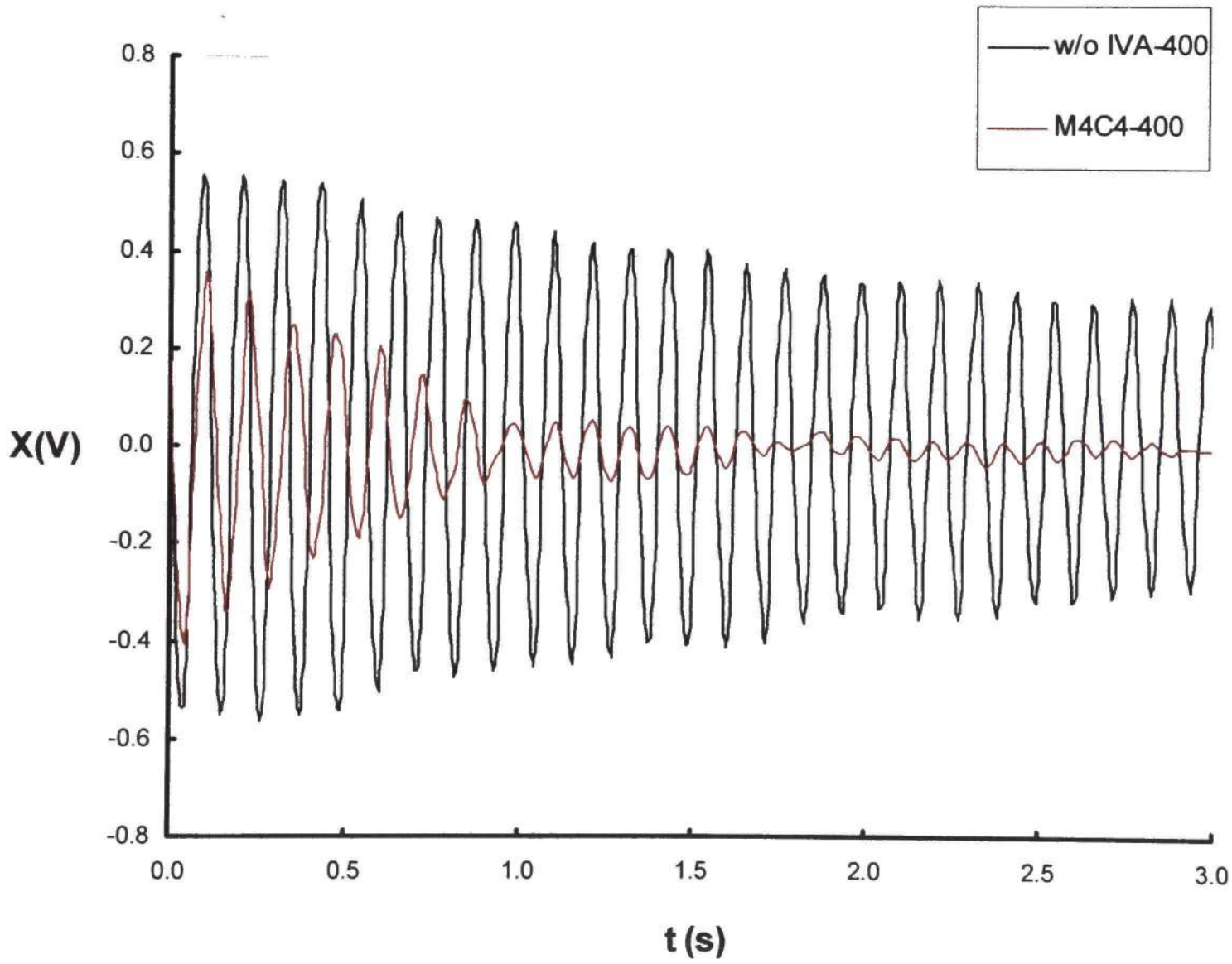

Figure 3.3: Decay of transient vibration with and without the IVA

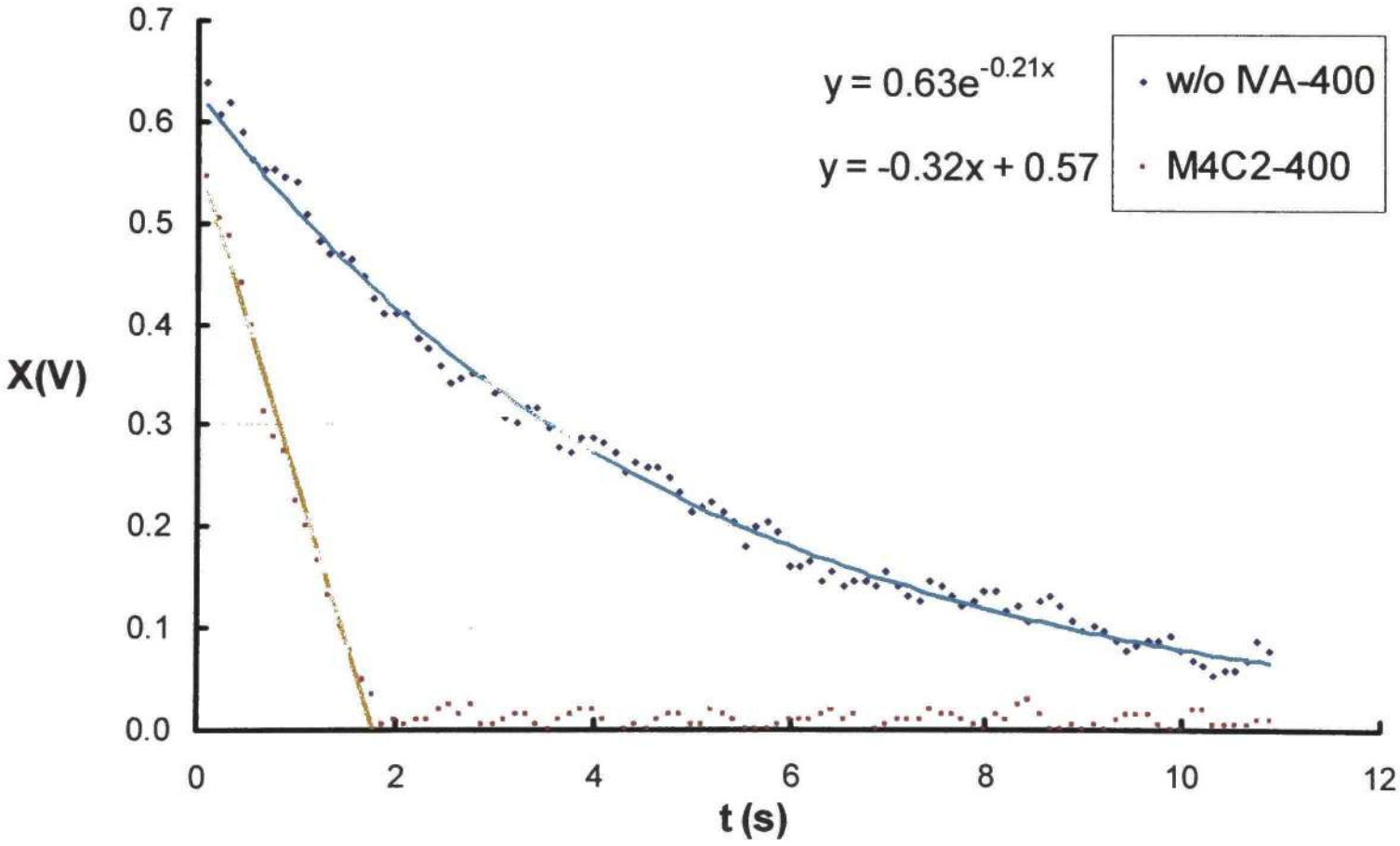

Figure 3.4: Exponential and linear decay

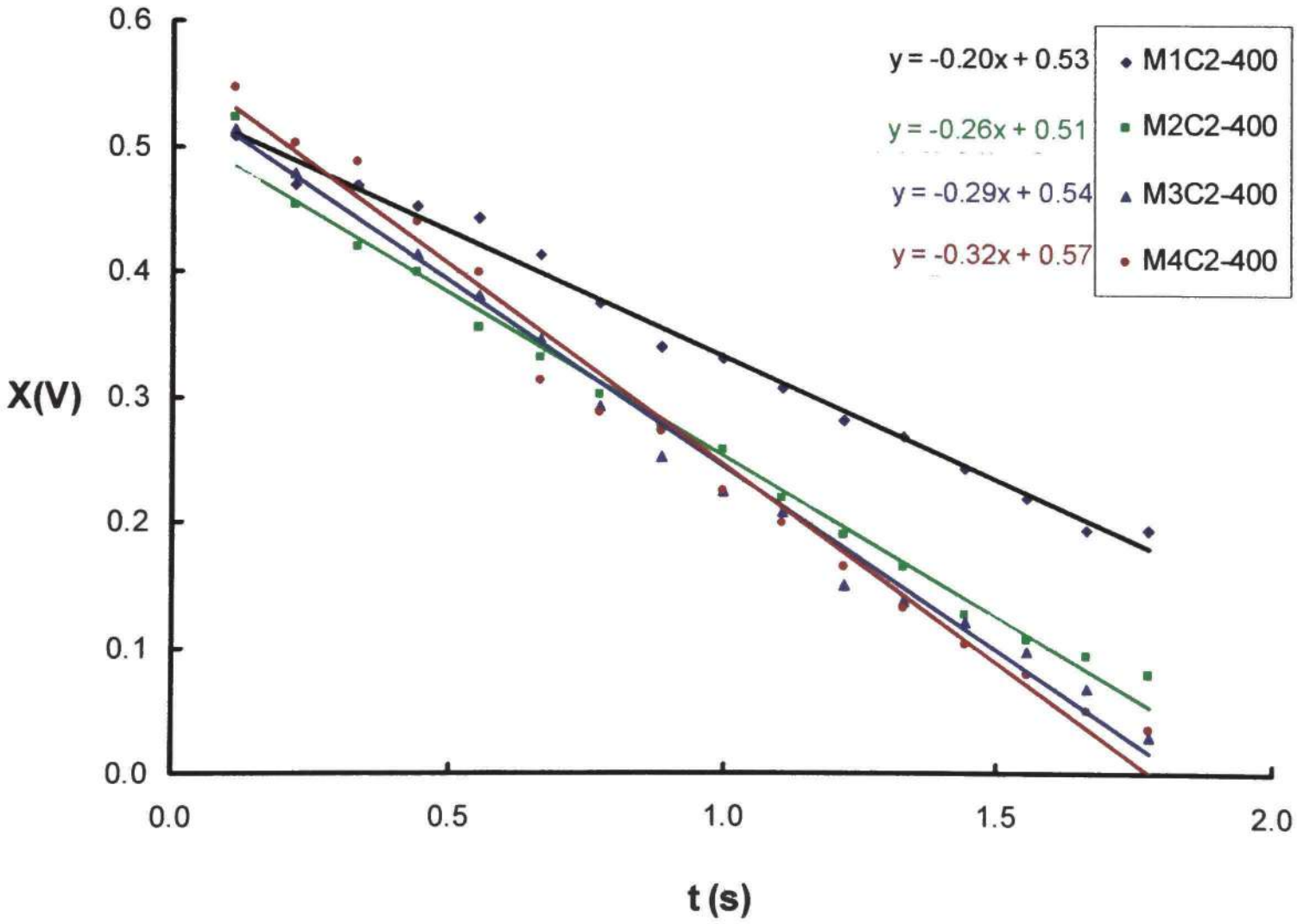

Figure 3.5: Effect of mass ratio on rate of decay

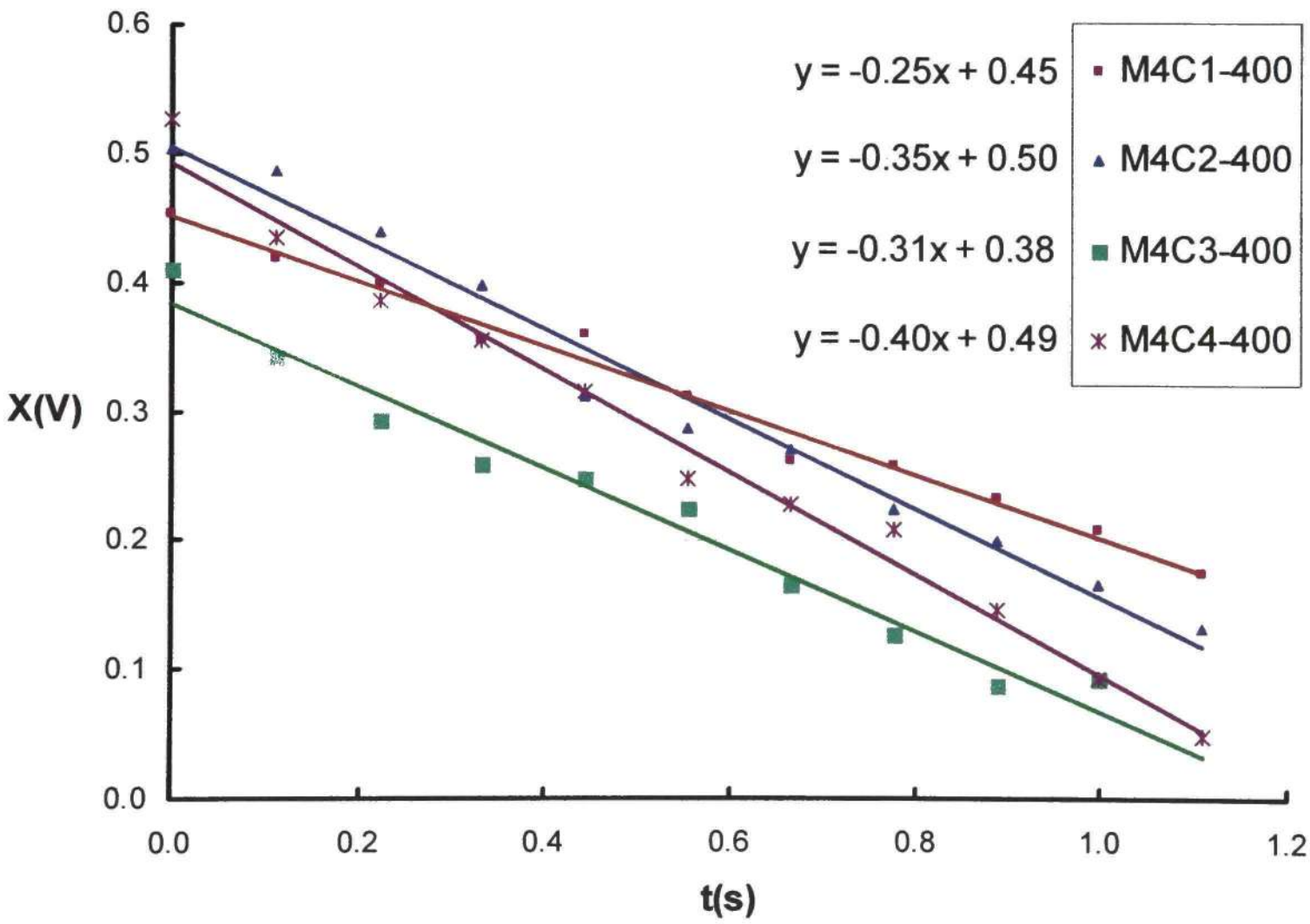

Figure 3.6: Effect of clearance on rate of decay

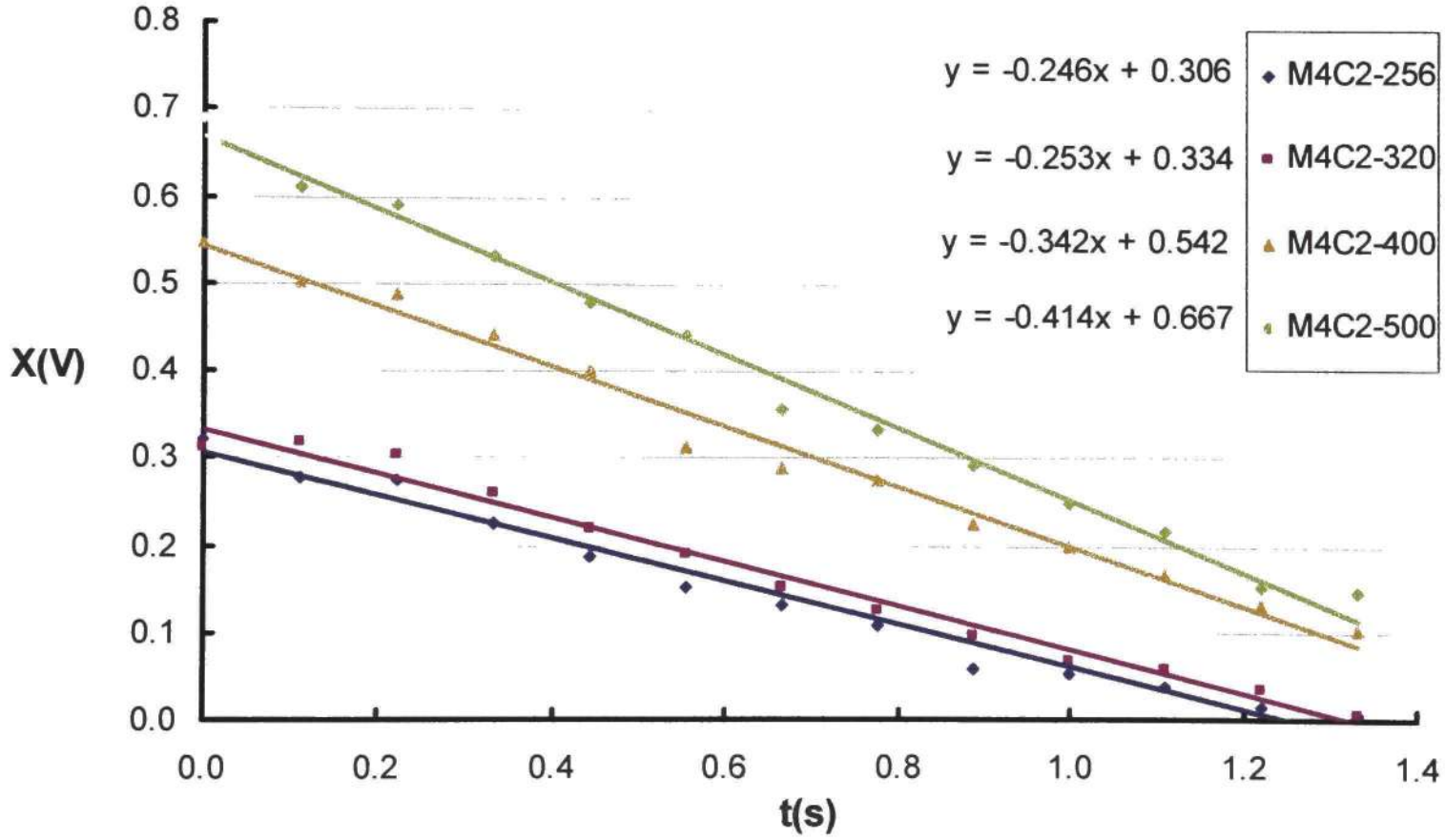

Figure 3.7: Effect of initial displacement on rate of decay

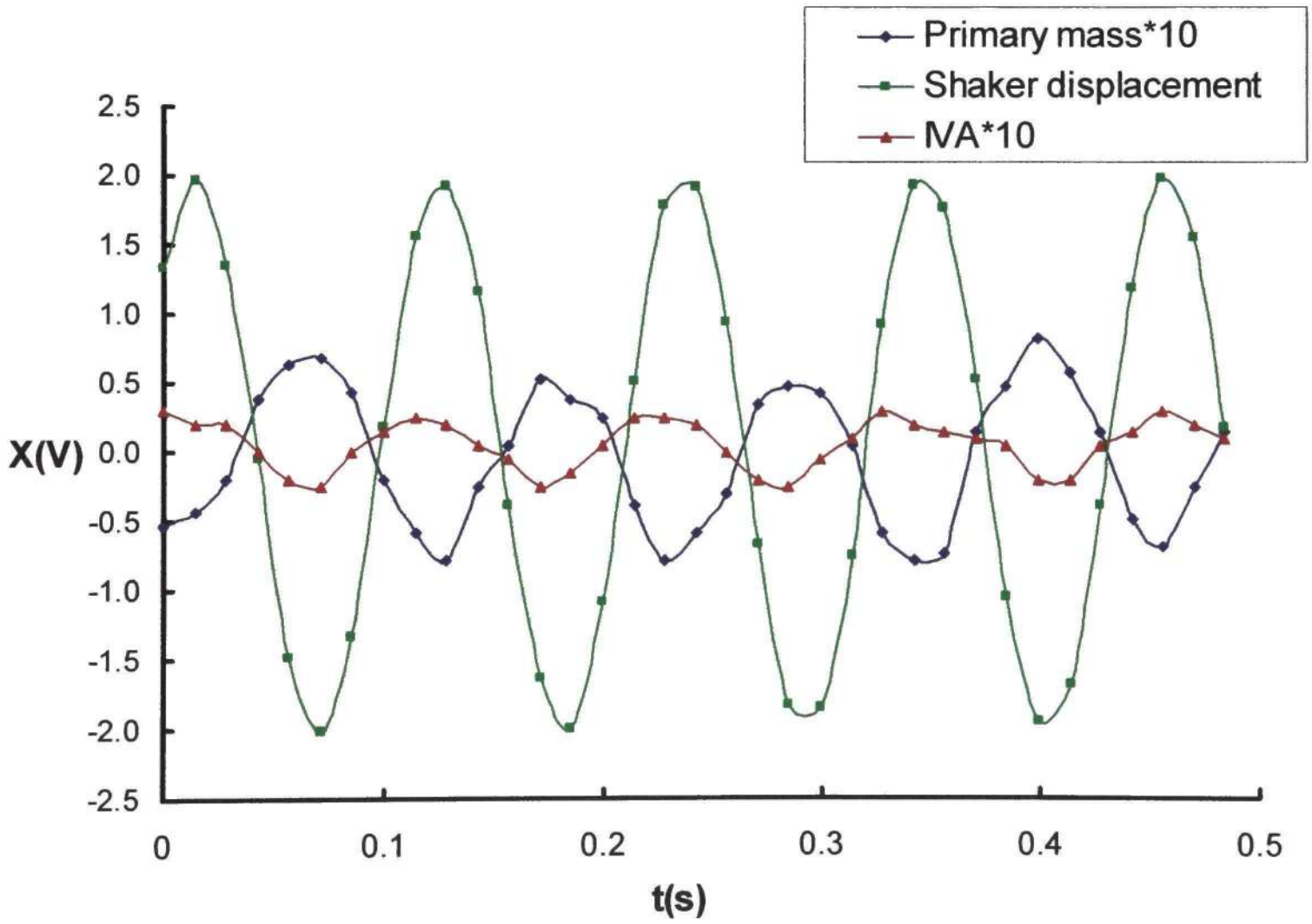

Figure 3.8: Time series data for A=0.254 mm, d=2.112 mm, μ=0.193, f=9 Hz

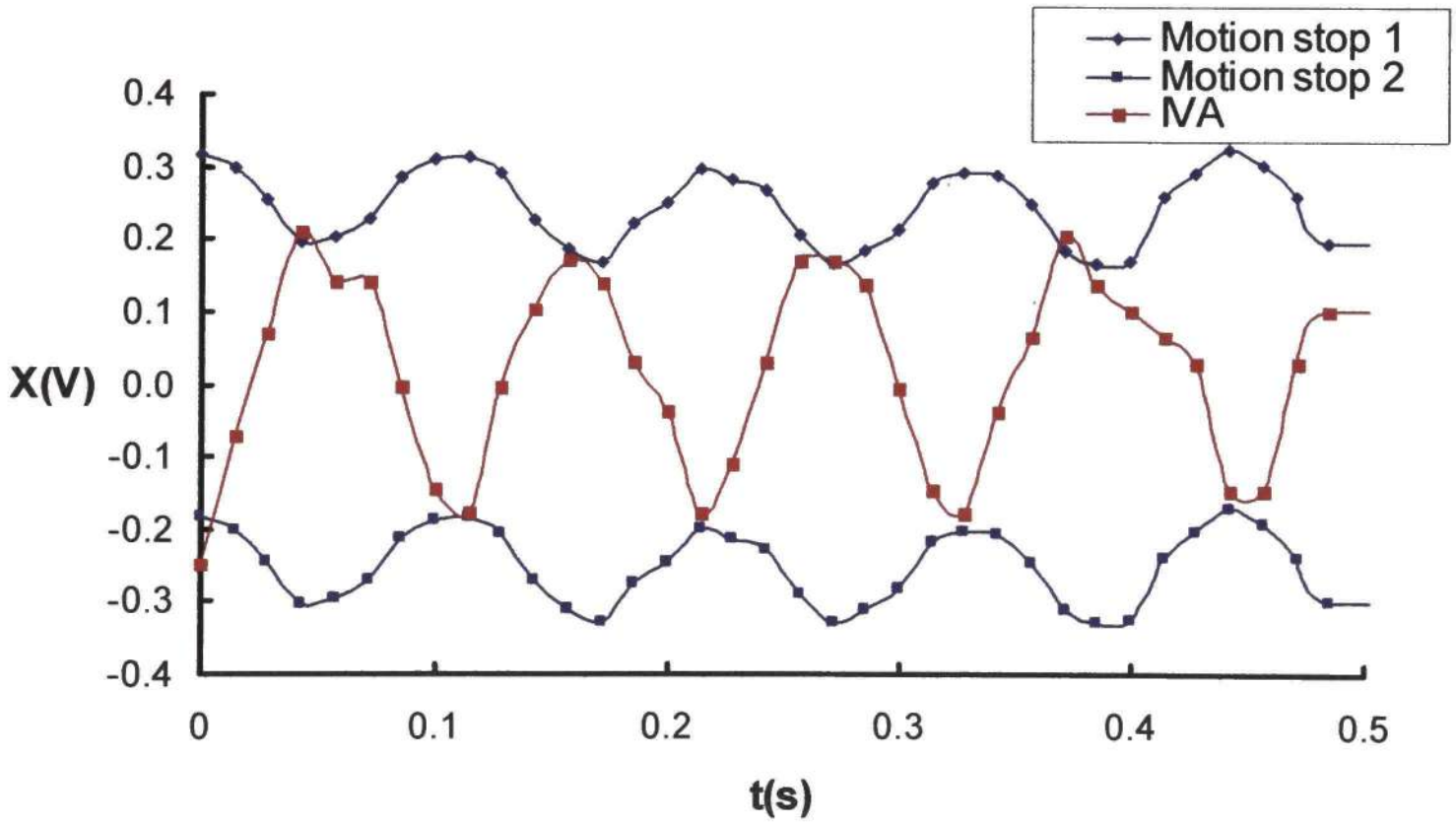

Figure 3.9: Motion Plot for A=0.254 mm, d=2.112 mm, μ=0.193, f=9 Hz

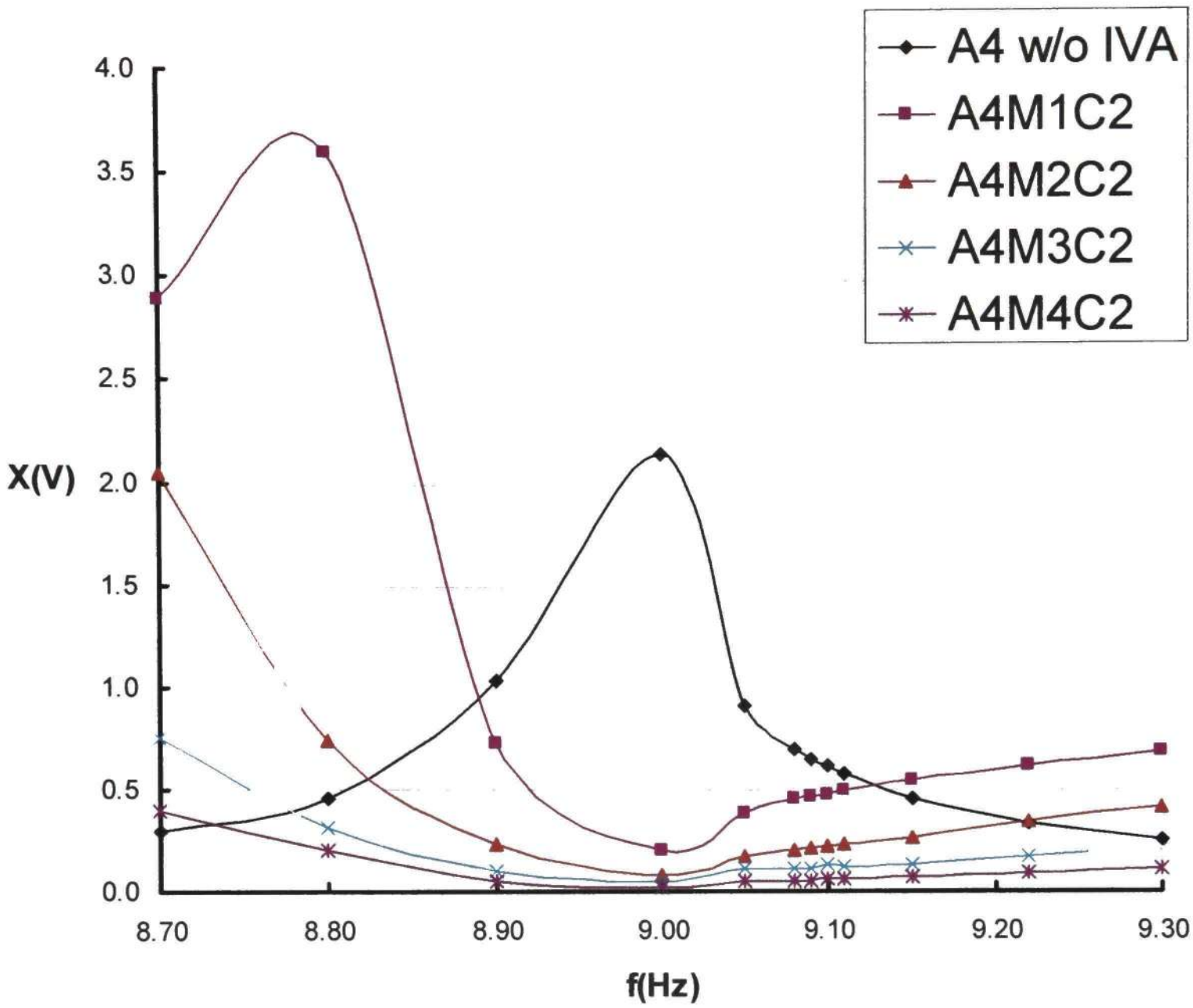

Figure 3.10: Effect of mass ratio on amplitude

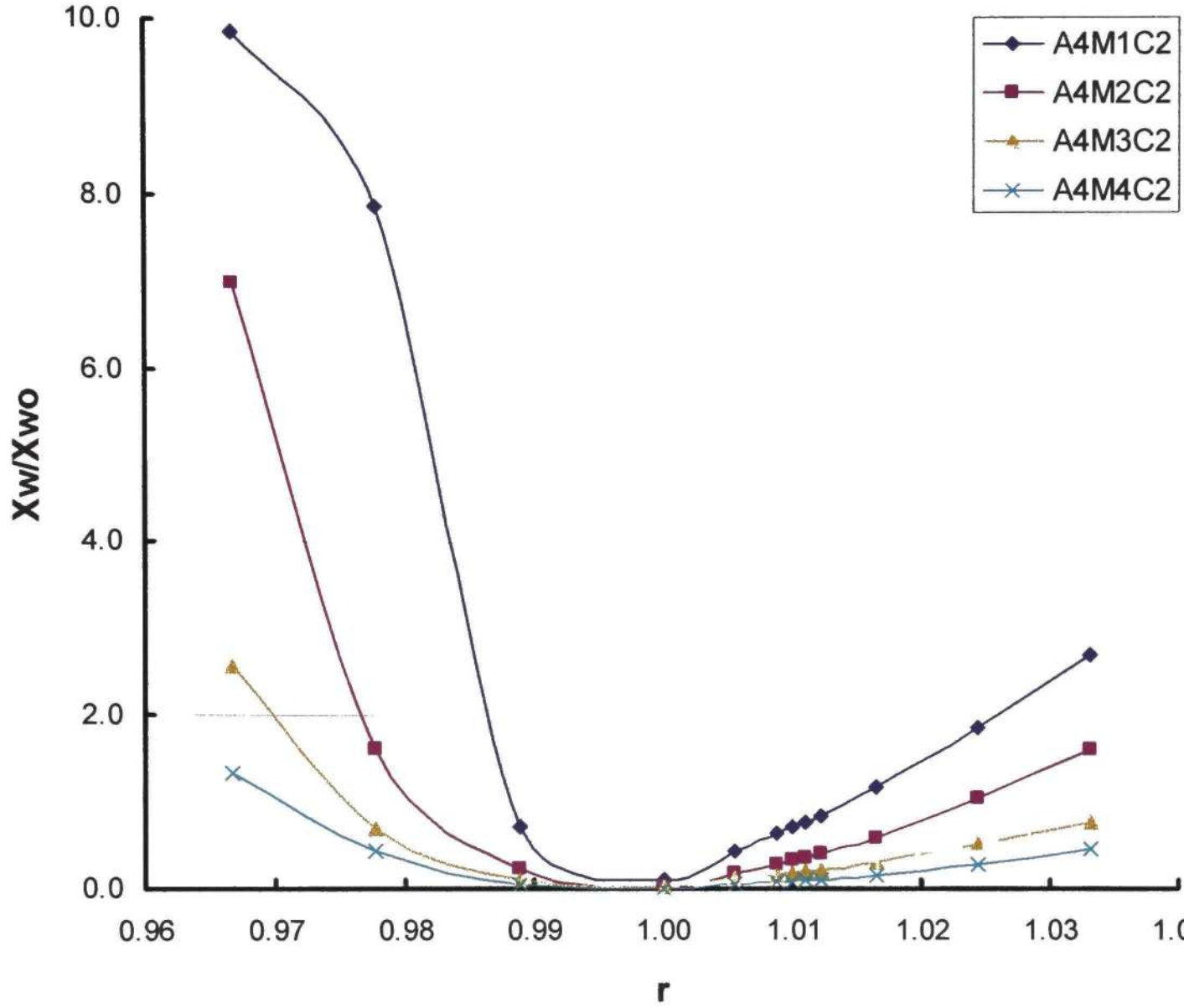

Figure 3.11: Effect of mass ratio on amplitude ratio

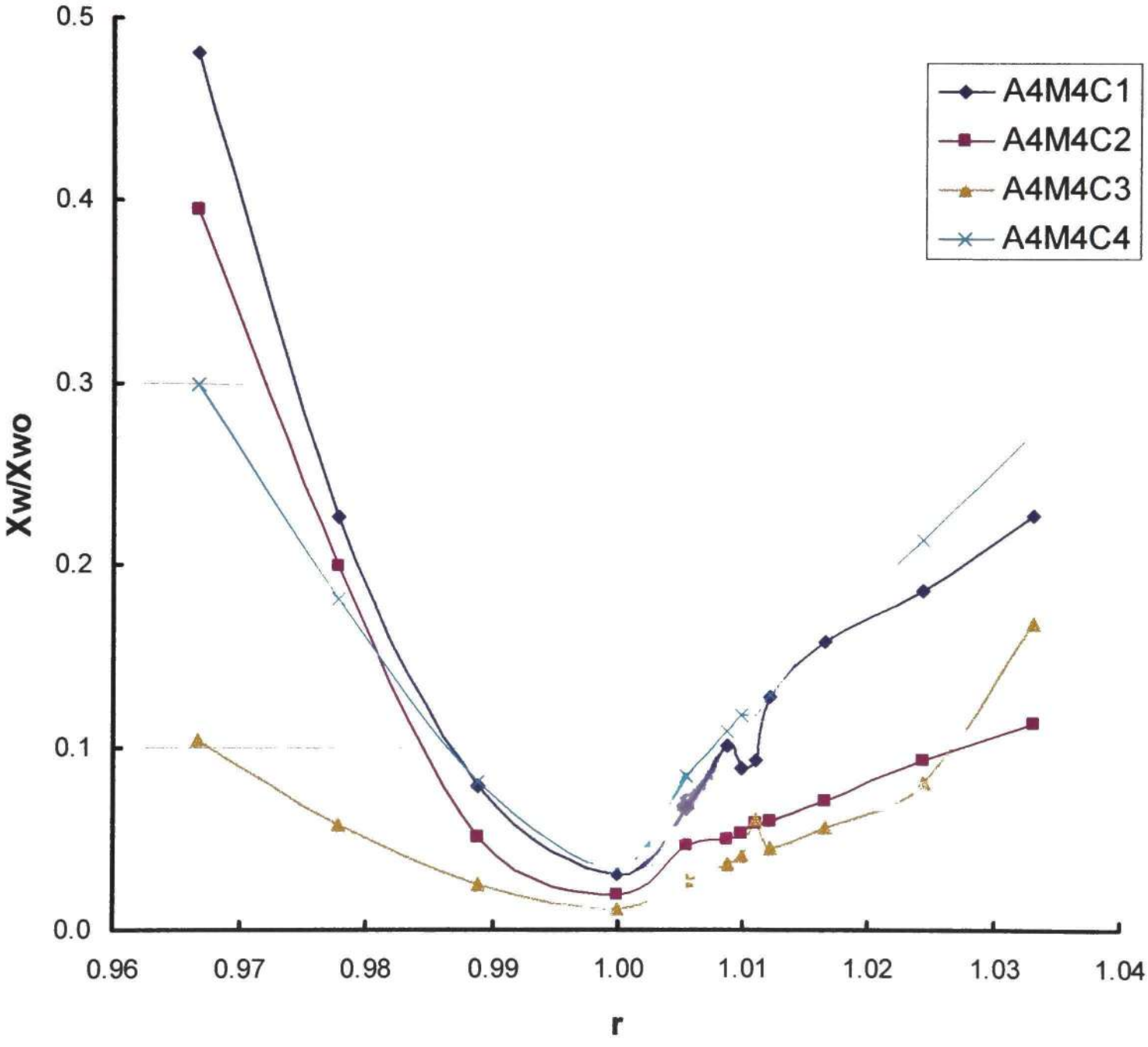

Figure 3.12: Effect of clearance on amplitude ratio

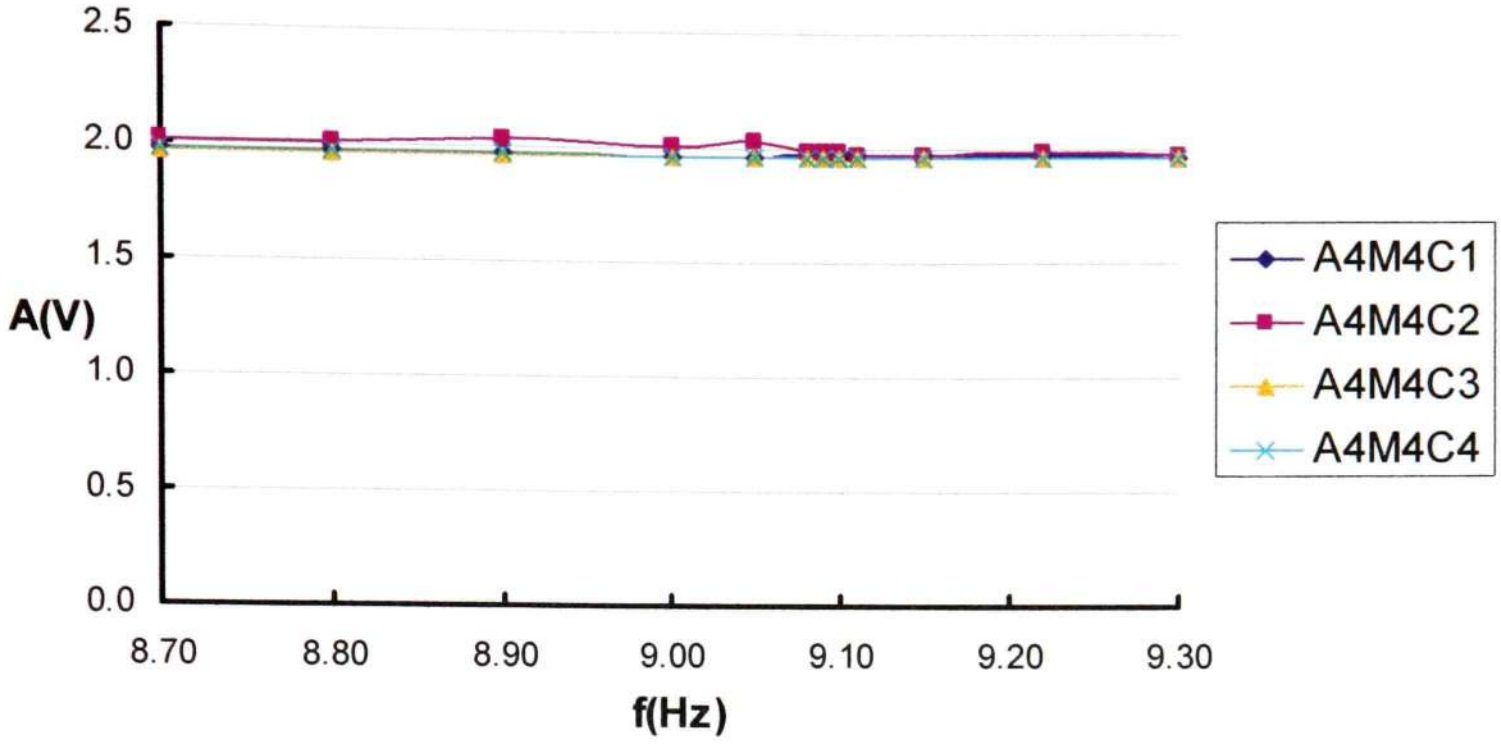

(a)

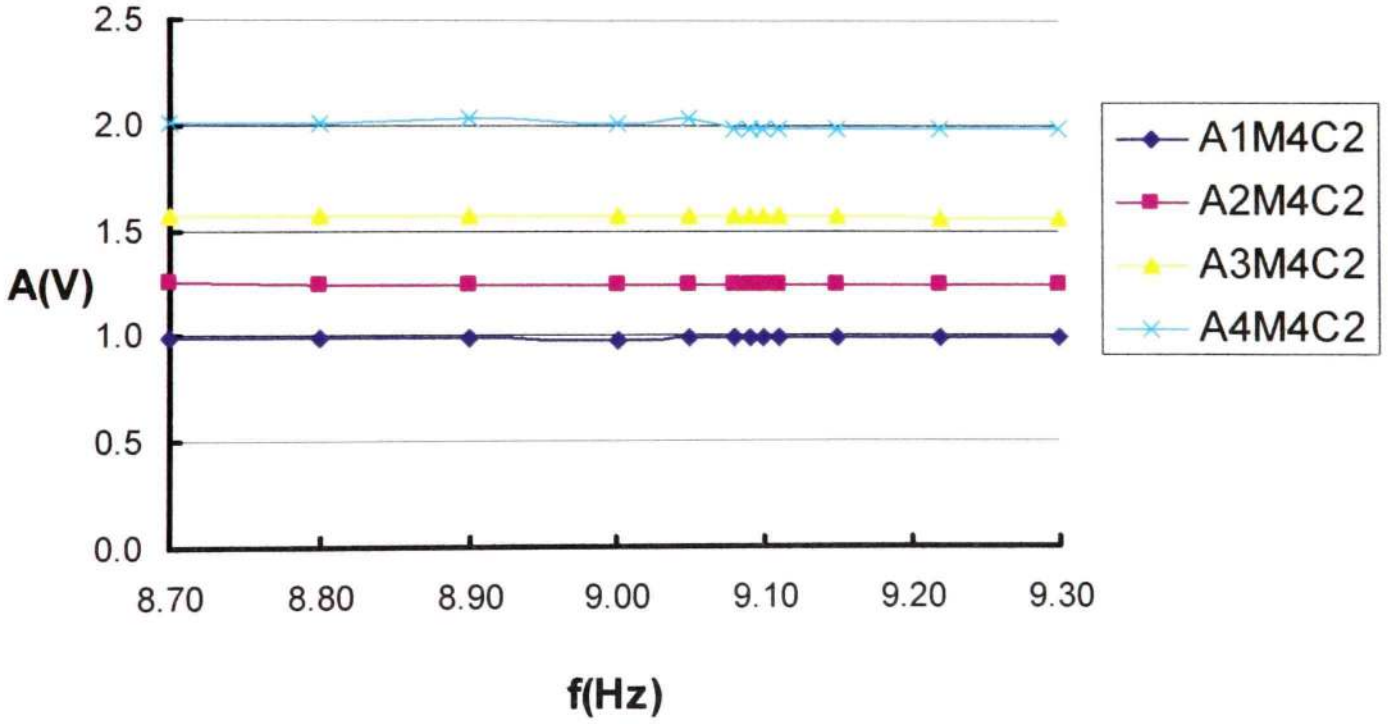

(b)

Figure 3.13: Typical shaker displacements for experiments

(a) Same excitation amplitude, (b) Different excitation amplitudes

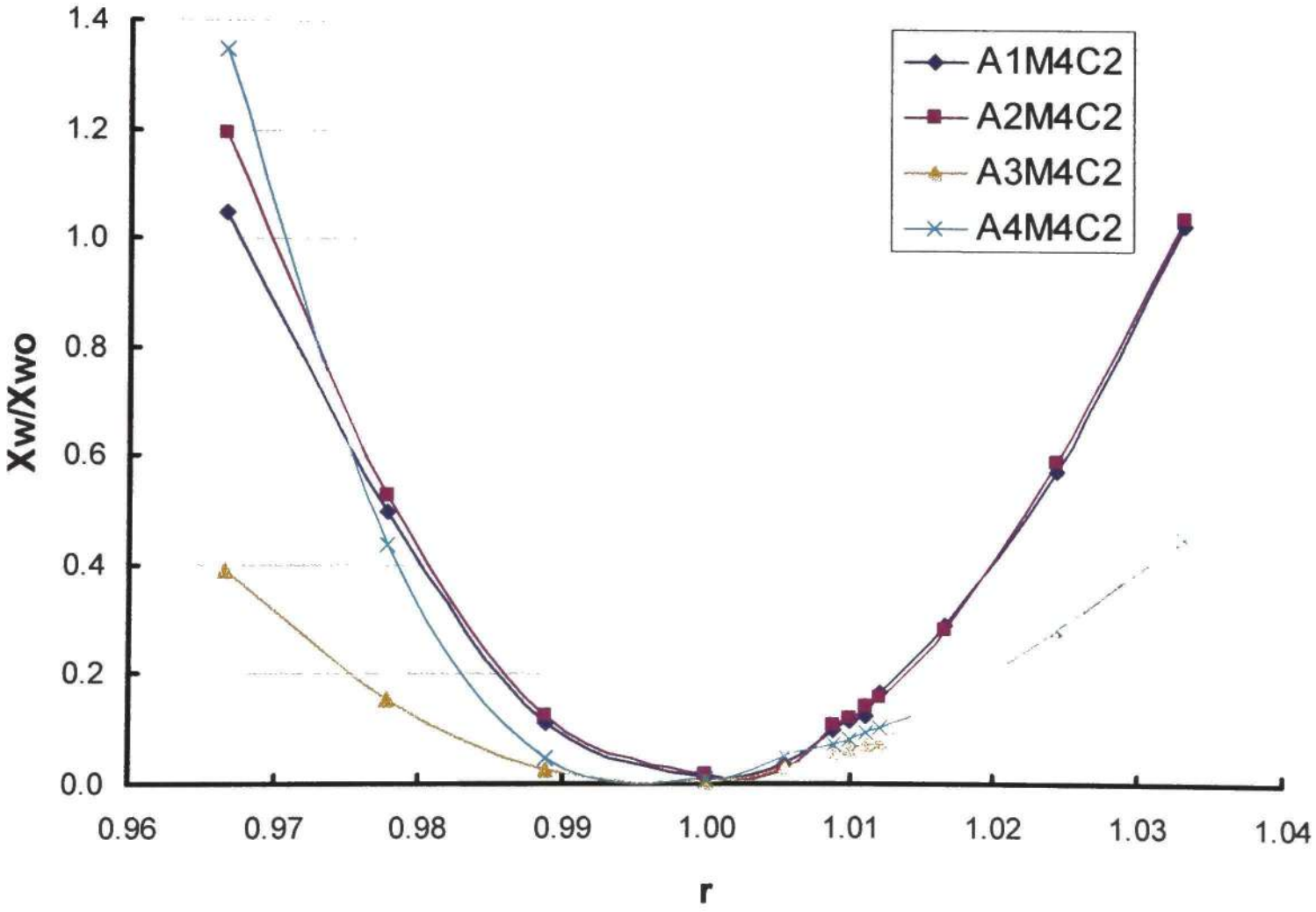

Figure 3.14: Effect of excitation amplitude on amplitude ratio

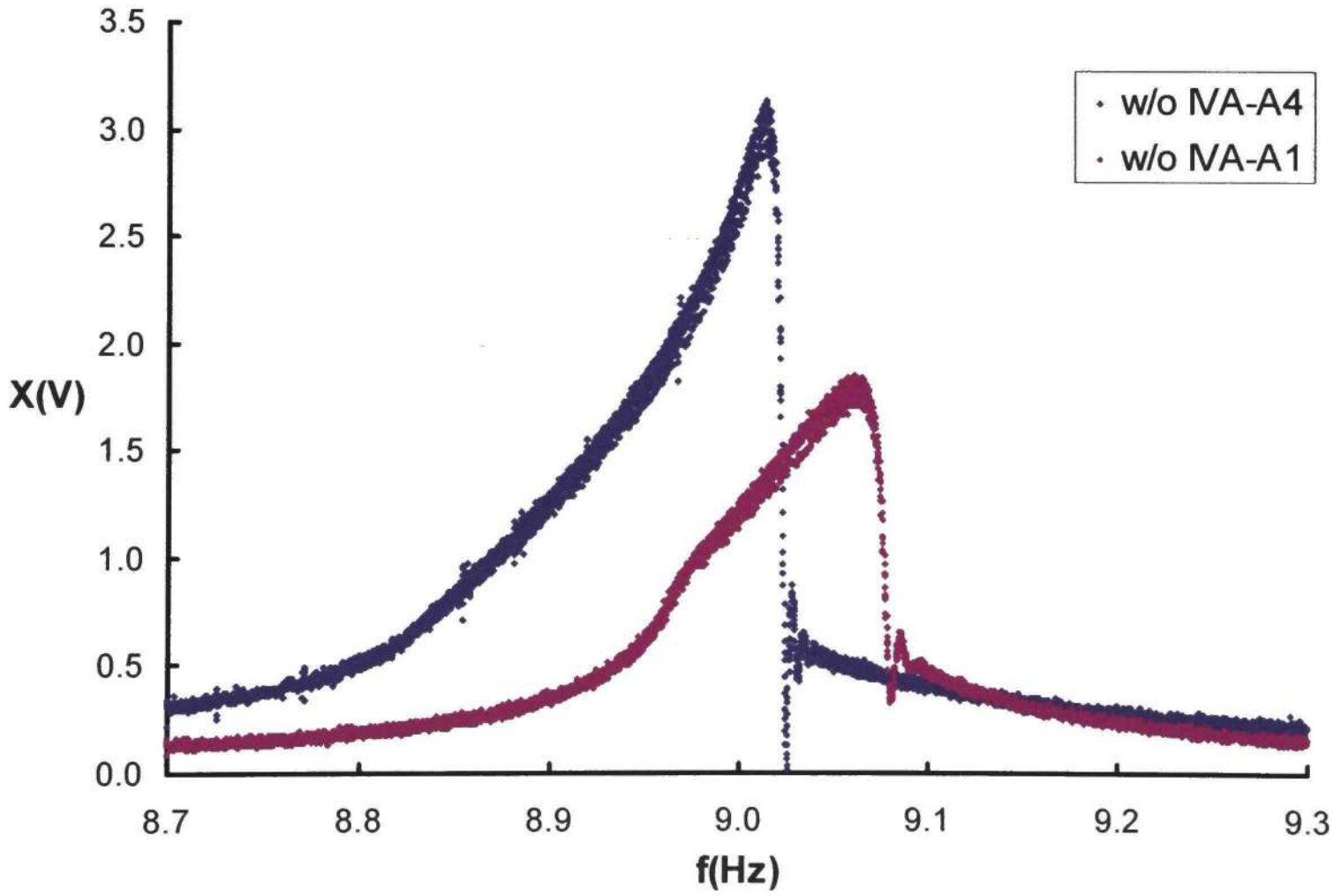

Figure 3.15: Upsweep without IVA for two amplitudes

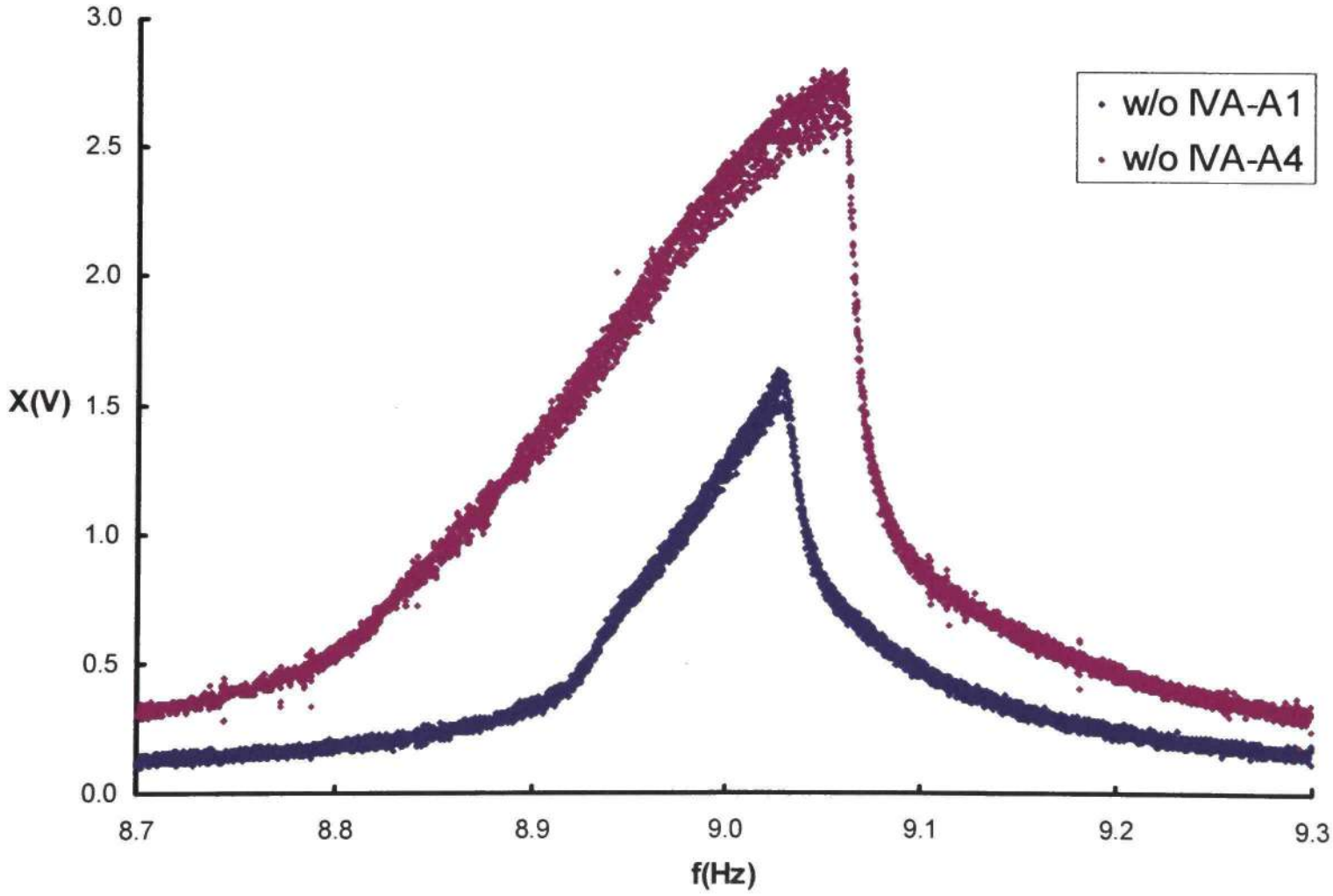

Figure 3.16: Downsweep without IVA for two amplitudes

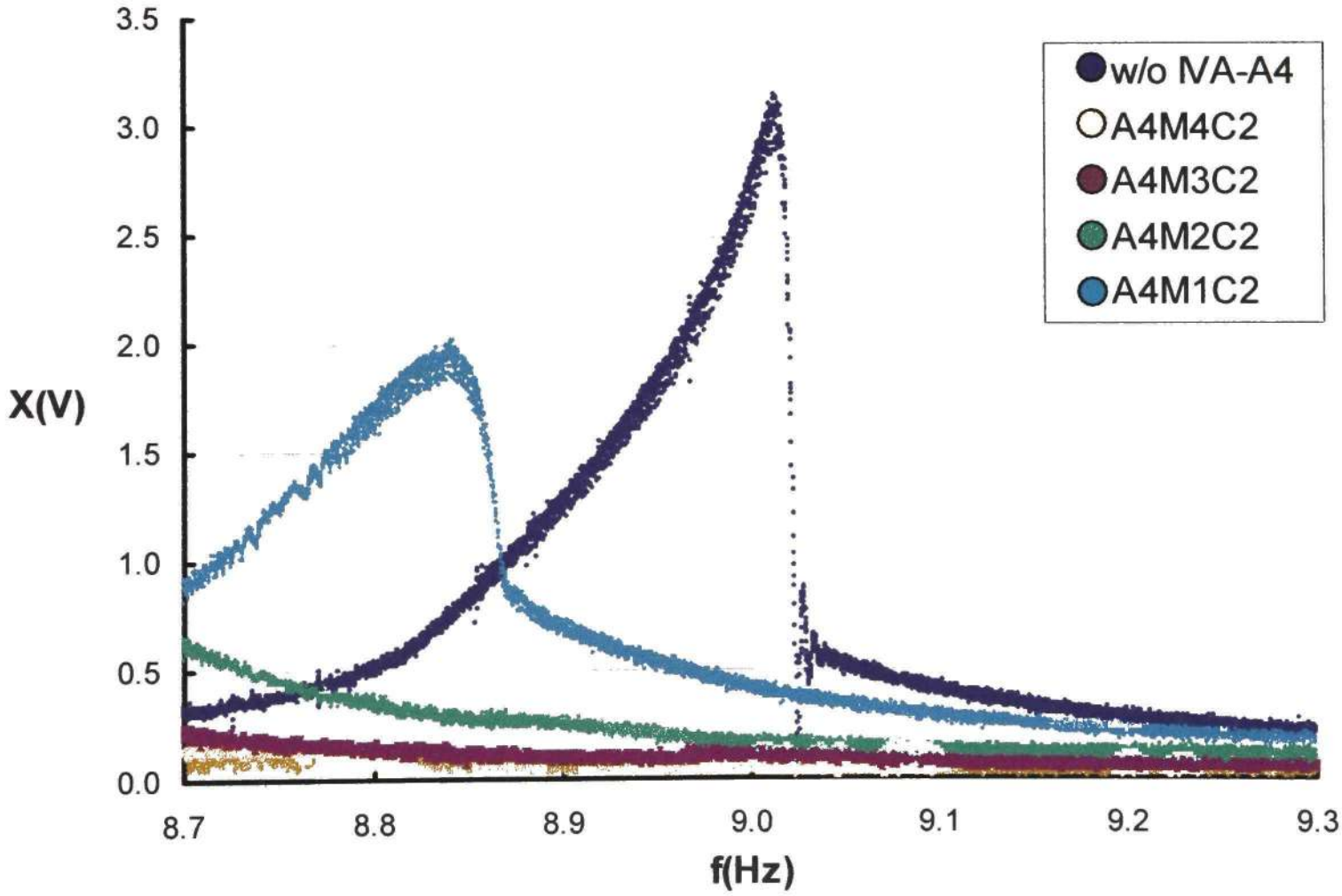

Figure 3.17: Effect of mass ratio on upsweep response

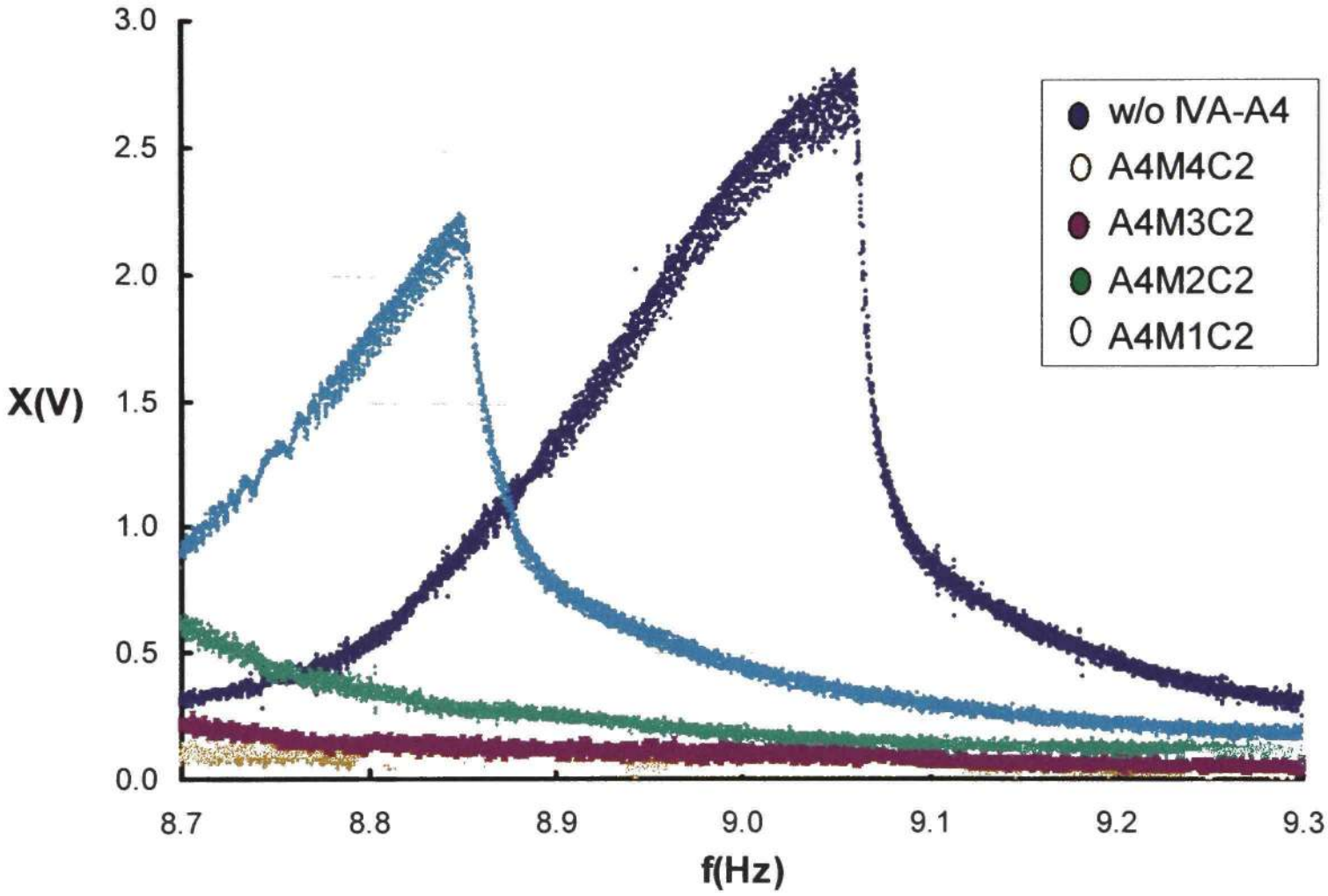

Figure 3.18: Effect of mass ratio on downsweep response

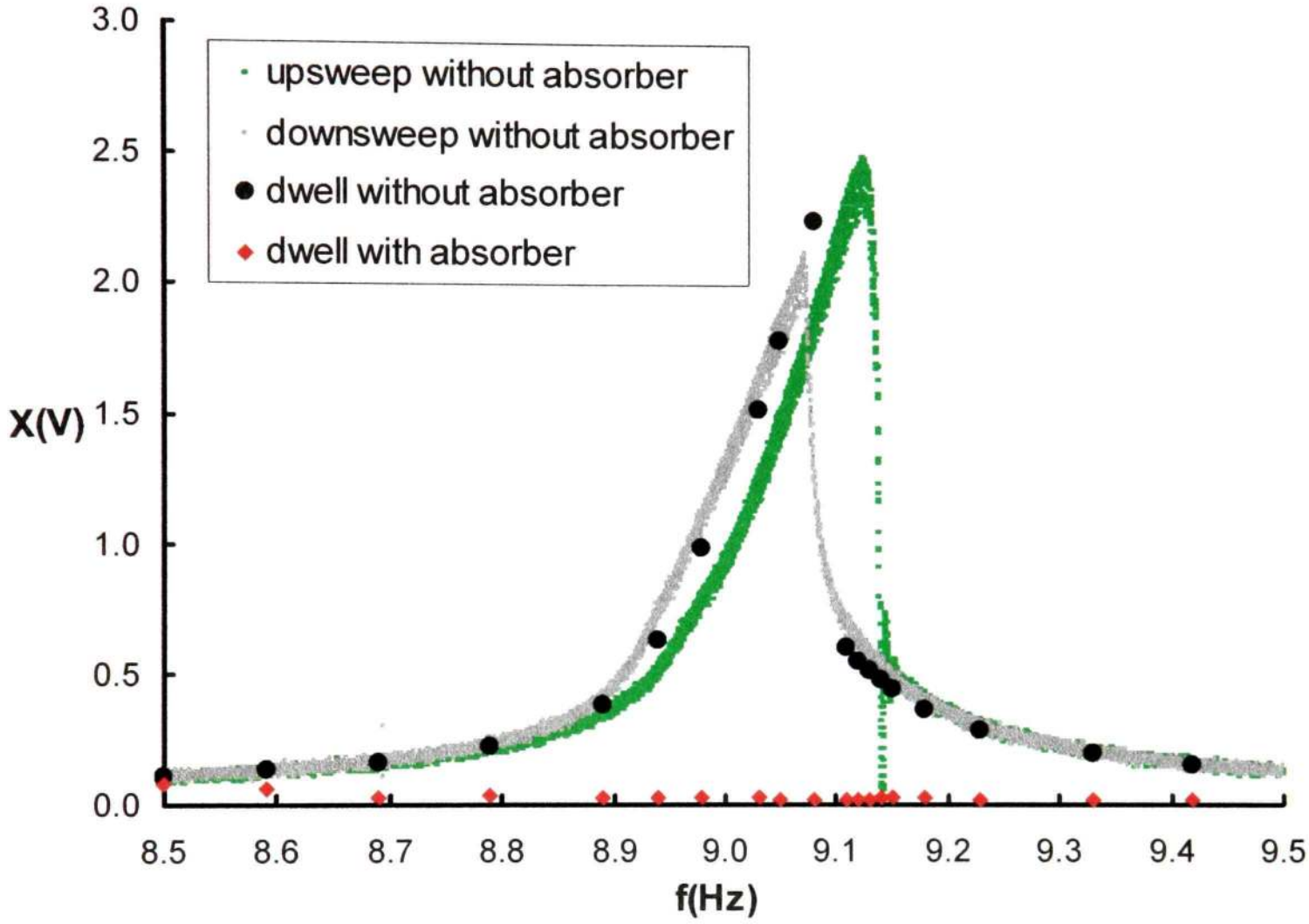

Figure 3.19: Frequency response of sweep and dwell data

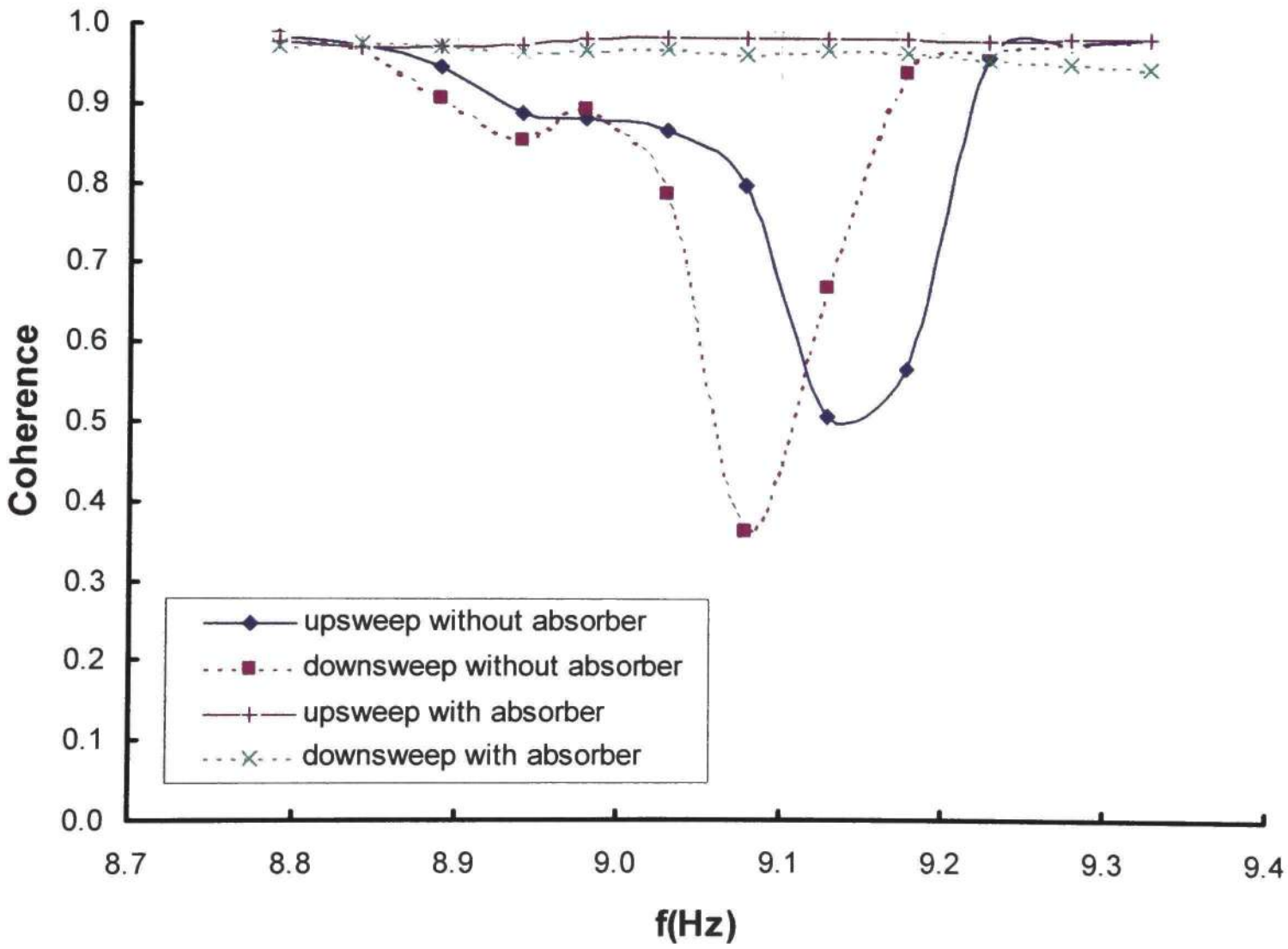

Figure 3.20: Coherence and absorption

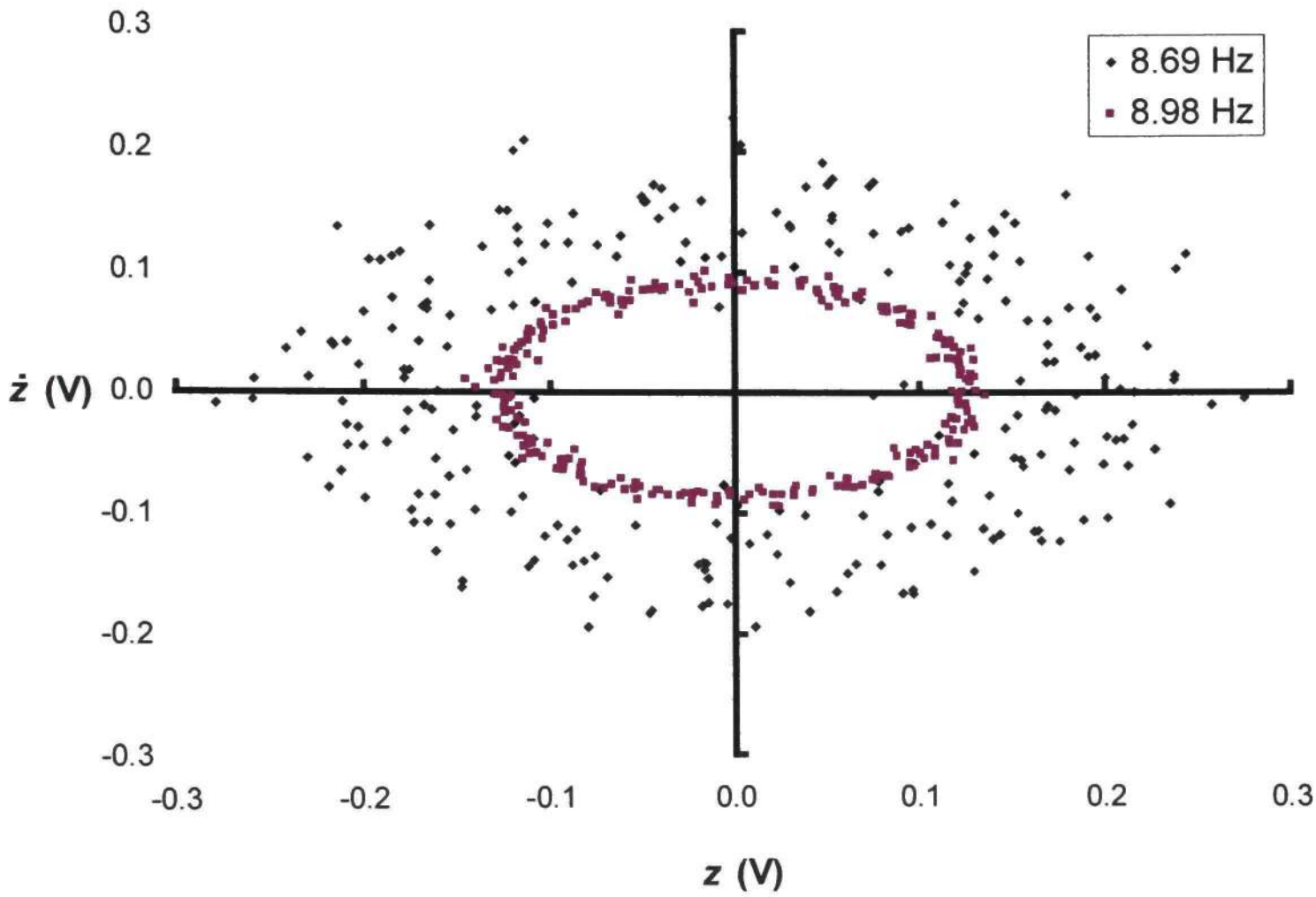

Figure 3.21: Phase portrait for efficient and inefficient operation

CHAPTER 4
CONCLUSIONS AND RECOMMENDATIONS

4.1 Conclusions

It has been shown that for the case without the IVA, the decay in vibration amplitude is exponential, whereas for the case with the IVA the decay is linear. It is seen that a higher mass ratio and higher initial displacement cause faster decay.

The position of a single-unit IVA has been measured experimentally for the first time, and dynamics of the IVA was shown. The effects of mass ratio, clearance, and excitation amplitude are studied by dwell and sweep experiments. It has been shown that a higher mass ratio increases the attenuations, and absorption is best around resonance. The use of coherence to determine absorption and vibration absorber efficiency is proposed. It has been confirmed experimentally for the first time that periodic, symmetric and steady state motion of the IVA enables efficient absorption, while the efficiency diminishes when the motion is unstable.

4.2 Recommendations

The effect of clearance ratio on system performance may be studied by combining the clearance and excitation amplitude parameters into a single parameter. The experimental data obtained from IVA position and coherence measurements may be used to design and build a feedback-controlled IVA with varying clearance. An IVA consisting of a hollow outer casing filled partially with a high-density fluid such as mercury, the impact-sloshing vibration absorber, can be designed and built. The performance of the abovementioned IVA can be compared with the single-unit IVA.

REFERENCES

Araki, Y., Jinnouchi, Y., Inoue, J., and Yokomichi, I., "Indicial Response of Impact Damper With Granular Material," *ASME Pressure Vessels and Piping Division (Publication) PVP Seismic Engineering-1989: Design, Analysis, Testing, and Qualification Methods*, pp. 73-79, 1989.

Babitsky, V. I., *Theory of Vibro-Impact Systems and Applications*, Springer, Berlin, 1998.

Bailey, T., and Semercigil, S. E., "A Passive Controller For Flexible L-Structures," *Journal of Sound and Vibration*, Vol. 173, pp. 131-136, 1994.

Bapat, C. N., "The General Motion of an Inclined Impact Damper With Friction," *Journal of Sound and Vibration*, Vol. 184, pp. 417-427, 1995.

Bapat, C. N., and Sankar, S., "Single Unit Impact Damper In Free and Forced Vibration," *Journal of Sound and Vibration*, Vol. 99, pp. 85-94, 1985.

Bendat, J. S., and Piersol, A. G., *Random Data*, Wiley, New York, 1986.

Cao, S., and Semercigil, S. E., "A Semi-Active Controller For Excessive Transient Vibrations of Light Structures," *Journal of Sound and Vibration*, Vol. 178, pp. 145-161, 1994.

Chalmers, R., and Semercigil, S. E., "Impact Damping the Second Mode of a Cantilevered Beam," *Journal of Sound and Vibration*, Vol. 146, pp. 157-161, 1991.

Chapra, S. C., and Canale, R. P., *Numerical Methods for Engineers, McGraw, Boston, 1998.*

Chatterjee, S., Mallik, A. K., and Ghosh, A., "Impact Dampers For Controlling Self-Excited Oscillations," *Journal of Sound and Vibration*, Vol. 193, pp. 1003-1014, 1996.

Chen, L. A., and Semercigil, S. E., "A Beam-Like Damper for Attenuating Transient Vibrations of Light Structures," *Journal of Sound and Vibration*, Vol. 164, pp. 53-65, 1993.

Collette, F. S., "A Combined Tuned Absorber and Pendulum Impact Damper Under Random Excitation," *Journal of Sound and Vibration*, Vol. 216, pp. 199-213, 1998.

Collette, F. S., and Semercigil, S. E., "Response of a Light Secondary System With a Modified Tuned Absorber To Transient Excitation," *Proceedings of the 16th International Modal Analysis Conference*, pp. 595-601, 1998.

Collette, F., Huynh, D., and Semercigil, S. E., "Further Results With Tuned Absorber-Impact Damper Combination," *Proceedings of the 17th International Modal Analysis Conference, San Antonio, TX*, February 2000.

Crandall, S. H., "The Role of Damping In Vibration Theory," *Journal of Sound and Vibration*, Vol. 11, pp. 3-18, 1970.

Crossley, F. R. E., "The Forced Oscillation of the Centrifugal Pendulum With Wide Angles," *Transactions of the ASME - Journal of Applied Mechanics*, pp. 41-47, 1953.

Cuvalci, O., and Ertas, A., "Pendulum as Vibration Absorber for Flexible Structures: Experiment and Theory," *Journal of Vibration and Acoustics*, Vol. 118, pp. 558-566, 1996.

Data Physics Corporation, *DP550Win Vibration Controller*, San Jose, CA, 1999.

El-Sayad, M. A., Hanna, S. N., and Ibrahim, R. A., "Parametric Excitation of Nonlinear Elastic Systems Involving Hydrodynamic Sloshing Impact," *Nonlinear Dynamics*, Vol. 18, pp. 25-50, 1999.

Ema, S., and Marui, E., "A Fundamental Study on Impact Dampers," *International Journal of Machine and Tools and Manufacture*, Vol. 34, pp. 407-421, 1994.

Ema, S., and Marui, E., "Damping Characteristics of an Impact Damper," *International Journal of Machine and Tools and Manufacture*, Vol. 36, pp. 293-306, 1995.

Ertas, A., and Mustafa, G., "Real-Time Response of the Simple Pendulum: An Experimental Technique," *Experimental Techniques*, Vol. 16, pp. 33-35, 1992.

Frahm, H., *Device for Damping Vibrations of Bodies*, US Patent No. 989958, 1909.

Fuse, T., "Prevention of Resonances By Impact Damper," *ASME Pressure Vessels and Piping Division (Publication) PVP Seismic Engineering-1989: Design, Analysis, Testing, and Qualification Methods*, pp. 57-66, 1989.

Grubin, C., "On the Theory of the Acceleration Damper," *Transactions of the ASME-Journal of Applied Mechanics*, Vol. 23, pp. 373-378, 1956.

Hoang, P., and Semercigil, S. E., "A Passive Controller For The Flexible Robot Arm," *Proceedings of the 1992 Engineering Systems Design and Analysis Conference-ASME*, pp. 197-202, 1992.

Ibrahim, R. A., Evans, M., and Yoon, Y. J., "Experimental Investigation of Random Excitation of Nonlinear Systems With Autoparametric Coupling," *Structural Safety*, Vol. 6, pp. 161-176, 1989.

Ibrahim, R. A., and Sullivan, D. G., "Experimental Investigation of Structural Linear and Autoparametric Interactions Under Random Excitation," *AIAA Journal*, Vol. 28, pp. 338-344, 1990.

Iemura, H., "Principles of TMD and TLD-Basic Principles and Design Procedure", *Passive and Active Structural Vibration Control in Civil Engineering*, Ed. Soong, T. T., and Costantinou, M. C., Springer, New York, 1994.

Jo, I., Kaneko, T., Nagatsu, S., Takahashi, C., and Kimura, M., "Development of Highway Light Pole woth Resistance to Wind Vortex-Induced Oscillations," *Kawasaki Steel Technical Report*, No. 21, pp. 86-94, 1989.

Kato, M., Dazai, M., and Takase, H., "Study on Impact Damper Having a Spring-supported Additional Mass," *Transactions of the Japanese Society of Mechanical Engineers*, Vol. 19, pp. 103-109, 1976.

Korenev, B. G., and Reznikov, L. M., *Dynamic Vibration Absorbers*, Wiley, West Sussex, England, 1993.

Koss, L. L., and Melbourne, W. H., "Chain Dampers for Control of Wind-Induced Vibration of Tower and Mast Structures," *Engineering Structures*, Vol. 17, pp. 622-625, 1995.

Masri, S. F., "Analytical and Experimental Studies of Multiple-Unit Impact Dampers," *The Journal of the Acoustical Society of America*, Vol. 45, pp. 1111-1117, 1968.

Masri, S. F., "General Motion of Impact Dampers," *The Journal of the Acoustical Society of America*, Vol. 47, pp. 229-237, 1969.

Masri, S. F., "Steady-State Response of a Multidegree System With an Impact Damper," *Transactions of the ASME-Journal of Applied Mechanics*, Vol. 40, pp. 127-132, 1973.

Masri, S. F., and Caughey, T. K., "On the Stability of the Impact Damper," *Transactions of the ASME-Journal of Applied Mechanics*, Vol. 88, pp. 586-592, 1966.

Masri, S. F., and Ibrahim, A. M., "Response of the Impact Damper to Stationary Random Excitation," *The Journal of the Acoustical Society of America*, Vol. 53, pp. 200-211, 1973.

Masri, S. F., Miller, R. K., Dehghanyar, T. J., and Caughey, T. K., "Active Parameter Control of Nonlinear Vibrating Structures," *Transactions of the ASME-Journal of Applied Mechanics*, Vol. 56, pp. 658-666, 1989.

Mead, D. J., *Passive Vibration Control*, Wiley, West Sussex, England, 1998.

Modi, V. J., and Seto, M. L., "Passive Control of Flow-Induced Oscillations Using Rectangular Nutation Dampers," *Journal of Vibration and Control*, Vol. 4, pp. 381-404, 1998.

Moore, J. J., Palazzolo, A. B., and Gadangi, R., "A Forced Response Analysis and Application of Impact Dampers to Rotordynamic Vibration Supression in a Cryogenic Environment," *Journal of Vibration and Acoustics*, Vol. 117, pp. 300-310, 1995.

Moore, J. J., Palazzolo, A. B., Gadangi, R. K., Kascak, A. F., Brown, G., and Motague, G., "Hybrid Friction-Impact Vibration Damper for Cryogenic Rotating Machinery," *Journal of Propulsion and Power*, Vol. 13, pp. 495-501, 1997.

Mustafa, G., and Ertas, A., "Experimental Evidence of Quasiperiodicity and Its Breakdown I the Column-Pendulum Oscillator," *Journal of Dynamic Systems, Measurement and Control*, Vol. 117, pp. 218-225, 1995.

Nayfeh, A. H., and Mook, D. T., *Nonlinear Oscillations*, Wiley, New York, 1979.

Ogawa, K., Ide, T., and Saitou, T., "Application of Impact Mass Damper to a Cable-Stayed Bridge Pylon," *Journal of Wind Engineering and Industrial Aerodynamics*, Vol 72, pp. 301-312, 1997.

Ogawa, K., Sakai, Y., and Sakai, F., "Control of Wind-Induced Vibrations Using an Impact Mass Damper," *Journal of Wind Engineering and Industrial Aerodynamics Proceedings of the 8th International Conference on Wind Engineering*, Part 3 Vol. 43, pp. 1881-1882, 1992.

Oledzki, A. A., Siwicki, I., and Wisniewski, J., "Impact Dampers In Application For Tube, Rod And Rope Structures," *Mechanism and Machine Theory*, Vol. 34, pp. 243-253, 1999.

Paget, A. L., "Vibration In Steam-Turbine Buckets and Damping by Impact," *Engineering*, Vol. 143, pp. 305-307, 1937.

Papalou, A. and Masri, S. F., "An Experimental Investigation of Particle Dampers Under Harmonic Excitation," *Journal of Vibration and Control*, Vol. 4, pp. 361-179, 1998.

Penalba, C., "Vibration Control in Lattice Communication Towers," *Proceedings of the 1999 Structures Congress*, pp. 983-986, 1999.

Piersol, A. G., "Data Analysis," *Noise and Vibration Control Engineering: Principles and Applications*, Ed. Beranek, L. L., and Ver, I. L., Wiley, New York, 1992.

Popplewell, N. and Liao, M., "A Simple Design Procedure For Optimum Impact Dampers," *Journal of Sound and Vibration*, Vol. 146, pp. 519-526, 1991.

Popplewell, N., and Semercigil, S. E., "Performance of the Bean Bag Impact Damper for a Sinusoidal External Force," *Journal of Sound and Vibration*, Vol. 133, pp. 193-223, 1989.

Popplewell, N., Bapat, C. N., and McLachlan, K., "Stable Periodic Vibroimpacts of an Oscillator," *Journal of Sound and Vibration*, Vol. 87, pp. 41-59, 1983.

Rao, S. S., *Mechanical Vibrations*, Addison-Wesley, Reading, MA, 1995.

Reed, W. H.., "Hanging Chain Impact Dampers; A Simple Method of Damping Tall Flexible Structures," *Proceedings of the International Research Seminar; Wind Effects on Buildings and Structures*, 1967, Ottawa, Vol.2, pp. 283-321.

Roy, R. K., Rocke, R. D., and Foster, J. E., "The Application of Impact Dampers to Continuous Systems," *Transactions of the ASME-Journal of Engineering for Industry*, Vol. 97, pp. 1317-1324, 1975.

Semercigil, S. E., and Popplewell, N., "Impact Damping of Random Vibrations," *Journal of Sound and Vibration*, Vol. 121, pp. 178-184, 1988.

Sevin, E., "On the Parametric Excitation of Pendulum-Type Vibration Absorber," *Transactions of the ASME - Journal of Applied Mechanics*, Vol. 28, pp. 330-334, 1961.

Skipor, E. and Bain, L. J., "Application of Impact Damping to Rotary Printing Equipment," *Transactions of the ASME-Journal of Mechanical Design*, Vol. 102, pp. 338-343, 1980.

Steinberg, D. S., "Snubbers Calm PCB Vibration," *Machine Design*, Vol. 49, pp 71-73, 1977.

Thomas, M. D., Knight, W. A., and Sadek, M. M., "The Impact Damper as a Method of Improving Cantilever Boring Bars," *Transactions of the ASME-Journal of Engineering for Industry*, Vol. 97, pp. 859-866, 1975.

Ungar, E. E., "Structural Damping," *Noise and Vibration Control Engineering: Principles and Applications*, Ed. Beranek, L. L., and Ver, I. L., Wiley, New York, 1992.

Ungar, E. E., "Vibration Isolation," *Noise and Vibration Control Engineering: Principles and Applications*, Ed. Beranek, L. L., and Ver, I. L., Wiley, New York, 1992.

Ying, Z., and Semercigil, S. E., "Response of a New Tuned Vibration Absorber to an Earthquake-like Random Excitation," *Journal of Sound and Vibration*, Vol. 150, pp. 520-530, 1991.

Yokomichi, I., Araki, Y., Jinnouchi, Y., and Inoue, J., "Impact Damper With Granular Materials for Multibody System," *Transactions of the ASME-Journal of Pressure Vessel Technology*, Vol. 118, pp. 95-103, 1996.

APPENDIX A

TABLE OF EXPERIMENTS

Table A.1

EXPERIMENT	MASS		FREQUENCY			EXCITATION and CLEARANCE				
	Impact Mass M2 (kg)	Mass Ration M2/M1	Exc. Freq. (Start Freq.) W1 (Hz)	End Frequency W2 (Hz)	Frequency Ratio r1	Excitation Ampl. A (mm)	Initial Displ. X1 (micstr)	Wall-to-Wall Gap (mm)	Clearance d (mm)	Clearance Ratio d/A
1	0.000	**0.000**	-		-	-	256		-	
2	0.000	**0.000**	8.700		**0.967**	0.127			-	-
3	0.000	**0.000**	8.800		**0.978**	0.127				-
4	0.000	**0.000**	8.900		**0.989**	0.127			-	-
5	0.000	**0.000**	9.000		**1.000**	0.127				-
6	0.000	**0.000**	9.050		**1.006**	0.127			-	-
7	0.000	**0.000**	9.080		**1.009**	0.127			-	-
8	0.000	**0.000**	9.090		**1.010**	0.127			-	-
9	0.000	**0.000**	9.100		**1.011**	0.127			-	-
10	0.000	**0.000**	9.110		**1.012**	0.127				
11	0.000	**0.000**	9.150		**1.017**	0.127				
12	0.000	**0.000**	9.220		**1.024**	0.127				
13	0.000	**0.000**	9.300		**1.033**	0.127				
14	0.000	**0.000**	8.700	9.300		0.127				-
15	0.000	**0.000**	9.300	8.700		0.127				-
16	0.000	**0.000**			-	-	320			
17	0.000	**0.000**	8.700		**0.967**	0.160			-	-
18	0.000	**0.000**	8.800		**0.978**	0.160			-	-
19	0.000	**0.000**	8.900		**0.989**	0.160			-	-
20	0.000	**0.000**	9.000		**1.000**	0.160			-	-
21	0.000	**0.000**	9.050		**1.006**	0.160			-	-
22	0.000	**0.000**	9.080		**1.009**	0.160			-	-
23	0.000	**0.000**	9.090		**1.010**	0.160			-	-
24	0.000	**0.000**	9.100		**1.011**	0.160				-
25	0.000	**0.000**	9.110		**1.012**	0.160			-	-
26	0.000	**0.000**	9.150		**1.017**	0.160			-	-
27	0.000	**0.000**	9.220		**1.024**	0.160			-	-
28	0.000	**0.000**	9.300		**1.033**	0.160			-	-
29	0.000	**0.000**	8.700	9.300	-	0.160				-
30	0.000	**0.000**	9.300	8.700	-	0.160			-	-

Table A.1 Continued

EXPERIMENT	MASS		FREQUENCY			EXCITATION and CLEARANCE				
	Impact Mass M2 (kg)	Mass Ration M2/M1	Exc. Freq. (Start Freq.) W1 (Hz)	End Frequency W2 (Hz)	Frequency Ratio r1	Excitation Ampl. A (mm)	Initial Displ. X1 (micstr)	Wall-to-Wall Gap (mm)	Clearance d (mm)	Clearance Ratio d/A
31	0.000	**0.000**	-		-		400			
32	0.000	**0.000**	8.700		**0.967**	0.202				-
33	0.000	**0.000**	8.800		**0.978**	0.202			-	-
34	0.000	**0.000**	8.900		**0.989**	0.202			-	-
35	0.000	**0.000**	9.000		**1.000**	0.202			-	-
36	0.000	**0.000**	9.050		**1.006**	0.202			-	-
37	0.000	**0.000**	9.080		**1.009**	0.202			-	-
38	0.000	**0.000**	9.090		**1.010**	0.202			-	-
39	0.000	**0.000**	9.100		**1.011**	0.202			-	-
40	0.000	**0.000**	9.110		**1.012**	0.202			-	-
41	0.000	**0.000**	9.150		**1.017**	0.202			-	-
42	0.000	**0.000**	9.220		**1.024**	0.202			-	-
43	0.000	**0.000**	9.300		**1.033**	0.202			-	
44	0.000	**0.000**	8.700	9.300		0.202			-	-
45	0.000	**0.000**	9.300	8.700		0.202			-	-
46	0.000	**0.000**			-	-	500			
47	0.000	**0.000**	8.700		**0.967**	0.254			-	
48	0.000	**0.000**	8.800		**0.978**	0.254			-	-
49	0.000	**0.000**	8.900		**0.989**	0.254			-	-
50	0.000	**0.000**	9.000		**1.000**	0.254			-	
51	0.000	**0.000**	9.050		**1.006**	0.254			-	-
52	0.000	**0.000**	9.080		**1.009**	0.254			-	
53	0.000	**0.000**	9.090		**1.010**	0.254			-	-
54	0.000	**0.000**	9.100		**1.011**	0.254			-	-
55	0.000	**0.000**	9.110		**1.012**	0.254			-	-
56	0.000	**0.000**	9.150		**1.017**	0.254			-	-
57	0.000	**0.000**	9.220		**1.024**	0.254			-	-
58	0.000	**0.000**	9.300		**1.033**	0.254			-	-
59	0.000	**0.000**	8.700	9.300	-	0.254			-	-
60	0.000	**0.000**	9.300	8.700	-	0.254			-	-

Table A.1 Continued

EXPERIMENT	MASS		FREQUENCY			EXCITATION and CLEARANCE				
	Impact Mass M2 (kg)	Mass Ration M2/M1	Exc. Freq. (Start Freq.) W1 (Hz)	End Frequency W2 (Hz)	Frequency Ratio r1	Excitation Ampl. A (mm)	Initial Displ. X1 (micstr)	Wall-to-Wall Gap (mm)	Clearance d (mm)	Clearance Ratio d/A
61	0.370	**0.193**	-		-	-	256	40.640		
62	0.370	**0.193**	8.700		**0.967**	0.127		40.640	**3.252**	**25.606**
63	0.370	**0.193**	8.800		**0.978**	0.127		40.640	**3.252**	**25.606**
64	0.370	**0.193**	8.900		**0.989**	0.127		40.640	**3.252**	**25.606**
65	0.370	**0.193**	9.000		**1.000**	0.127		40.640	**3.252**	**25.606**
66	0.370	**0.193**	9.050		**1.006**	0.127		40.640	**3.252**	**25.606**
67	0.370	**0.193**	9.080		**1.009**	0.127		40.640	**3.252**	**25.606**
68	0.370	**0.193**	9.090		**1.010**	0.127		40.640	**3.252**	**25.606**
69	0.370	**0.193**	9.100		**1.011**	0.127		40.640	**3.252**	**25.606**
70	0.370	**0.193**	9.110		**1.012**	0.127		40.640	**3.252**	**25.606**
71	0.370	**0.193**	9.150		**1.017**	0.127		40.640	**3.252**	**25.606**
72	0.370	**0.193**	9.220		**1.024**	0.127		40.640	**3.252**	**25.606**
73	0.370	**0.193**	9.300		**1.033**	0.127		40.640	**3.252**	**25.606**
74	0.370	**0.193**	8.700	9.300		0.127		40.640	**3.252**	**25.606**
75	0.370	**0.193**	9.300	8.700		0.127		40.640	**3.252**	**25.606**
76	0.370	**0.193**			-	-	320	40.640		
77	0.370	**0.193**	8.700		**0.967**	0.160		40.640	**3.252**	**20.325**
78	0.370	**0.193**	8.800		**0.978**	0.160		40.640	**3.252**	**20.325**
79	0.370	**0.193**	8.900		**0.989**	0.160		40.640	**3.252**	**20.325**
80	0.370	**0.193**	9.000		**1.000**	0.160		40.640	**3.252**	**20.325**
81	0.370	**0.193**	9.050		**1.006**	0.160		40.640	**3.252**	**20.325**
82	0.370	**0.193**	9.080		**1.009**	0.160		40.640	**3.252**	**20.325**
83	0.370	**0.193**	9.090		**1.010**	0.160		40.640	**3.252**	**20.325**
84	0.370	**0.193**	9.100		**1.011**	0.160		40.640	**3.252**	**20.325**
85	0.370	**0.193**	9.110		**1.012**	0.160		40.640	**3.252**	**20.325**
86	0.370	**0.193**	9.150		**1.017**	0.160		40.640	**3.252**	**20.325**
87	0.370	**0.193**	9.220		**1.024**	0.160		40.640	**3.252**	**20.325**
88	0.370	**0.193**	9.300		**1.033**	0.160		40.640	**3.252**	**20.325**
89	0.370	**0.193**	8.700	9.300	-	0.160		40.640	**3.252**	**20.325**
90	0.370	**0.193**	9.300	8.700	-	0.160		40.640	**3.252**	**20.325**

4 x 1M = 4

Table A.1 Continued

EXPERIMENT	MASS		FREQUENCY			EXCITATION and CLEARANCE				
	Impact Mass M2 (kg)	Mass Ration M2/M1	Exc. Freq. (Start Freq.) W1 (Hz)	End Frequency W2 (Hz)	Frequency Ratio r1	Excitation Ampl. A (mm)	Initial Displ. X1 (micstr)	Wall-to-Wall Gap (mm)	Clearance d (mm)	Clearance Ratio d/A
91	0.370	**0.193**	-		-	-	400	40.640		
92	0.370	**0.193**	8.700		**0.967**	0.202		40.640	**3.252**	**16.099**
93	0.370	**0.193**	8.800		**0.978**	0.202		40.640	**3.252**	**16.099**
94	0.370	**0.193**	8.900		**0.989**	0.202		40.640	**3.252**	**16.099**
95	0.370	**0.193**	9.000		**1.000**	0.202		40.640	**3.252**	**16.099**
96	0.370	**0.193**	9.050		**1.006**	0.202		40.640	**3.252**	**16.099**
97	0.370	**0.193**	9.080		**1.009**	0.202		40.640	**3.252**	**16.099**
98	0.370	**0.193**	9.090		**1.010**	0.202		40.640	**3.252**	**16.099**
99	0.370	**0.193**	9.100		**1.011**	0.202		40.640	**3.252**	**16.099**
100	0.370	**0.193**	9.110		**1.012**	0.202		40.640	**3.252**	**16.099**
101	0.370	**0.193**	9.150		**1.017**	0.202		40.640	**3.252**	**16.099**
102	0.370	**0.193**	9.220		**1.024**	0.202		40.640	**3.252**	**16.099**
103	0.370	**0.193**	9.300		**1.033**	0.202		40.640	**3.252**	**16.099**
104	0.370	**0.193**	8.700	9.300		0.202		40.640	**3.252**	**16.099**
105	0.370	**0.193**	9.300	8.700	-	0.202		40.640	**3.252**	**16.099**
106	0.370	**0.193**	-		-	-	500	40.640		
107	0.370	**0.193**	8.700		**0.967**	0.254		40.640	**3.252**	**12.803**
108	0.370	**0.193**	8.800		**0.978**	0.254		40.640	**3.252**	**12.803**
109	0.370	**0.193**	8.900		**0.989**	0.254		40.640	**3.252**	**12.803**
110	0.370	**0.193**	9.000		**1.000**	0.254		40.640	**3.252**	**12.803**
111	0.370	**0.193**	9.050		**1.006**	0.254		40.640	**3.252**	**12.803**
112	0.370	**0.193**	9.080		**1.009**	0.254		40.640	**3.252**	**12.803**
113	0.370	**0.193**	9.090		**1.010**	0.254		40.640	**3.252**	**12.803**
114	0.370	**0.193**	9.100		**1.011**	0.254		40.640	**3.252**	**12.803**
115	0.370	**0.193**	9.110		**1.012**	0.254		40.640	**3.252**	**12.803**
116	0.370	**0.193**	9.150		**1.017**	0.254		40.640	**3.252**	**12.803**
117	0.370	**0.193**	9.220		**1.024**	0.254		40.640	**3.252**	**12.803**
118	0.370	**0.193**	9.300		**1.033**	0.254		40.640	**3.252**	**12.803**
119	0.370	**0.193**	8.700	9.300	-	0.254		40.640	**3.252**	**12.803**
120	0.370	**0.193**	9.300	8.700	-	0.254		40.640	**3.252**	**12.803**

Table A.1 Continued

EXPERIMENT	MASS		FREQUENCY			EXCITATION and CLEARANCE				
	Impact Mass M2 (kg)	Mass Ration M2/M1	Exc. Freq. (Start Freq.) W1 (Hz)	End Frequency W2 (Hz)	Frequency Ratio r1	Excitation Ampl. A (mm)	Initial Displ. X1 (micstr)	Wall-to-Wall Gap (mm)	Clearance d (mm)	Clearance Ratio d/A
213	0.278	**0.145**	-		-	-	400	40.640		
121	0.278	**0.145**	8.700		**0.967**	0.254		40.640	**3.252**	**12.803**
122	0.278	**0.145**	8.800		**0.978**	0.254		40.640	**3.252**	**12.803**
123	0.278	**0.145**	8.900		**0.989**	0.254		40.640	**3.252**	**12.803**
124	0.278	**0.145**	9.000		**1.000**	0.254		40.640	3.252	**12.803**
125	0.278	**0.145**	9.050		**1.006**	0.254		40.640	**3.252**	**12.803**
126	0.278	**0.145**	9.080		**1.009**	0.254		40.640	**3.252**	**12.803**
127	0.278	**0.145**	9.090		**1.010**	0.254		40.640	**3.252**	**12.803**
128	0.278	**0.145**	9.100		**1.011**	0.254		40.640	**3.252**	**12.803**
129	0.278	**0.145**	9.110		**1.012**	0.254		40.640	**3.252**	**12.803**
130	0.278	**0.145**	9.150		**1.017**	0.254		40.640	**3.252**	**12.803**
131	0.278	**0.145**	9.220		**1.024**	0.254		40.640	**3.252**	**12.803**
132	0.278	**0.145**	9.300		**1.033**	0.254		40.640	**3.252**	**12.803**
133	0.278	**0.145**	8.700	9.300		0.254		40.640	**3.252**	**12.803**
134	0.278	**0.145**	9.300	8.700	-	0.254		40.640	**3.252**	**12.803**
135	0.184	**0.096**	-		-	-	400	40.640		
136	0.184	**0.096**	8.700		**0.967**	0.254		40.640	**3.252**	**12.803**
137	0.184	**0.096**	8.800		**0.978**	0.254		40.640	**3.252**	**12.803**
138	0.184	**0.096**	8.900		**0.989**	0.254		40.640	**3.252**	**12.803**
139	0.184	**0.096**	9.000		**1.000**	0.254		40.640	**3.252**	**12.803**
140	0.184	**0.096**	9.050		**1.006**	0.254		40.640	**3.252**	**12.803**
141	0.184	**0.096**	9.080		**1.009**	0.254		40.640	**3.252**	**12.803**
142	0.184	**0.096**	9.090		**1.010**	0.254		40.640	**3.252**	**12.803**
143	0.184	**0.096**	9.100		**1.011**	0.254		40.640	**3.252**	**12.803**
144	0.184	**0.096**	9.110		**1.012**	0.254		40.640	**3.252**	**12.803**
145	0.184	**0.096**	9.150		**1.017**	0.254		40.640	**3.252**	**12.803**
146	0.184	**0.096**	9.220		**1.024**	0.254		40.640	**3.252**	**12.803**
147	0.184	**0.096**	9.300		**1.033**	0.254		40.640	**3.252**	**12.803**
148	0.184	**0.096**	8.700	9.300	-	0.254		40.640	**3.252**	**12.803**
149	0.184	**0.096**	9.300	8.700	-	0.254		40.640	**3.252**	**12.803**

$1A \times 3M = 3$

Table A.1 Continued

EXPERIMENT	MASS		FREQUENCY			EXCITATION and CLEARANCE				
	Impact Mass M2 (kg)	Mass Ration M2/M1	Exc. Freq. (Start Freq.) W1 (Hz)	End Frequency W2 (Hz)	Frequency Ratio r1	Excitation Ampl. A (mm)	Initial Displ. X1 (micstr)	Wall-to-Wall Gap (mm)	Clearance d (mm)	Clearance Ratio d/A
150	0.086	**0.045**	-			-	400	40.640		
151	0.086	**0.045**	8.700		**0.967**	0.254		40.640	**3.252**	**12.803**
152	0.086	**0.045**	8.800		**0.978**	0.254		40.640	**3.252**	**12.803**
153	0.086	**0.045**	8.900		**0.989**	0.254		40.640	**3.252**	**12.803**
154	0.086	**0.045**	9.000		**1.000**	0.254		40.640	**3.252**	**12.803**
155	0.086	**0.045**	9.050		**1.006**	0.254		40.640	**3.252**	**12.803**
156	0.086	**0.045**	9.080		**1.009**	0.254		40.640	**3.252**	**12.803**
157	0.086	**0.045**	9.090		**1.010**	0.254		40.640	**3.252**	**12.803**
158	0.086	**0.045**	9.100		**1.011**	0.254		40.640	**3.252**	**12.803**
159	0.086	**0.045**	9.110		**1.012**	0.254		40.640	**3.252**	**12.803**
160	0.086	**0.045**	9.150		**1.017**	0.254		40.640	**3.252**	**12.803**
161	0.086	**0.045**	9.220		**1.024**	0.254		40.640	**3.252**	**12.803**
162	0.086	**0.045**	9.300		**1.033**	0.254		40.640	**3.252**	**12.803**
163	0.086	**0.045**	8.700	9.300	-	0.254		40.640	**3.252**	**12.803**
164	0.086	**0.045**	9.300	8.700	-	0.254		40.640	**3.252**	**12.803**
165	0.086	**0.045**			-	-	400	39.500		
166	0.370	**0.193**	-		-	-	400	39.500		
167	0.370	**0.193**	8.700		**0.967**	0.254		39.500	**2.112**	**8.315**
168	0.370	**0.193**	8.800		**0.978**	0.254		39.500	**2.112**	**8.315**
169	0.370	**0.193**	8.900		**0.989**	0.254		39.500	**2.112**	**8.315**
170	0.370	**0.193**	9.000		**1.000**	0.254		39.500	**2.112**	**8.315**
171	0.370	**0.193**	9.050		**1.006**	0.254		39.500	**2.112**	**8.315**
172	0.370	**0.193**	9.080		**1.009**	0.254		39.500	**2.112**	**8.315**
173	0.370	**0.193**	9.090		**1.010**	0.254		39.500	**2.112**	**8.315**
174	0.370	**0.193**	9.100		**1.011**	0.254		39.500	**2.112**	**8.315**
175	0.370	**0.193**	9.110		**1.012**	0.254		39.500	**2.112**	**8.315**
176	0.370	**0.193**	9.150		**1.017**	0.254		39.500	**2.112**	**8.315**
177	0.370	**0.193**	9.220		**1.024**	0.254		39.500	**2.112**	**8.315**
178	0.370	**0.193**	9.300		**1.033**	0.254		39.500	**2.112**	**8.315**
179	0.370	**0.193**	8.700	9.300	-	0.254		39.500	**2.112**	**8.315**
180	0.370	**0.193**	9.300	8.700		0.254		39.500	**2.112**	**8.315**

1M x 1A x 3C

Table A.1 Continued

EXPERIMENT	MASS		FREQUENCY			EXCITATION and CLEARANCE				
	Impact Mass M2 (kg)	Mass Ration M2/M1	Exc. Freq. (Start Freq.) W1 (Hz)	End Frequency W2 (Hz)	Frequency Ratio r1	Excitation Ampl. A (mm)	Initial Displ. X1 (micstr)	Wall-to-Wall Gap (mm)	Clearance d (mm)	Clearance Ratio d/A
181	0.086	**0.045**	-		-		400	42.300		
182	0.370	**0.193**	-		-	-	400	42.300		
183	0.370	**0.193**	8.700		**0.967**	0.254		42.300	**4.912**	**19.339**
184	0.370	**0.193**	8.800		**0.978**	0.254		42.300	**4.912**	**19.339**
185	0.370	**0.193**	8.900		**0.989**	0.254		42.300	**4.912**	**19.339**
186	0.370	**0.193**	9.000		**1.000**	0.254		42.300	**4.912**	**19.339**
187	0.370	**0.193**	9.050		**1.006**	0.254		42.300	**4.912**	**19.339**
188	0.370	**0.193**	9.080		**1.009**	0.254		42.300	**4.912**	**19.339**
189	0.370	**0.193**	9.090		**1.010**	0.254		42.300	**4.912**	**19.339**
190	0.370	**0.193**	9.100		**1.011**	0.254		42.300	**4.912**	**19.339**
191	0.370	**0.193**	9.110		**1.012**	0.254		42.300	**4.912**	**19.339**
192	0.370	**0.193**	9.150		**1.017**	0.254		42.300	**4.912**	**19.339**
193	0.370	**0.193**	9.220		**1.024**	0.254		42.300	**4.912**	**19.339**
194	0.370	**0.193**	9.300		**1.033**	0.254		42.300	**4.912**	**19.339**
195	0.370	**0.193**	8.700	9.300		0.254		42.300	**4.912**	**19.339**
196	0.370	**0.193**	9.300	8.700		0.254		42.300	**4.912**	**19.339**
197	0.086	**0.045**			-	-	400	41.500		
198	0.370	**0.193**	-			-	400	41.500		
199	0.370	**0.193**	8.700		**0.967**	0.254		41.500	**4.112**	**16.189**
200	0.370	**0.193**	8.800		**0.978**	0.254		41.500	**4.112**	**16.189**
201	0.370	**0.193**	8.900		**0.989**	0.254		41.500	**4.112**	**16.189**
202	0.370	**0.193**	9.000		**1.000**	0.254		41.500	**4.112**	**16.189**
203	0.370	**0.193**	9.050		**1.006**	0.254		41.500	**4.112**	**16.189**
204	0.370	**0.193**	9.080		**1.009**	0.254		41.500	**4.112**	**16.189**
205	0.370	**0.193**	9.090		**1.010**	0.254		41.500	**4.112**	**16.189**
206	0.370	**0.193**	9.100		**1.011**	0.254		41.500	**4.112**	**16.189**
207	0.370	**0.193**	9.110		**1.012**	0.254		41.500	**4.112**	**16.189**
208	0.370	**0.193**	9.150		**1.017**	0.254		41.500	**4.112**	**16.189**
209	0.370	**0.193**	9.220		**1.024**	0.254		41.500	**4.112**	**16.189**
210	0.370	**0.193**	9.300		**1.033**	0.254		41.500	**4.112**	**16.189**
211	0.370	**0.193**	8.700	9.300	-	0.254		41.500	**4.112**	**16.189**
212	0.370	**0.193**	9.300	8.700	-	0.254		41.500	**4.112**	**16.189**

M1 is the primary mass. M2 is the IVA mass. M2/M1 is the mass ratio. W1 and W2 are the starting and ending frequencies for frequency sweep experiments. For dwells. W1 is the excitation frequency and W2 is not defined. r1 is the frequency ratio for dwell

experiments, corresponding to W1. Amplitude A is the zero-to-peak excitation amplitude for forced vibration experiments. A is not defined for free vibration, instead, X1 is defined as the initial excitation. X1 is measured in microstrains, using the strain gage. d is the free clearance between the walls, in which the IVA can move. It is found by subtracting the IVA diameter from the wall gap. d/A is the non-dimensional clearance, clerance divided by excitation amplitude A. This quantity is not defined for free vibration.

PERMISSION TO COPY

In presenting this thesis in partial fulfillment of the requirements for a master's degree at Texas Tech University or Texas Tech University Health Sciences Center, I agree that the Library and my major department shall make it freely available for research purposes. Permission to copy this thesis for scholarly purposes may be granted by the Director of the Library or my major professor. It is understood that any copying or publication of this thesis for financial gain shall not be allowed without my further written permission and that any user may be liable for copyright infringement.

Agree (Permission is granted.)

Student's Signature _____ Date _____

Disagree (Permission is not granted.)

Student's Signature _____ Date _____